An important role of ceramide metabolism in diseases, which are caused by oxidative stress

An important role of ceramide metabolism in diseases, which are caused by oxidative stress

2016

Keiko Kobayashi

Contents

General Introduction

It is generally assumed that the oxidative stress has a major role in aging and pathogenesis of diseases such as atherosclerosis, diabetes, non-alcoholic fatty liver disease (NAFLD), and Alzheimer's disease (1-5). It is important to clarify the events caused by oxidative stress leading to these diseases, although it is very difficult to evaluate the oxidative stress in tissues. Hydrogen peroxide is assumed to be the functional molecule causing oxidative stress but its concentration is too low and besides it is decomposed too fast to allow us its accurate determination.

There are some indicators, which reflect the oxidative state indirectly; vitamin C, vitamin E, and the ratio of reduced (GSH) and oxidized glutathione (GSSG). These are factors cooperating each other to protect the cell from oxidative stress. Then they have been used as parameters of oxidative stress.

Ceramide is a well-known lipid, which causes apoptosis in a variety of cells. When HL-60 cell was treated with antineoplastic agents, the ceramide concentration in the cell was increased and this increase was inhibited by catalase (6). This result suggested that the increase of ceramide was caused by oxidative stress involving hydrogen peroxide.

Ceramide is generated by two pathways; de novo and salvage pathways. In the de novo pathway, serine-palmitoyl transferase is the rate determining enzyme, while in the salvage pathway, sphingomyelinase (SMase) hydrolyzes sphingomyelin to yield ceramide (7).

It is reported that carbon tetrachloride (CCl_4) intoxication, which has been used as a typical model of oxidative stress in the liver, increased the ceramide content in rat tissues (8). Combining the results from the apoptosis of HL-60 by oxidative stress (6), it is possible that ceramide is increased by oxidative stress *in vivo*.

Based on this hypothesis, I investigated whether the ceramide metabolism was affected by oxidative stress and the underlying mechanism of this change *in vivo* by animal experiments.

In Chapter 1, I showed that the total ceramide concentration significantly increased in the liver, brain, kidney, and plasma of CCl_4-intoxicated rats. The ratio of GSH/GSSG decreased in the liver, plasma, kidney, and brain 2 h after CCl_4 intoxication. In addition, the level of vitamin C was decreased in the liver and kidney. On the other hand, the level of vitamin E was decreased in the liver, kidney, and plasma. The increase of ceramide was derived from the increase of neutral sphingomyelinase (nSMase) activity in the liver, kidney, and brain. The increase in nSMase activity was induced significantly in the liver 2 h after intoxication with CCl_4, when the ratio of GSH/GSSG in the liver decreased. These results indicated that acute oxidative stress stimulated nSMase activity resulting in the production of ceramide.

In Chapter 2, I found that the increase of plasma ceramide was inhibited by celecoxib, a selective cyclooxygenase-2 (COX-2) inhibitor in CCl_4-intoxicated rats. CCl_4-induced hepatic injury is divided into two phases; in the initial phase trichloromethyl radical is generated by P450 dependent dehalogenation and in the second phase Kupffer cells are activated leading to the increase in the activities of phospholipase A_2 and COX-2. Since the increase of plasma ceramide 24 h after oral administration of CCl_4 was significantly reduced by celecoxib treatment, this observation indicated that celecoxib ameliorated the toxicity of CCl_4 by inhibiting COX-2 in the second phase. Indeed it was shown later that Kupffer cells were activated in the second phase of CCl_4 intoxication utilizing Nucling-knockout mice, in which the number of Kupffer cells was largely reduced (9).

In Chapter 3, I evaluated the change in ceramide metabolism by oxidative stress during diabetes. Streptozotocin (STZ) was used to induce diabetes in Wistar male rats. After 2 weeks of the drug administration, the activity of secretory sphingomyelinase (sSMase) was significantly increased in the plasma, while the activity of nSMase was not changed in the kidney and liver. In addition, the ceramide concentration in plasma was significantly increased because of the elevated sSMase activity. On the other hand, the ceramide concentration in the kidney was significantly increased at 8 weeks after STZ administration, while the nSMase activity was not increased. These observations supported the view that prolonged oxidative stress stimulated plasma sSMase activity in the chronic state of diabetes.

In Chapter 4, I showed that the ceramide concentration and sSMase activity also increased in the plasma of aged apolipoprotein E knock out ($apoE^{-/-}$) mice. Although the total ceramide level in plasma was always higher in $apoE^{-/-}$ mice than that in wild-type (WT) mice, it decreased by aging in both WT and $apoE^{-/-}$ mice. The ceramide level in the aorta of $apoE^{-/-}$ mice was increased at 15 weeks of age when $apoE^{-/-}$ mice developed atherosclerosis. These results indicated that sSMase activity was increased by oxidative stress and generated ceramide, leading to atherogenesis during aging.

In Chapter 5, I found that the sSMase activity depended on the redox state. Namely sSMase was activated by oxidation with hydrogen peroxide and the activated sSMase was inactivated by GSH. In addition I searched a possible inhibitor of sSMase among food factors. Based on the previous results, sSMase has an important role in progression of metabolic syndrome. Considering that sSMase is activated in oxidative state, I examined effects of antioxidants on sSMase. As a result, (-)-epicatechin 3-*O*-gallate (ECg) and (-)-

3′-*O*-methylepigallocatechin 3-*O*-gallate (EGCg-3′-O-Me) showed strong inhibitory effect on sSMase. These observations support the view that antioxidants possibly prevent the progress of diseases caused by oxidative stress through inhibiting sSMase.

This thesis shows that ceramide, a well known lipid to cause apoptosis, is increased in CCl_4-intoxicated liver, diabetes mellitus, and atherogenesis during aging, namely in tissues with enhanced oxidative stress. Especially, I show that the ceramide salvage pathway is directly activated by oxidative stress. These results clearly show that the cell has a physiological mechanism causing ceramide synthesis to respond to oxidative stress. The nSMase activation and ceramide production in the early phase of CCl_4-intoxicated liver show that the liver cell has a very sensitive antenna to detect oxidative stress resulting in causing apoptosis in cells under oxidative stress. This is a physiologically reasonable response of cells, because oxidative stress causes caricinogenesis in the cell and animals must effectively eliminate transformed cells.

When radical reactions in biology caught attentions about 40 years ago, scientists assumed that radical reactions, usually called as lipid peroxidation were unphysiological reactions and that the cell had no physiological response to cope with them. Later it is clarified that oxidative stress activates many physiological proteins including MAPK (mitogen-activated protein kinase), Nrf2, heme oxygenase, and so on (10). In this thesis I clarified that SMase is directly activated by oxidative stress. It is worthwhile to note that among enzymes activated by oxidative stress, SMase is closely related with pathogenesis of atherosclerosis and diabetes, which are very serious problems in developed countries.

My studies further reveral that sSMase is inhibited by antioxidants. This finding will be very useful to prevent these diseases by improvement of diets.

References

1) Madamanchi, N. R., Vendrov, A., Runge, M. S. Oxidative stress and vascular disease. *Arterioscler. Thromb. Vasc. Biol.* **25**, 29-38 (2005).

2) Giacco, F., Brownlee, M., Oxidative stress and diabetic complications. *Circ. Res*. **107**, 1058-1070 (2010).

3) Finkel, T., Holbrook, N. J. Oxidants, oxidative stress and the biology of ageing. *Nature* **408**, 239-247 (2000).

4) Narasimhan, S., Gokulakrishnan, K., Sampathkumar, R., Farooq, S., Ravikumar, R., Mohan, V., Balasubramanyam, M. Oxidative stress is independently associated with non-alcoholic fatty liver disease (NAFLD) in subjects with and without type 2 diabetes. *Clin. Biochem.* **43**, 815-821 (2010).

5) Zhao, Y., Zhao, B. Oxidative stress and the pathogenesis of Alzheimer's disease. *Oxid. Med. Cell Longev.* **2013** (2013).

6) Yamada, Y., Kajiwara, K., Yano, M., Kishida, E., Masuzawa, Y., Kojo, S., Increase of ceramides and its inhibition by catalase during chemically induced apoptosis of HL-60 cells determined by electrospray ionization tandem mass spectrometry. *Biochim. Biophys. Acta*. **1532**, 115–120 (2001).

7) Mullen, T. D., Hannun, Y. A., Obeid, L. M. Ceramide synthases at the centre of sphingolipid metabolism and biology. *Biochem. J.* **441**, 789-802 (2012).

8) Ichi, I., Nakahara, K., Fujii, K., Iida, C., Miyashita, Y., Kojo, S. Increase of ceramide in the liver and plasma after carbon tetrachloride intoxication in the rat. *J. Nutr. Sci. Vitaminol.* **53**, 53-56 (2007).

9) Kiso, K., Ueno, S., Fukuda, M., Ichi, I., Kobayashi, K., Sakai, T., Fukui, K., Kojo, S. The role of Kupffer cells in carbon tetrachloride intoxication in mice. *Biol. Pharm. Bull.* **35**, 980-983 (2012).

10) Schieber, M., Chandel, N. S. ROS function in redox signaling and oxidative stress. *Curr. Biol.* **24**, R453-462 (2014).

Chapter 1

Neutral sphingomyelinase-induced ceramide accumulation by oxidative stress during carbon tetrachloride intoxication

Abstract

Ceramide is a biologically active lipid causing apoptosis in a variety of cells. In this study, we examined the effect of CCl_4 on the ceramide metabolism and indicators of oxidative stress. After 12 h of oral administration of CCl_4 (4 ml/kg body weight as a 1:1 mixture of CCl_4 and mineral oil) to rats, aspartate aminotransferase (AST) and alanine aminotransferase (ALT) were increased. Antioxidants such as vitamins C and E were decreased in the liver and kidney. In addition, the ratio of GSH/GSSG in the liver, plasma, kidney, and brain decreased at 2 h. The total ceramide in the liver significantly increased as early as 2 h after CCl_4 administration. After 24 and 36 h, the total ceramide in plasma and the kidney was also augmented. In the brain, the total ceramide dramatically increased at 36 h. These results suggested that the increased ceramide in plasma was transferred to the kidney and the brain. The activity of neutral sphingomyelinase (SMase), which was reported to be enhanced by the decrease of GSH, was significantly increased after CCl_4 treatment in the liver, kidney, and brain. However, acid SMase activities were not increased in the liver and kidney. Thus, the activation of neutral SMase via oxidative stress induced the increase of ceramide during CCl_4 intoxication in not only the liver but also other tissues. These results suggested that the excess accumulation of ceramide causes damage in other organs including the kidney and brain during fulminant hepatic failure.

Abbreviations: aSMase, acid sphingomyelinase; ALT, alanine aminotransferase; AST, aspartate aminotransferase; BUN, blood urea nitrogen; GSH, reduced glutathione; GSSG, oxidized glutathione; LC-MS/MS, liquid chromatography-electrospray tandem mass spectrometry; NBD, nitrobenzofurazan; nSMase, neutral sphingomyelinase; ROS, reactive oxygen species; SM, sphingomyelin; SMase, sphingomyelinase

1. Introduction

Carbon tetrachloride (CCl_4) is metabolized by P450-dependent dehalogenation to trichloromethyl radical, which deranges the cellular metabolism, including alteration of membrane proteins and lipids by their covalent binding to cellular macromolecules (1). CCl_4 intoxication has been used as an animal model of fulminant hepatic failure to develop artificial liver support (2, 3). The mechanism of liver injury by CCl_4 has received more attention than that by any other chemical (4).

Ceramide has been implicated in regulating cell-cycle arrest, apoptosis, and cell senescence (5-7) and serves as an intracellular second messenger (8). Ceramide is generated by sphingomyelin (SM) hydrolysis by sphingomyelinase (SMase) (9). SMases are classified based on pH optima, subcellular localization, and cation dependence (10). Neutral SMase (nSMase) is localized in the plasma membrane and exhibits an optimum pH of about 7.5 and Mg^{2+}-dependence. Acid SMase (aSMase), with an optimum pH of about 4.8, operates at the endosomal-lysosomal compartments or plasma membrane. Some studies report that a negative correlation exists between nSMase activity and reduced glutathione (GSH) (11, 12) and partially purified nSMase is dose-dependently inhibited by GSH (13). Because GSH is the major antioxidant defense system that eliminates toxic oxygen radical (14), the activation of SMase might be accompanied with the enhancement of oxidative stress by CCl_4 administration.

Oxidative stress such as UV-light and irradiation induced the ceramide accumulation in the injured cells (15, 16). In addition, the hydrophobic nature of CCl_4 allows it to permeate cell membranes and CCl_4 is distributed and accumulated in organs such as the liver, brain, kidney, and heart (17). Therefore, the radical derived from CCl_4 might affect the synthesis of ceramide in these organs. In fulminant hepatic failure, which

induces massive necrosis of the liver via oxidative stress, toxic substances and cytokines released into the circulation are assumed to cause encephalopathy and renal dysfunction (18). Our previous study showed that hepatic and plasma ceramides were increased by the administration of CCl_4 to rats (19). Therefore, it is possible that the increased ceramide in the liver and plasma during fulminant hepatic failure is one of the important toxins causing damage in other organs including the kidney and the brain. In the present study, we show that oxidative stress via CCl_4 administration induces the changes of ceramide metabolism in not only the liver but also other organs such as the kidney and brain.

2. Materials and methods

2.1. Animals

This study was approved by the Animal Care Committee of Nara Women's University. Eight-week-old male rats (SLC: Wistar strain) were obtained from Japan SLC Co. (Hamamatsu, Shizuoka, Japan). The animals were housed in a room at 24±2°C, with a 12 h/12 h light-dark cycle. Animals were fed commercial laboratory chow (MF, Oriental Yeast Co., Osaka, Japan) and water ad libitum. Eight-week-old rats were administered a mixture of CCl_4 and mineral oil (1:1, 4 ml/kg body weight) through an intragastric tube as previously described (20). The control rats received mineral oil alone (4 ml/kg body weight).

2.2. Analytical methods

Rats were anesthetized with diethyl ether and killed by collecting the blood from the inferior vena cava using a syringe containing sodium heparin as an anticoagulant. After perfusion of ice-cooled saline through the portal vein, organs were removed. After perfusion, the liver, kidney, and brain were dissected out. Blood was centrifuged to separate the plasma. The activities of plasma aspartate aminotransferase (AST) and alanine aminotransferase (ALT) were determined using diagnostic kits (GOT and GPT-UV Test Wako, Wako Pure Chemicals Co., Osaka) and expressed as Karmen Units.

The determination of vitamin C was made according to a specific and sensitive method involving chemical derivatization and HPLC (21). The excised tissue was homogenized in 5 volumes of 10 mmol/L phosphate buffered saline (pH 7.2) under ice cooling. All determinations were made by duplicated experiments. One hundred microliters of tissue homogenate or plasma was added to 900 μL of metaphosphoric acid solution (200 g/L) containing stannous chloride (10 g/L) followed by centrifugation at 10,000 g for 10 min at 4 °C to get a deproteinized sample. A 100 μL sample of the supernatant was taken out and mixed with 100μL of 2,6-dichloroindophenol (2 g/L) to oxidize ascorbic acid. The solution was mixed with 50 μL of stannous chloride (10 g/L) in a metaphosphoric acid solution (50 g/L) and with 120 μL of 2,4-dinitrophenylhydrazine (20 g/L) in 4.5 mol/L of sulfuric acid. The mixture was incubated for 3 h at 37 °C. After cooling in an ice bath, ethyl acetate (1 mL) and water (1 mL) were added to the reaction mixture. After shaking and centrifugation (1,000 g) for 10 min, 600 μL of the ethyl acetate layer was taken out and evaporated to dryness. The residue was dissolved in 100 μL of acetonitrile, and 10 μL of the sample was applied to HPLC. For HPLC analysis, a Shimadzu LC-9A pump was used. The sample was applied to μ-Bondasphere column (5 μm C_{18} 100A, Waters), eluted with a 1:1 mixture of acetonitrile and water adjusted at pH 3.5 with triethylamine

(10 g/ L) and phosphoric acid at the rate of 1 mL/min. The absorption at 505 nm was recorded with a spectrophotometer (type SPD-10A manufactured by Shimadzu, Kyoto, Japan). The detection limit was 1 pmol, which was identical with the literature (21).

The concentration of vitamin E was determined by HPLC (22). The levels of total GSH and oxidized glutathione (GSSG) were determined by the enzymatic method (23). The levels of blood urea nitrogen (BUN) were measured using diagnostic kit (Urea B Test Wako, Wako Pure Chemicals Co., Osaka).

2.3. Measurement of ceramide

Lipid of each tissue was extracted according to the method of Folch et al. (24). In brief, the excised tissue was homogenized in 9.9 ml of a mixture of $CHCl_3$ and CH_3OH (2:1, v/v) and added 2.2 ml of water. After vigorous shaking and centrifugation for 5 min at 1,000 g, the $CHCl_3$ layer was collected. To the residue, 6.6 ml of $CHCl_3$ was added and the extraction was performed again. The collected $CHCl_3$ solution was evaporated. The resulting lipid was dissolved in 120 μl of chloroform to perform Silica gel 60 TLC (Merck, Darmstadt, Germany). The TLC separation method was previously described (25). In brief, the first elution was made with a mixture of *n*-butanol/acetic acid/water (3:1:1, v/v/v) to the one third mark of the plate and the second elution was made to the top of the plate with a mixture of diethyl ether/*n*-hexane/acetic acid (90:10:1, v/v/v). Ceramide spot was visualized under UV by staining with primulin spray. The ceramide spot was scratched from TLC plate and collected into a glass tube. Extraction from TLC plate was conducted with 2 ml of a mixture of $H_2O/CH_3OH/CHCl_3$ (8:20:10, v/v/v) under shaking for 30 min. After centrifugation, the $CHCl_3$ layer was collected. One mililitter of H_2O and 2 ml of $CHCl_3$ were added to the residue and the extraction was repeated. The $CHCl_3$ layer was collected in a glass tube. To the residue, 1.5 ml of $CHCl_3$ was added. The

extraction was performed additional one more time. The collected solution was evaporated and suspended in 200 μl of a mixture of $CHCl_3$ and CH_3OH (1:1, v/v). Quantitative measurements of ceramide species were made using a triple-quadrupole mass spectrometer (Finnigan MAT TSQ 7000). ESI-MS/MS was performed as previously described (25). HPLC was conducted using a Waters 600S system equipped with a μ-Bondasphere column (5 μm C_{18} 100A Waters). Elution was performed at a flow rate of 0.2 ml/min with a mixture of 5 mM ammonium formate, methanol, and tetrahydrofuran (1:2:7, v/v/v). Mass analysis was perfomed in the positive ion mode in a heated capillary tube at 250 °C with an electrospray potential of 4.5 kV, a seath gas pressure of 70 psi, and a collision gas pressure of 1.6-2.0 mTorr. Under optimized conditions, monitoring ions were ceramide molecular species $[M+H]^+$ for the product ion at *m/z* 264 of sphingoid base. Standard and samples were injected with 5 μl of 5 pmol/μl C8:0 ceramide ratio, assuming that the calibration curve of ceramide bearing C16-24 acyl chains was similer to that of C16:0 ceramide. Each sample was analyzed in duplicate.

2.4. Assay of SMase activity

The enzyme assay of SMase was performed basically as previously described (26). The excised tissues were homogenized in 3 volumes of phosphate buffered saline (10 mM, pH 7.4) under ice cooling. Protein concentrations were determined according to the method of Lowry et al. (27). Homogenization (10-20 mg protein/ml) was dissolved in 0.2% Triton X-100 in 10 mM Tris, pH 7.4 (supplemented with 25 μM genistein) for 10 min on ice. The lysates were homogenized with three passes through a 25-G needle. Nitrobenzofurazan (NBD) C_6-SM (Molecular Probes Inc., Eugene, OR, USA) was added to the lysates to give a final concentration of 20 μM and they were incubated at 4°C for 10 min. The lysates were added to 5 mM $MgCl_2$ in 10 mM Tris, pH 7.4 for nSMase or

0.5 M acetate buffer, pH 4.5 for the aSMase. The final volume was 300 μl. After incubation for 1 h at 37°C, the reaction was stopped by adding 1 ml of methanol. The samples (20 μl each) were directly analyzed by HPLC, which was conducted using a Nova Pak 4 μm C18 column (3.9×150 mm, Waters). Elution was performed at a flow rate of 1 ml/min with a mixture of methanol, water, and phosphoric acid at a volume ratio of 35:65:0.2. In this condition NBD C_6-SM and NBD C_6-ceramide were eluted at about 3 and 11 min, respectively. Fluorescence of these compounds was determined using a fluorescence detector (Shimadzu, RF-10AXL, excitation at 466 nm and emission at 536 nm). Authentic NBD C_6-ceramide was purchased from Molecular Probes Inc.

3. Results

3.1. Liver injury caused by CCl_4

The plasma ALT level tended to increase 6 h after administration of CCl_4 and at 12 h it was significantly higher than that in the control group (Fig. 1a). At 12 h, the plasma AST level was also significantly higher than that of the control group (Fig. 1b). These results show the extensive cell death 12 h after CCl_4 administration. After 24 and 36 h, AST and ALT levels were increased further.

3.2. Changes in the level of vitamin C and vitamin E in rats treated with CCl_4

To examine the effect of CCl_4 intoxication on oxidative stress, we analyzed antioxidant vitamins. The hepatic level of vitamin C significantly decreased 6 h after CCl_4 administration. After 24 and 36 h, vitamin C in the liver decreased drastically to about 9-11% of the control liver (Fig. 2a). However, vitamin C in plasma increased 2, 6, 12,

and 36 h after CCl_4 intoxication (Fig. 2b). Although vitamin C in the kidney was temporarily increased at 2 h, the kidney vitamin C level at 24 and 36 h was lower than that of the control group (Fig. 2c). Vitamin C in the brain 6 h after CCl_4 administration decreased compared to the control group (Fig. 2 d), but the levels of vitamin C were almost the same as in the control group from 12 to 36 h.

The hepatic vitamin E level was significantly decreased 6 h after CCl_4 intoxication compared to the control group (Fig. 3a). In plasma, vitamin E was also decreased at 6 h and declined thereafter (Fig. 3b). The level of vitamin E in the kidney was decreased by administration of CCl_4 except at 6 h (Fig. 3c). However, the vitamin E in the brain increased 6 and 12 h after administration of CCl_4 (Fig. 3d).

3.3. Effect of CCl_4 intoxication on the GSH/GSSG ratio

It is reported that partially purified nSMase is dose-dependently inhibited by GSH in vitro (13). To reveal the relationship of GSH and ceramide metabolism in vivo, the GSH/GSSG ratios were determined during CCl_4 intoxication. The GSH/GSSG ratios of the liver and plasma decreased significantly 2 h after CCl_4 administration and declined thereafter (Fig. 4a, b). The GSH/GSSG ratio of the kidney was significantly decreased 2, 6, and 24 h after CCl_4 intoxication (Fig. 4c). In the brain, the ratio of GSH/GSSG was also significantly diminished from 2 h to 36 h after CCl_4 treatment compared to the control group (Fig. 4d).

3.4. Changes in the level of ceramides in rats treated with CCl_4

In the control rat liver, the major ceramides were C24:0, C24:1, C16:0, C24:2, and C22:0 in decreasing order (Fig. 5a). As early as 2 h after CCl_4 intoxication, significant increases of C22:0, C24:0, C24:1, and C24:2 in the liver were observed compared to the

control group. Twenty-four hours after administration of CCl_4, all ceramide species in the liver were significantly increased. Especially, the increase of C18:0 was striking. Total hepatic ceramide was significantly increased 2 and 12, and 24 h after CCl_4 intoxication. However, all ceramide species and total ceramide showed almost the same levels as in the control group 36 h after CCl_4 intoxication.

Major ceramides of plasma were C24:0 and C24:1 (Fig. 5b). All ceramides were significantly increased 24 h after CCl_4 intoxication, and after 36 h the total ceramide in plasma significantly increased to 5.9 times that in the control group.

In the kidney, major ceramides were C24:0, C24:1, and C16:0 (Fig. 5c). C22:0 and C24:0, and C24:2 were significantly increased 2 h after CCl_4 administration. After 24 and 36 h, total ceramide in the kidney was significantly increased compared to the control group.

The major ceramide in the brain was C18:0, which accounted for about 80-85% of total ceramide (Fig. 5d). Although total ceramide in the brain did not increase until 24 h, the total ceramide 36 h after CCl_4 administration was remarkably higher than that of the control group. Among the ceramides, the increase of C18:0 was the most striking at 36 h.

3.5. Changes in the SMase activity in rats treated with CCl_4

In the liver, nSMase activity was significantly increased 2 and 24 h after CCl_4 treatment (Fig. 6a). However, aSMase activity in the liver was significantly decreased by CCl_4 intoxication except at 24 h (Fig. 6b). In the kidney, nSMase activity was significantly increased 2 and 24 h after CCl_4 administration (Fig. 6c). ASMase in the kidney was significantly decreased 12 and 36 h after intoxication of CCl_4 (Fig. 6d). In the brain, nSMase and aSMase were significantly increased 2-24 h after treatment with CCl_4 (Fig.

6e, f). In particular, nSMase and aSMase activities were dramatically increased to 51- and 27-fold that of the control group at 24 h, respectively. However, both SMase activities were almost equal to those of the control group at 36 h.

3.6. Effect of CCl_4 intoxication on the level of plasma BUN

To examine the effect of CCl_4 intoxication on renal injury, we measured the level of BUN. Although the level of BUN was not significantly increased from 2 to 24 h after CCl_4 intoxication, the BUN 36 h after CCl_4 administration was significantly higher than that of the control group (Fig. 7).

4. Discussion

The accumulation of ceramide is implicated in diseases such as atherosclerosis (28, 29) and Alzheimer's disease (30), which accompany the enhancement of oxidative stress. In this study, we examined whether ceramides were increased in tissues via oxidative stress in rats intoxicated with CCl_4.

The primary defense against oxidative stress in the tissue rests with antioxidants such as antioxidant vitamins and GSH. Our previous studies demonstrated that the concentration of vitamin C, abundant and the strongest antioxidant in animal tissues, reflected oxidative stress most sensitively in the rat liver during chemical intoxication (20, 31). In the liver, vitamin C was decreased by CCl_4 intoxication, showing that oxidative stress was enhanced. Although vitamin C is not a vitamin for Wistar rats, oxidative stress caused by CCl_4 led to a depletion of vitamin C. The level of vitamin E in the liver was also reduced 6 h after CCl_4 intoxication. It was reported that vitamin E inhibited

the oxidative stress caused by CCl_4, resulting in a decrease of necrosis of the liver cells (32). Therefore, hepatic vitamin E might also be a marker to evaluate oxidative stress of the liver by CCl_4 intoxication, although the rate of decrease of the liver vitamin E is considerably smaller than that of vitamin C.

Total hepatic ceramide increased significantly 2 h after CCl_4 intoxication. The nSMase activity also increased 2 h after CCl_4 administration in the liver. Ceramide was generated by a single class of enzyme, SMase, and it was reported that the early ceramide changes were related with SMase activities (33). Therefore, the increase of hepatic ceramide by CCl_4 intoxication at the early stage may be due to increased nSMase activity. In addition, hepatic ceramides in rats undergoing liver ischemia/reperfusion (I/R) increased and aSMase activity increased during reperfusion of the ischemic liver, in contrast to nSMase activity (34). Whether nSMase or aSMase is activated may depend on the type of injury.

In addition, a negative correlation between nSMase activity and GSH concentration is reported in liver cells (11) and cells of other types (13, 35). In the liver, the present study showed that both the decrease of GSH/GSSG ratio and the increase of ceramide were observed from 2 to 24 h after CCl_4 administration. The decrease of GSH/GSSG ratio preceded the onset of apoptosis induced by various agents (36). These results suggest that oxidative stress-induced change of ceramide metabolism causes hepatic damage.

In plasma, vitamin C concentration increased 2, 6, 12, and 36 h after CCl_4 treatment. This may be ascribed to the release from the necrotized liver, which contains a 40-fold concentration of vitamin C (about 2,000 versus 50 μM) compared to plasma. In addition, vitamin E and the GSH/GSSG ratio in plasma were also diminished by CCl_4 treatment suggesting that the oxidative stress in plasma increased as well as in the liver. Plasma ceramide was dramatically increased 24-36 h after CCl_4 intoxication. Because the

ceramide composition in plasma was similar to that in the liver, the accumulation of hepatic ceramide by the enhancement of oxidative stress and resulting release from the necrotized liver may increase plasma ceramide by CCl_4 intoxication. Furthermore, it is possible that the increased ceramides in plasma during hepatic failure is one of the important toxic factors causing damage in other organs.

In the kidney, the decrease of vitamin E and the GSH/GSSG ratio was earlier than that of vitamin C, suggesting that vitamin E and the GSH/GSSG ratio are sensitive markers of oxidative stress in the kidney. The total ceramide at 24 and 36 h in the kidney was significantly increased compared to the control group. Particularly, ceramides with long chain such as C22 and C24 in the kidney were markedly increased compared to those of the liver. The nSMase activity in the kidney was increased by CCl_4 administration similarly to the liver. The change of renal ceramide metabolism via the oxidative stress may be also a cause of the dysfunction.

In the brain, vitamin C was decreased only 6 h after CCl_4 treatment. It was reported that the rate of decrease of cerebral vitamin C is slower than that in the other organs such as the liver and the kidney, when vitamin C deficiency was induced in ODS rats which lack the key enzyme for ascorbate synthesis (37). The vitamin E level in the brain was even increased 2, 6, and 12 h after CCl_4 administration. In rats fed a vitamin E-deficient diet, the decrease of vitamin E in the brain was the slowest among the tissues including the liver and the kidney (38). These results indicated the presence of unknown mechanisms to maintain the levels of these vitamins in the brain.

Ceramide with 18-carbon atom side chains in the brain predominated and the ceramide profile of the brain was very different from that of other tissues. Ceramides were reported to increase following brain injury such as ischemia (39, 40). This study showed that the total ceramide, especially C18:0, in the brain was dramatically increased 36 h

after CCl_4 administration. However, both SMase activities at 36 h were almost the same as in the control group in spite of the low GSH/GSSG ratio, suggesting that the dysfunction of the brain 36 h after CCl_4 intoxication caused the decrease of SMase activities. Since intravenously injected fluorescent C_6-ceramide is able to cross blood-brain-barrier (41), the increased ceramide in plasma may be transferred to the brain at the late stage, especially at 36 h, and the increase of ceramide may lead to brain damage. This idea is supported by the result that the increase of C18:0 was the most conspicuous among the ceramides and was 4.7, 18.6, and 3.8 times the control value in the liver, plasma, and brain, respectively. In addition, both nSMase and aSMase activities were dramatically increased compared to the control group 24 h after CCl_4 treatment. Although the increase of these SMase activities may be involved in the augmentation of some brain ceramides, which did not include C18:0 2-24 h after CCl_4 intoxication, further studies are necessary to clarify the cause of the change of ceramide levels in the brain.

In this study, the activity of nSMase was significantly increased after CCl_4 treatment in all organs examined. The decrease of the ratio of GSH/GSSG in the early stage was also observed, although neither the increase of GSH nor the decrease of GSSG was observed by CCl_4 intoxication (data not shown). The other study demonstrated that a correlation between the SMase activity and the decrease of oxidation products caused by GSH was observed (11). However, the mechanism of nSMase activation by oxidative stress is not fully understood. GSH dose-dependently inhibited nSMase activity in vitro and the γ-glutamylcysteine part in GSH was suggested to function as an allosteric regulator of nSMase (13). Therefore, the GSH and the GSH/GSSG ratio may be a negative regulator of nSMase in the animal model of oxidative stress such as CCl_4 intoxication. Our previous study showed that the concentration of lipid hydroperoxides also increased significantly in liver mitochondria after 6 h of intragastric administration of CCl_4 (42).

Other report demonstrated that the administration of bilirubin, an antioxidant inhibited the activation of nSMase during the increase of lipid peroxidation by UV irradiation (43). These results suggested that oxidative stress such as lipid peroxidation also induced the activation of nSMase by CCl_4 intoxication.

Our previous study demonstrated that the activation of caspase-3 in the liver took place 12 h after CCl_4 administration (20). Therefore, the accumulation of hepatic ceramide may be one of causes that induce apoptosis in the liver. In addition, the level of BUN, which is a clinical parameter of renal function, was increased 36 h after CCl_4 injection. Because the level of ceramide in the kidney was increased at 24 and 36 h, the accumulation of ceramide may also contribute to renal cell death. In the brain, the ceramide also increased 36 h after CCl_4 administration. Therefore, further study is required to reveal the relation between the accumulation of ceramide and cell death in the brain.

In conclusion, antioxidants such as vitamins C and E, and GSH/GSSG ratio were decreased and the levels of ceramide were increased not only in the liver but also in other tissues by CCl_4 administration. In addition, it was suggested that the activation of nSMase via oxidative stress during CCl_4 intoxication induced the increase of ceramide. Our data support the view that the excess accumulation of ceramide plays an important role to cause the injury in the kidney and brain during fulminant hepatic failure.

References

1) Racknagel, R.O., Glende, E.J.R, Dolak, J.A., Waller, R.I. Mechanism of carbon tetrachloride toxicity. *Pharmacol. Ther.* **43**, 139-154 (1989).

2) Soloviev, V., Hassan, A.N., Akatov, V., Lezhnev, E., Ghaffar, T.Y., Ghaffar, Y.A. A novel bioartificial liver containing small tissue fragments: efficiency in the treatment of acute hepatic failure induced by carbon tetrachloride in rats. *Int. J. Artif. Organs* **26**, 735-742 (2003).

3) Shnyra, A., Bocharov, A., Bochkova, N., Spirov, V. Bioartificial liver using hepatocytes on biosilon microcarriers: treatment of chemically induced acute hepatic failure in rats. *Artif. Organs* **15**, 189-197 (1991).

4) Bruckner, J.V., Warren, D.A. Toxic effect of solvents and vapors. *In:Casarett & Doull's Toxicology. The Basic Science of Poisons. (Klaassen CD, ed), 6th Ed. McGraw-Hill. New York*, pp.869-916 (2001).

5) Hannum, Y.A., Luberto, C. Ceramide in the eukaryotic stress response. *Trends Cell Biol.* **10**, 73-80 (2000).

6) Merrill, A.H. De novo sphingolipid biosynthesis: a necessary, but dangerous, pathway. *J. Biol. Chem.* **277**, 25843-25846 (2002).

7) Hannun, Y.A., Obeid, L.M. The ceramide-centric universe of lipid-mediated cell regulation: stress encounters of the lipid kind. *J. Biol. Chem.* **277**, 25847-25850 (2002).

8) Kolesnick, R. Ceramide: a novel second messenger. *Trends Cell Biol.* **2**, 232–236 (1992).

9) Merrill, A.H., Jones, D.D. An update of the enzymology and regulation of sphingomyelin metabolism. *Biochim. Biophys. Acta* **1044**, 1–12 (1990).

10) Goni, F.M., Alonso, A. Sphingomyelinases: enzymology and membrane activity. *FEBS Lett.* **531**, 38-46 (2002).

11) Tsyupko, A. N., Dudnik, L. B., Evstigneeva, R. P., Alessenko, A. V. Effects of reduced and oxidized glutathione on sphingomyelinase activity and contents of sphingomyelin and lipid peroxidation products in murine liver. *Biochemistry (Mosc)* **66**, 1028-1034 (2001).

12) Rutkute, K., Asmis, R. H., Nikolova-Karakashian, M. N. Regulation of neutral sphingomyelinase-2 by GSH: a new insight to the role of oxidative stress in aging-associated inflammation. *J. Lipid Res.* **48**, 2443-2452 (2007).

13) Liu, B., Hannun, Y. A. Inhibition of the neutral magnesium dependent sphingomyelinase by glutathione. *J. Biol. Chem.* **272**, 16281-16287 (1997).

14) Han, D., Hanawa, N., Saberi, B., Kaplowitz, N. Mechanisms of liver injury. III. Role of glutathione redox status in liver injury. *Am. J. Physiol. Gastrointest. Liver Physiol.* **291**, G1-7 (2006).

15) Farrell, A. M., Uchida, Y., Nagiec, M. M., Harris, I. R., Dickson, R. C., Elias, P. M., Holleran, W. M. UVB irradiation up-regulates serine palmitoyl transferase in cultured human keratinocytes. *J. Lipid Res.* **39**, 2031-2038 (1998).

16) Santana, P., Pena, L.A., Haimovitz-Friedman, A., Martin, S., Green, D., McLoughlin, M., Cordon-Cardo, C., Schuchman, E.H., Fuks, Z., Kolesnick, R. Acid sphingomyelinase-deficient human lymphoblasts and mice are defective in radiation-induced apoptosis. *Cell* **86**, 189-199 (1996).

17) Melin, A.M., Perromat, A., Deleris, G. Pharmacologic application of Fourier transform IR spectroscopy: in vivo toxicity of carbon tetrachloride on rat liver. *Biopolymers* **57**, 160–168 (2000).

18) Laleman, W., Wilmer, A., Evenepoel, P., Verslype, C., Fevery, J., Nevens, F. Review article: non-biological liver support in liver failure. *Aliment. Pharmacol. Ther.* **23**, 351-363 (2006).

19) Ichi, I., Nakahara, K., Fujii, K., Iida, C., Miyashita, Y., Kojo, S. Increase of ceramide in the liver and plasma after carbon tetrachloride intoxication in the rat. *J. Nutr. Sci. Vitaminol.* **53**, 53-56 (2007).

20) Sun, F., Tsutsui, C., Hamagawa, E., Ono, Y., Ogiri, Y., Kojo, S. Evaluation of oxidative stress during apoptosis and necrosis caused by carbon tetrachloride in rat liver. *Biochim. Biophys. Acta* **1535**, 186-191 (2001).

21) Kishida, E., Nishimoto, Y., Kojo, S. Specific determination of ascorbic acid with chemical derivatization and high-performance liquid chromatography. *Anal. Chem.* **64**, 1505-1507 (1992).

22) Sun, F., Hayami, S., Ogiri, Y., Haruna, S., Tanaka, K., Yamada, Y., Tokumaru, S., Kojo, S. Evaluation of oxidative stress based on lipid hydroperoxide, vitamin C and vitamin E during apoptosis and necrosis caused by thioacetamide in rat liver. *Biochim. Biophys. Acta* **1500**, 181-185 (2000).

23) Anderson, M.E. Determination of glutathione and glutathione disulfide in biological samples. *Methods Enzymol.* **113**, 548-555 (1985).

24) Folch, J., Ascoli, I., Lees, M., Meath, J.A., LeBaron, N. Preparation of lipid extracts from brain tissues. *J. Biol. Chem*. **191**, 833-841 (1966).

25) Yamada, Y., Kajiwara, K., Yano, M., Kishida, E., Masuzawa, Y., Kojo, S. Increase of ceramides and its inhibition by catalase during chemically induced apoptosis of HL-60 cells determined by electrospray ionization tandem mass spectrometry. *Biochim. Biophys. Acta* **1532**, 115-120 (2001).

26) Lightle, S.A., Oakley, J.I., Nikolova-Karakashian, M.N. Activation of sphingolipid turnover and chronic generation of ceramide and sphingosine in liver during aging. *Mech. Ageing Dev.* **120**, 111-125 (2000).

27) Lowry, O.H., Rosebrough, N.J., Farr, A.L., Randall, J. Protein measurement with Folin phenol reagent. *J. Biol. Chem.* **19**, 265-275 (1951).

28) Ichi, I., Takashima, Y., Adachi, N., Nakahara, K., Kamikawa, C., Harada-Shiba, M., Kojo, S. Effects of dietary cholesterol on tissue ceramides and oxidation products of apolipoprotein B-100 in apoE-deficient mice. *Lipids* **42**, 893-900 (2007).

29) Park, T.S., Rosebury, W., Kindt, E.K., Kowala, M.C., Panek, R.L. Serine palmitoyl transferase inhibitor myriocin induces the regression of atherosclerotic plaques in hyperlipidemic apoE-deficient mice. *Pharmacol. Res.* **58**, 45-51 (2008).

30) Cutler, R.G., Kelly, J., Storie, K., Pedersen, W.A., Tammara, A., Hatanpaa, K., Troncoso, J.C., Mattson, M.P. Involvement of oxidative stress-induced abnormalities in ceramide and cholesterol metabolism in brain aging and Alzheimer's disease. *Proc. Natl. Acad. Sci. USA* **101**, 2070-2075 (2004).

31) Kojo, S. Vitamin C, basic metabolism and its function as an index of oxidative stress, *Curr. Med. Chem.* **11**, 1041–1064 (2004).

32) Yoshida, Y., Itoh, N., Hayakawa, M., Piga, R., Cynshi, O., Jishage, K., Niki, E. Lipid peroxidation induced by carbon tetrachloride and its inhibition by antioxidant as evaluated by an oxidative stress marker, HODE, *Toxicol. Appl. Pharmacol.* **208**, 87-97 (2005).

33) Cremesti, A.E., Goni, F.M., Kolesnick, R. Role of sphingomyelinase and ceramide in modulating rafts: do biophysical properties determine biologic outcome? *FEBS Lett.* **531**, 47-53 (2002).

34) Llacuna, L., Mari, M., Garcia-Ruiz, C., Fernandez-Checa, J.C., Morales, A. Critical role of acidic sphingomyelinase in murine hepatic ischemia-reperfusion injury. *Hepatology* **44**, 561-572 (2006).

35) Martin, S.F., Sawai, H., Villalba, J.M., Hannun, Y.A. Redox regulation of neutral sphingomyelinase-1 activity in HEK293 cells through a GSH-dependent mechanism. *Arch. Biochem. Biophys.* **459**, 295-300 (2007).

36) Ghibelli, L., Coppola, S., Fanelli, C., Rotilio, G., Civitareale, P., Scovassi, A.I., Ciriolo, M.R. Glutathione depletion causes cytochrome c release even in the absence of cell commitment to apoptosis. *FASEB J.* **13**, 2031-2036 (1999).

37) Tokumaru, S., Takeshita, S., Nakata, R., Tsukamoto, I., Kojo, S. Change in the level of vitamin C and lipid peroxidation in tissues of the inherently scorbutic rat during ascorbate deficiency. *J. Agric. Food Chem.* **44**, 2748-2753 (1996).

38) Tokumaru, S., Ogino, R., Shiromoto, A., Iguchi, H., Kojo, S. Increase of lipid hydroperoxides in tissues of vitamin E-deficient rats. *Free Radic. Res.* **26**, 169-174 (1997).

39) Nakane, M., Kubota, M., Nakagomi, T., Tamura, A., Hisaki, H., Shimasaki, H., Ueta, N. Lethal forebrain ischemia stimulates sphingomyelin hydrolysis and ceramide generation in the gerbil hippocampus. *Neurosci. Lett.* **296**, 89-92 (2000).

40) Ohtani, R., Tomimoto, H., Kondo, T., Wakita, H, Akiguchi, I., Shibasaki, H., Okazaki, T. Upregulation of ceramide and its regulating mechanism in a rat model of chronic cerebral ischemia. *Brain Res.* **1023**, 31-40 (2004).

41) Zimmermann, C., Ginis, I., Furuya, K., Klimanis, D., Ruetzler, C., Spatz, M., Hallenbeck, J.M. Lipopolysaccharide-induced ischemic tolerance is associated with increased levels of ceramide in brain and in plasma. *Brain Res.* **895**, 59-65 (2001).

42) Ikeda, K., Toda, M., Tanaka, K., Tokumaru, S., Kojo, S. Increase of lipid hydroperoxides in liver mitochondria and inhibition of cytochrome oxidase by carbon tetrachloride intoxication in rats. *Free Radic Res.* **28**, 403-410 (1998).

43) Dudnik, L.B., Tsyupko, A.N., Khrenov, A.V., Alessenko, A.V. Effect of bilirubin on lipid peroxidation, sphingomyelinase activity, and apoptosis induced by sphingosine and UV irradiation. *Biochemistry (Mosc)* **66**, 1019-1027 (2001).

Figures and legends

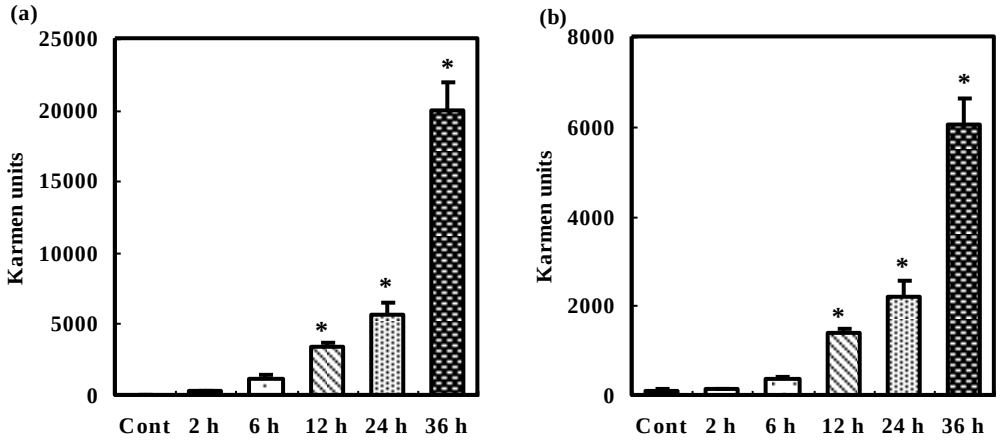

Fig. 1. CCl_4 (4 ml/kg; as a mixture of CCl_4:mineral oil=1:1) was orally administered to rats. After 1, 2, 3, 6, 12, and 24 h, plasma AST (a) and ALT (b) activities were assayed as described in the text. Control rats received mineral oil (4 ml/kg) and the enzyme activity was determined after 12 h. Values are means ± S.E. for 4-5 rats and asterisks indicate significant differences from the corresponding control group (ANOVA Fisher's protected least significant difference test (PLSD), *P<0.05).

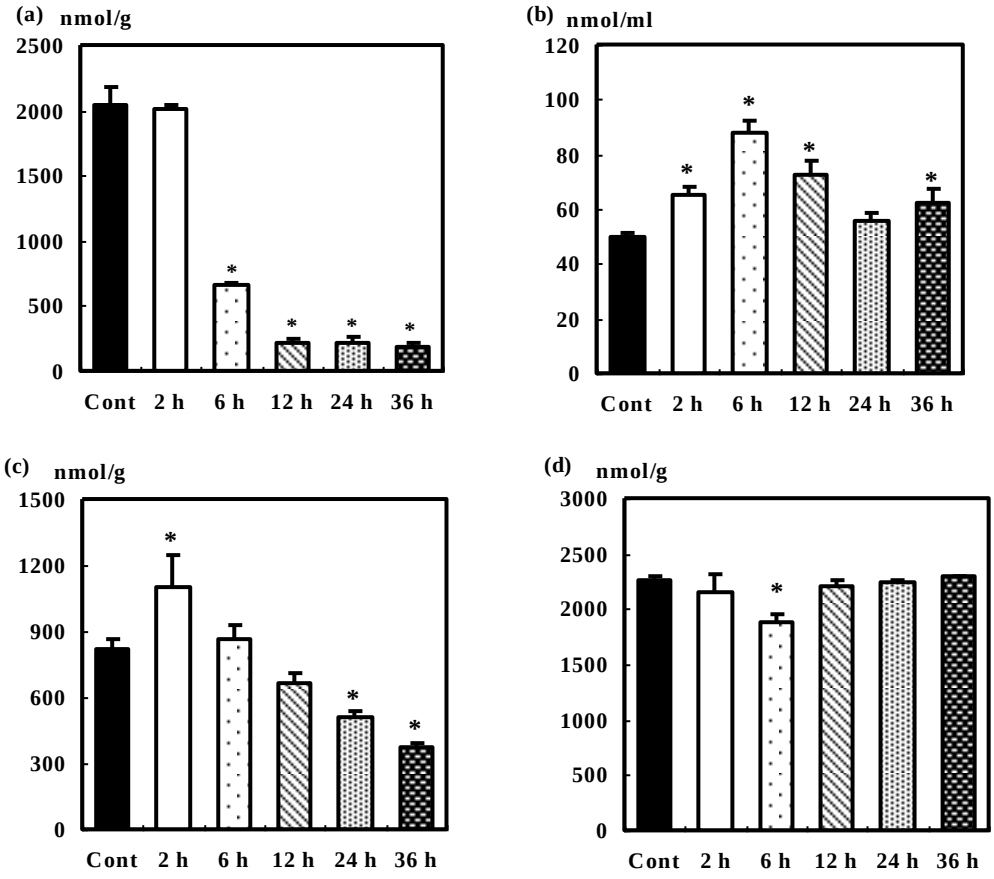

Fig. 2. The level of vitamin C in the liver(a), plasma (b), kidney (c), and brain (d) of rats after CCl_4 administration and the control group. After 2, 6, 12, 24, and 36 h, the level of vitamin C in these tissues were determined as described in the text. After 12 h of the administration of mineral oil, determinations were made for control rats. Values are means ± S.E. for 4-5 rats and asterisks indicate a significant difference from the control group (ANOVA Fisher's protected least significant difference test (PLSD), *$P<0.05$).

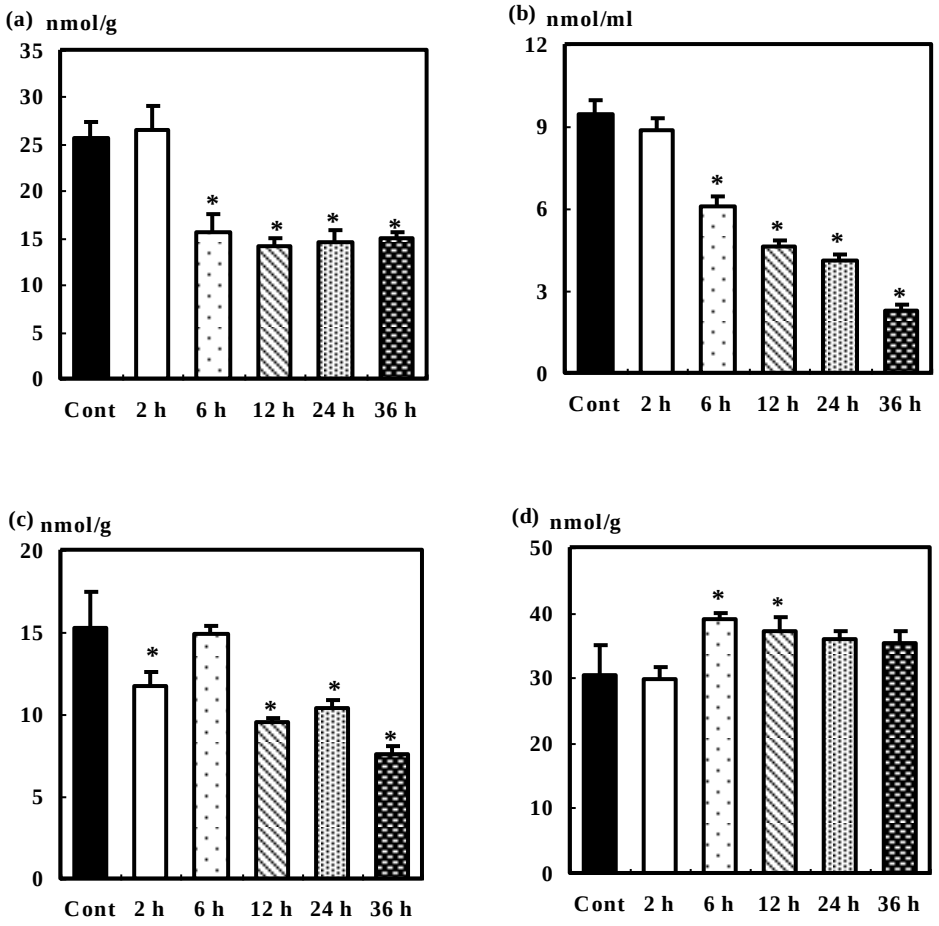

Fig. 3. The level of vitamin E in the liver (a), plasma (b), kidney (c), and brain (d) of rats after CCl_4 administration and the control group. After 2, 6, 12, 24, and 36 h, the level of vitamin E in these tissues were determined as described in the text. After 12 h of the administration of mineral oil, determinations were made for control rats. Values are means ± S.E. for 4-5 rats and asterisks indicate a significant difference from the control group (ANOVA Fisher's protected least significant difference test (PLSD), *$P<0.05$).

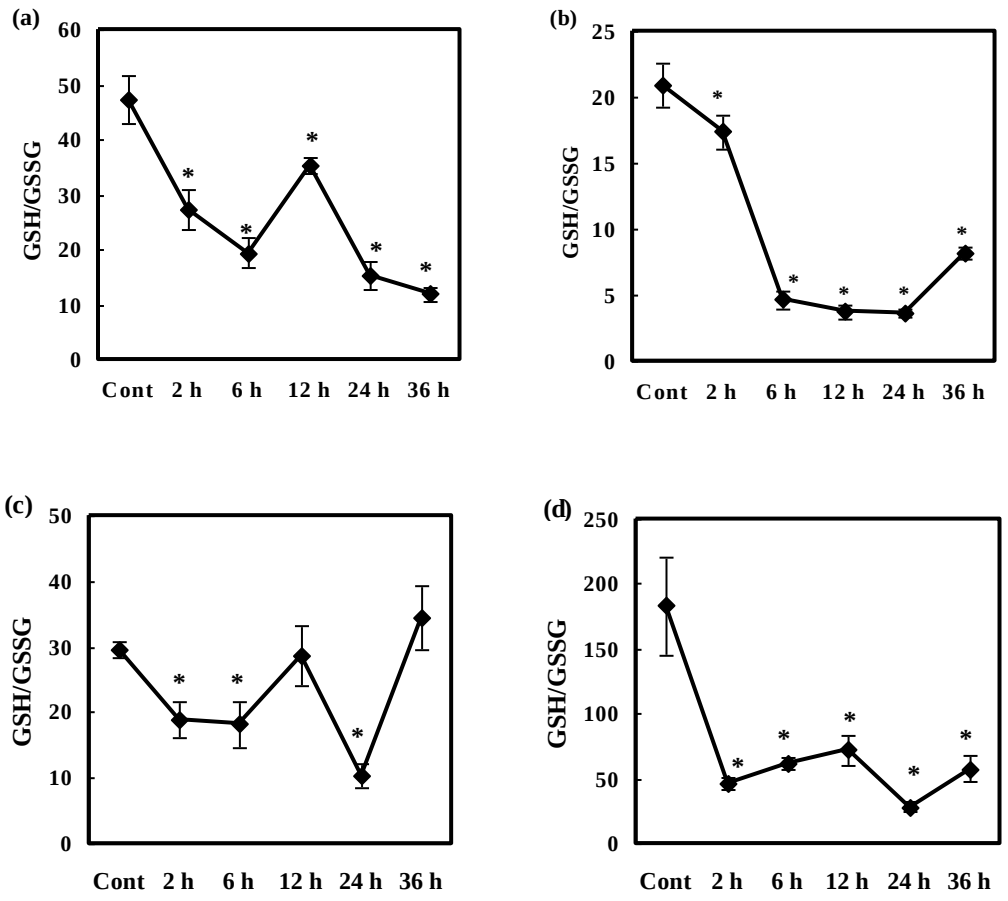

Fig. 4. The ratios of GSH/GSSG in the liver (a), plasma (b) the kidney (c), and the brain (d) of rats after CCl_4 administration and the control group. After 2, 6, 12, 24, and 36 h, the ratios of GSH/GSSG were assayed as described in the text. Control rats received mineral oil and the ratio of GSH/GSSG was determined after 12 h. Values are means ± S.E. for 4-5 rats and asterisks indicate significant differences from the corresponding control group (ANOVA Fisher's protected least significant difference test (PLSD), *P<0.05)

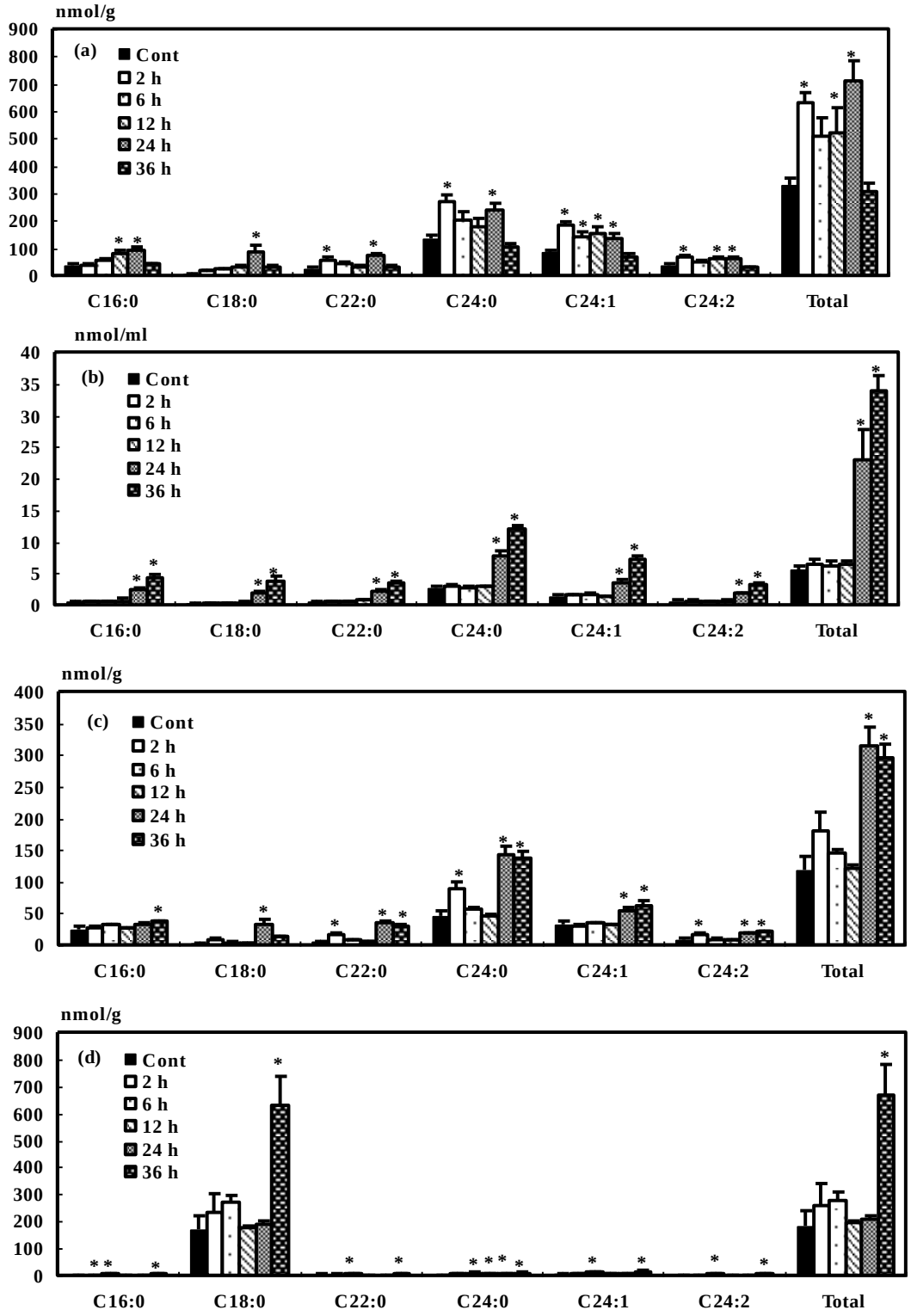
nmol/g
(a)
Cont
2 h
6 h
12 h
24 h
36 h
C16:0
C18:0
C22:0
C24:0
C24:1
C24:2
Total
nmol/ml
(b)
nmol/g
(c)
nmol/g
(d)

Fig. 5. The level of ceramides in the liver (a), plasma (b), kidney (c), and brain (d) of rats after CCl_4 administration and the control group. After 2, 6, 12, 24, and 36 h, the level of ceramides in these tissues were determined as described in the text. After 12 h of the administration of mineral oil, determinations were made for control rats. Values are means ± S.E. for 4-5 rats and asterisks indicate a significant difference from the control group (ANOVA Fisher's protected least significant difference test (PLSD), *$P<0.05$).

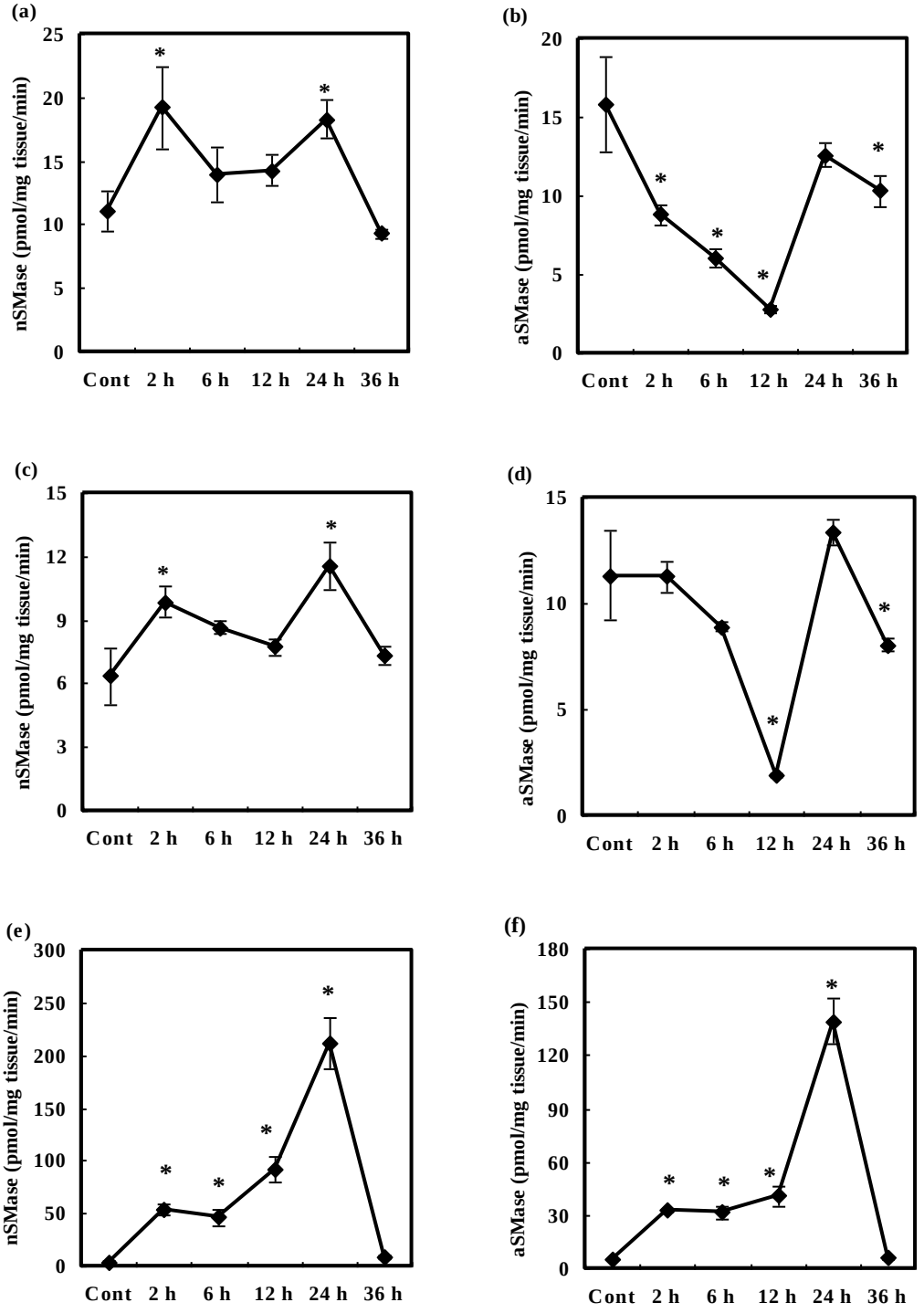
(a)
nSMase (pmol/mg tissue/min)
25
20
15
10
5
0
Cont 2 h 6 h 12 h 24 h 36 h
(b)
aSMase (pmol/mg tissue/min)
20
15
10
5
0
Cont 2 h 6 h 12 h 24 h 36 h
(c)
nSMase (pmol/mg tissue/min)
15
12
9
6
3
0
Cont 2 h 6 h 12 h 24 h 36 h
(d)
aSMase (pmol/mg tissue/min)
15
10
5
0
Cont 2 h 6 h 12 h 24 h 36 h
(e)
nSMase (pmol/mg tissue/min)
300
250
200
150
100
50
0
Cont 2 h 6 h 12 h 24 h 36 h
(f)
aSMase (pmol/mg tissue/min)
180
150
120
90
60
30
0
Cont 2 h 6 h 12 h 24 h 36 h

Fig. 6. The activities of nSMase and aSMase in the liver (a, b), the kidney (c, d), and the brain (e, f) of rats after CCl_4 administration and the control group. After 2, 6, 12, 24, and 36 h, nSMase and aSMase activities were assayed as described in the text. Control rats received mineral oil and the enzyme activity was determined after 12 h. Values are means ± S.E. for 4-5 rats and asterisks indicate significant differences from the corresponding control group (ANOVA Fisher's protected least significant difference test (PLSD), *$P<0.05$).

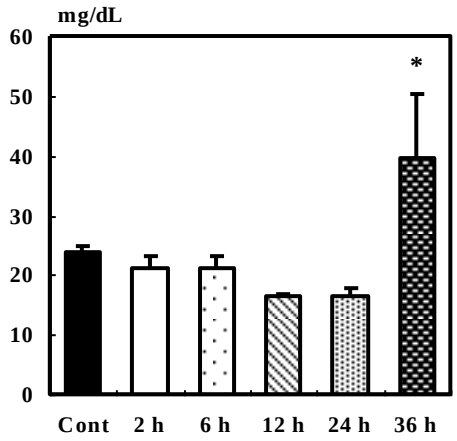

Fig. 7. The level of BUN of rats after CCl_4 administration and the control group. After 2, 6, 12, 24, and 36 h, the level of BUN in these tissues were determined as described in the text. After 12 h of the administration of mineral oil, determinations were made for control rats. Values are means ± S.E. for 4-5 rats and asterisks indicate a significant difference from the control group (ANOVA Fisher's protected least significant difference test (PLSD), *P<0.05).

Chapter 2

Effect of celecoxib, a selective cyclooxygenase-2 inhibitor on carbon tetrachloride intoxication in rats

Abstract

CCl_4 (0.5 ml/kg as CCl_4) was orally administered to rats. Twelve hours after administration of CCl_4, plasma ALT (alanine aminotransferase) and AST (aspartate aminotransferase) levels, indicators of liver necrosis, were significantly higher than those in the control group showing that active liver necrosis took place. At the same time the level of liver vitamin C was decreased significantly compared to that in the control group. Oral administration of 100 mg/kg each of celecoxib 3 and 8 h after CCl_4 treatment did not change plasma ALT and AST and liver vitamin C levels 12 h after CCl_4 treatment, but 24 h after CCl_4 treatment, significantly decreased plasma ALT and AST levels and elevated liver vitamin C level. These finding suggested that celecoxib effectively ameliorated the necrotic action and the oxidative stress induced by CCl_4 in the second phase. Although the plasma levels of all ceramide species were significantly increased 24 h after CCl_4 intoxication, treatment with celecoxib significantly reduced the total ceramide concentration in plasma. These results indicated that celecoxib significantly ameliorated the toxicity of CCl_4 in the second phase.

Abbreviations: ALT, alanine aminotransferase; AST, aspartate aminotransferase; COX-2, cyclooxygenase-2; IL, interleukin; TNF-α, tumor necrosis factor-α

1. Introduction

In the study of radical reactions in biology, one of the most studied models is drug-induced hepatitis. Carbon tetrachloride (CCl_4) is a well-known typical hepatotoxin causing centrizonal necrosis (1). CCl_4-induced hepatic injury is assumed to involve two phases. The initial phase is generation of radicals and the second phase is activation of Kupffer cells (2), which release various pro-inflammatory mediators (3). In the second phase, activities of phospholipase A_2 (4) and cyclooxygenase-2 (COX-2) (5-7) are increased. While COX-2-dependent response is assumed to be an important factor to link between oxidative stress and inflammation (5), COX-2 is also suggested to be hepatoprotective (8). In this study we evaluated the effect of celecoxib, a specific inhibitor of COX-2 in CCl_4 intoxication.

In addition, CCl_4 intoxication has been used as an animal model of fulminant hepatic failure to develop artificial liver support (9). In fulminant hepatic failure, toxic substances and cytokines released into the circulation are assumed to cause encephalopathy and renal dysfunction (10). Recently, we reported that plasma ceramides are increased in severe liver failure caused by D-galactosamine (11) or CCl_4 (12, 13). It is well established that ceramides cause apoptosis in a variety of cells (14). In this study, we evaluated the effect of celecoxib on the increase of plasma ceramide caused by CCl_4. Since extensive liver damage and the increase in plasma ceramide concentration occurred 24 h after CCl_4 administration (12, 13), we focused our study on the change in ceramides at this time.

2. Materials and methods

2.1. Animals

This study was approved by the Animal Care Committee of Nara Women's University. Eight-week-old male rats (SLC: Wistar strain) were obtained from Japan SLC Co. (Hamamatsu, Shizuoka, Japan). The animals were housed in a room at 24±2˚C, with a 12 h/12 h light-dark cycle. Animals were fed commercial laboratory chow (MF, Oriental Yeast Co., Osaka, Japan) and water ad libitum. To detect the effect of celecoxib definitely, the oral doses of CCl_4 and celecoxib were examined based on preliminary experiments changing the dose of CCl_4 at 0.5, 1, and 2 ml/kg body weight and that of celecoxib at 50 and 100 mg/kg body weight. The dose of CCl_4 was determined to be 0.5 ml/kg as CCl_4. Celecoxib (100 mg /kg body weight 3 h before or after administration of CCl_4) did not give sufficiently high protective effect, then the same dose of celecoxib was added 8 h after administration of CCl_4. Based on these preliminary experiments, after 12 h fasting, CCl_4 groups were orally administered 1 ml/kg of a mixture of CCl_4 and mineral oil (0.5 ml/kg as CCl_4) as previously described (15). Three and eight hours after administration of CCl_4, the CCl_4+celecoxib group orally received 100 mg/kg each of celecoxib twice. The CCl_4+vehicle group received vehicle (0.5% methylcellulose, 0.025% Tween 20). Analysis of plasma and the liver for the CCl_4+celecoxib group and the CCl_4+vehicle group were made 12 and 24 h after CCl_4 administration. The sham and control groups were administered 1 ml/kg of mineral oil. The sham group received celecoxib 3 and 8 h after administration of mineral oil. Analysis of plasma and the liver for the control and sham were made 24 h after mineral oil administration.

2.2. Analytical methods

Rats were anesthetized with diethyl ether and killed by collecting the blood from the inferior vena cava using a syringe containing sodium heparin as an anticoagulant. After perfusion of ice-cooled saline through the portal vein, the liver was removed. The excised tissue was homogenized in 5 volumes of phosphate buffered saline (10 mM, pH 7.4) under ice cooling. All determinations were made in duplicate experiments with 4-5 animals in each group.

The determination of total vitamin C was made according to a specific and sensitive method (16) involving chemical derivatization and HPLC as mentioned in Chapter 1.

Blood was centrifuged at 8,400 g for 5 min at 4˚C to separate plasma. The activities of plasma aspartate aminotransferase (AST: EC 2.6.1.1) and alanine aminotransferase (ALT: EC 2.6.1.2) were determined using diagnostic kits (GOT and GPT-UV Test Wako, Wako Pure Chemicals Co., Osaka) and expressed as Karmen Units. The levels of plasma ceramides were determined as described previously (13) and mentioned in Chapter 1. Briefly, ceramides were extracted with a mixture of $CHCl_3/CH_3OH$, followed by sequential TLC separations (17). The ceramide spot was extracted with a mixture of $H_2O/CH_3OH/CHCl_3$ (0.8:2:1, v/v/v) and subjected to LC-MS/MS analysis (17)。

Statistical analysis was carried out with Statcel (Excel 2000). Differences between the group means were considered significant at $P<0.05$ using Bonferroni/ Dunn procedure.

3. Results

3.1. Effect of celecoxib on the necrosis and oxidative stress caused by CCl_4

To evaluate the extent of liver necrosis, plasma ALT and AST levels were determined. Twelve hours after administration of CCl_4, plasma ALT level of the CCl_4+vehicle and the

CCl_4+celecoxib groups were 600±101 and 706±35.4 Karmen units, respectively (n=5). No significant difference was observed between these values, while these values were significantly higher than those in control group shown in Table 1. The data of the control group were determined 24 h after administration of mineral oil and the ALT and AST values were identical with normal rats without any treatment (data not shown). Plasma AST level of the CCl_4+vehicle and the CCl_4+celecoxib groups were 1278±207.5 and 1351±68.8 Karmen units, respectively (n=5). No significant difference was also observed between these values, while these values were significantly higher than those in control group shown in Table 1. At the same time the levels of liver vitamin C, a sensitive indicator of oxidative stress (18), in the CCl_4+vehicle and the CCl_4+celecoxib were decreased to 636.4±71.0 and 583.7±43.4 nmol/g liver, respectively (n=5). These values were significantly low compared to those in the control group (Table 1), the vitamin C level of which was identical with normal rats without any treatment (data not shown). The effect of celecoxib on plasma ALT and AST and liver vitamin C were not observed 12 h after CCl_4 treatment, i.e., during the initial phase of intoxication.

Plasma ALT and AST levels were further increased and the level of liver vitamin C remained at a low level 24 h after CCl_4 intoxication (Table 1). Treatment with celecoxib significantly decreased plasma ALT and AST levels compared to the CCl_4+vehicle group, showing that celecoxib effectively ameliorated the necrotic action of CCl_4 at the second phase. Consistent with this observation, the liver vitamin C level in the CCl_4+celecoxib group was higher than that in the CCl_4+vehicle group (Table 1).

No difference was observed between the control and the sham groups, showing that celecoxib did not affect these parameters (Table 1).

3.2. *Effect of celecoxib on plasma ceramide after CCl_4 treatment*

The plasma levels of all ceramide species were significantly increased 24 h after the treatment with CCl_4 (0.5 ml/kg) (Table 2). Treatment with celecoxib significantly reduced the concentrations of total ceramide and major ceramide species, which were C24:0 and C24:1 in plasma (Table 2), although all ceramide levels were significantly higher than those in the control and sham groups. The decrease in plasma ceramides corresponded with the decreased liver damage as evidenced by decreased ALT and AST by celecoxib.

4. Discussion

This study demonstrated that treatment with celecoxib significantly ameliorated liver cell necrosis based on plasma ALT and AST levels 24 h after CCl_4 intoxication. At the same time, celecoxib significantly reduced the oxidative stress in the liver during the second phase of CCl_4 intoxication based on hepatic vitamin C level, which was the most sensitive indicator of oxidative stress during hepatitis caused by chemicals such as CCl_4 (15), thioacetamide (19), or D-galatosamine (20). Although an antioxidant such as α-tocopherol inhibited liver necrosis caused by CCl_4 via direct reduction of oxidative stress (21), a different mechanism should operate in the inhibition of oxidative stress by celecoxib. Because it was unlikely that celecoxib functioned as a radical scavenger.

CCl_4 activated Kupffer cells (2), causing secretion of chemical mediators such as TNF-α (tumor necrosis factor-α), IL (interleukin)-1, and IL-6 (3, 22), and induction of COX-2 (23). Soluble TNF-α receptor prevented the increase in serum ALT 24 h after CCl_4 intoxication and thereafter, showing an important role of TNF-α in the second phase of liver cell injury (24). Upregulation of TNF-α associated with the induction of COX-2 (25, 26), products of which might have a conceivable link between inflammatory response

and oxidative injury (5). Over-expression of COX-2 in the mouse liver resulted in a marked induction of the proinflammatory cytokines such as TNF-α, IL-1β, and IL-6, inducing hepatitis, which was recovered by celecoxib administration (27). These results indicated the close link among COX-2, proinflammatory cytokines, and oxidative stress.

On the other hand, inhibition of COX-2 with NS-398, another selective COX-2 inhibitor, aggravated the liver injury caused by a higher dose of CCl_4 at 2 ml/kg (8). The reason of this difference is not easily explained but the effect of CCl_4 on COX-2 and inflammation may vary with an applied dose. Indeed, a moderately hepatotoxic dose of CCl_4 (2 ml/kg) increased hepatic COX-2, while a highly hepatotoxic dose of CCl_4 (3 ml/kg) was accompanied by minimal COX-2 activity (28).

The effect of celecoxib on the liver is still controversial. In chronic applications of CCl_4 to rodents, COX-2 inhibitor reduced (29-31), or potentiated (32) liver fibrosis. The critical role of COX-2 and the effect of celecoxib on liver inflammation remained to be explored.

Treatment with celecoxib significantly reduced the plasma level of ceramide, which caused cell death in a variety of cells (14) and we reported that it might be a cause of multi-organ failure in fulminant hepatic failure (13). Therefore it is possible that celecoxib is beneficial to prevent multi-organ failure in fulminant hepatic failure, although the role of COX-2 in ceramide metabolism is not clear at present.

In contrast to our study, celecoxib induced de novo synthesis of sphingolipids including ceramide in human cancer cell lines (33). The difference may be explained thus: ceramide is produced by neutral sphingomyelinase, via a salvage pathway in CCl_4 intoxication (13).

References

1) Zimmerman, H. J., "Hepatotoxicity, The Adverse Effects of Drugs and Other Chemicals on the Liver" Appleton-Century-Crofts, New York, 1978.

2) Edwards, M. J., Keller, B. J., Kauffman, F. C., Thurman, R. G. The involvement of Kupffer cells in carbon tetrachloride toxicity. *Toxicol. Appl. Pharmacol.* **119**, 275-279 (1993).

3) Ramadori, G., Moriconi F., Malik I., Dudas J., Physiology and pathophysiology of liver inflammation, damage and repair. *J. Physiol. Pharmacol*. **59**, Suppl. 1, 107-117 (2008).

4) Ryu, A., Itabe, H., Mutoh, M., Kudo, I., Arai, H., Inoue, K. Enhanced degradation of phospholipids by phospholipase A2 in liver of carbon tetrachloride-treated rat. *J. Health Sci.* **46**, 275-281 (2000).

5) Basu S. Carbon tetrachloride-induced lipid peroxidation: eicosanoid formation and their regulation by antioxidant nutrients. *Toxicology* **189**, 113-127 (2003).

6) Kim, S.-H., Cheon, H. J., Yun, N., Oh, S.-T., Shin, E., Shim, K. S., Lee, S.-M. Protective Effect of a Mixture of Aloe vera and Silybum marianum Against Carbon Tetrachloride–Induced Acute Hepatotoxicity and Liver Fibrosis. *J. Pharmacol. Sci.* **109**, 119-127 (2009).

7) Lee, C.-H., Park, S.-W., Kim, Y. S., Kang, S. S., Kim, J. A., Lee, S. H., Lee, S.-M. Protective Mechanism of Glycyrrhizin on Acute Liver Injury Induced by Carbon Tetrachloride in Mice. *Biol. Pharm. Bull.* **30**, 1898-1904 (2007).

8) Bhave, V. S., Donthamsetty, S., Latendresse, J. R., Mehendale, H. M. Inhibition of cyclooxygenase-2 aggravates secretory phospholipase A2-mediated progression of acute liver injury. *Toxicol. Appl. Pharmacol.* **228**, 239-246 (2008).

9) Soloviev, V., Hassan, A. N., Akatov, V., Lezhnev, E., Ghaffar, T. Y., Ghaffar, Y. A. A novel bioartificial liver containing small tissue fragments: efficiency in the treatment of acute hepatic failure induced by carbon tetrachloride in rats. *Int. J. Artif. Organs* **26**, 735-742 (2003).

10) Laleman, W., Wilmer, A., Evenepoel, P., Verslype, C., Fevery, J., Nevens, F. Review article: non-biological liver support in liver failure. *Aliment. Pharmacol. Ther.,* **23**, 351-363 (2006).

11) Yamaguchi, M., Miyashita, Y., Kumagai, Y, Kojo, S. Change in liver and plasma ceramides during D-galactosamine-induced acute hepatic injury by LC-MS/MS. *Bioorg. Med. Chem. Lett.* **14**, 4061-4064 (2004).

12) Ichi, I., Nakahara, K., Fujii, K., Iida, C., Miyashita, Y., Kojo, S. Increase of ceramide in the liver and plasma after carbon tetrachloride intoxication in the rat. *J. Nutr. Sci. Vitaminol.* **53**, 53-56 (2007).

13) Ichi, I., Kamikawa, C., Nakagawa, T., Kobayashi, K., Kataoka, R., Nagata, E., Kitamura, Y., Nakazaki, C., Matsura, T., Kojo, S. Neutral sphingomyelinase-induced ceramide accumulation by oxidative stress during carbon tetrachloride intoxication. *Toxicology* **261**, 33-40 (2009).

14) Hannun, Y. A., Obeid, L. M. The ceramide-centric universe of lipid-mediated cell regulation: stress encounters of the lipid kind. *J. Biol. Chem.* **277**, 25847-25850 (2002).

15) Sun F., Tsutsui C., Hamagawa E., Ono Y., Ogiri Y., Kojo S. Evaluation of oxidative stress during apoptosis and necrosis caused by carbon tetrachloride in rat liver. *Biochim. Biophys. Acta* **1535**, 186-191 (2001).

16) Kishid,a E., Nishimoto, Y., Kojo, S. Specific determination of ascorbic acid with chemical derivatization and high-performance liquid chromatography. *Anal. Chem.* **64**, 1505-1507 (1992).

17) Yamada, Y., Kajiwara K., Yano, M., Kishida, E., Masuzawa, Y., Kojo, S. Increase of ceramides and its inhibition by catalase during chemically induced apoptosis of HL-60 cells determined by electrospray ionization tandem mass spectrometry. *Biochim. Biophys. Acta* **1532**, 115-120 (2001).

18) Kojo, S. Vitamin C: basic metabolism and its function as an index of oxidative stress. *Curr. Med. Chem* **11**, 1041-1064 (2004).

19) Sun, F., Hayami, S., Ogiri, Y., Haruna, S., Tanaka, K., Yamada, Y., Tokumaru, S., Kojo, S. Evaluation of oxidative stress based on lipid hydroperoxide, vitamin C and vitamin E during apoptosis and necrosis caused by thioacetamide in rat liver. *Biochim. Biophys. Acta* **1500**, 181-185 (2000).

20) Sun, F., Hamagawa, E., Tsutsui, C., Sakaguchi, N., Kakuta, Y., Tokumaru, S., Kojo, S. Evaluation of oxidative stress during apoptosis and necrosis caused by d-galactosamine in rat liver. *Biochem. Pharmacol.* **65**, 101-107 (2003).

21) Iida, C., Fujii, K., Koga, E., Washino, Y., Kitamura, Y., Ichi, I., Abe, K., Matsura, T., Kojo, S. Effect of α-tocopherol on carbon tetrachloride intoxication in the rat liver. *Arch. Toxicol.* **83**, 477-483 (2009).

22) Czaja, M. J., Flanders, K. C., Biempica, l., Klein, C., Zern, M. A., Weiner, F. R., Expression of tumor necrosis factor-alpha and transforming growth factor-beta 1 in acute liver injury. *Growth Factors* **1**, 219-226 (1989).

23) Basu, S., Oxidative injury induced cyclooxygenase activation in experimental hepatotoxicity. *Biochem. Biophys. Res. Comm.* **254**, 764-767 (1999).

24) Czaja, M. J., Xu, J., Alt, E. Prevention of carbon tetrachloride-induced rat liver injury by soluble tumor necrosis factor receptor. *Gastroenterol.* **108**, 1849-1854 (1995).

25) Ferreri, N. R., An, S.-J., McGiff, J. C. Cyclooxygenase-2 expression and function in the medullary thick ascending limb. *Am. J. Physiol.* **277**, F360-F368 (1999).

26) Yu, J., Ip, E., dela Pena, A., Hou, J. Y., Sesha, J., Pera, N., Hall, P., Kirsch, R., Leclercq, I., Farrell, G. C. COX-2 induction in mice with experimental nutritional steatohepatitis: role as pro-inflammatory mediator. *Hepatology* **43**, 826-836 (2006).

27) Yu, J., Hui, A. Y., Chu, E. S., Cheng, A. S., Go, M. Y., Chan, H. L., Leung, W. K., Cheung, K. F., Ching, A. K., Chui, Y. L., Chan, K. K., Sung, J. J. Expression of a cyclo-oxygenase-2 transgene in murine liver causes hepatitis. *Gut* **56**, 991-999 (2007).

28) Bhave, V. S., Donthamsetty, S., Latendresse, J. R., Muskhelishvili, L., Mehendale, H. M. Secretory phospholipase A2 mediates progression of acute liver injury in the absence of sufficient cyclooxygenase-2. *Toxicol. Appl. Pharmacol.* **228**, 225-238 (2008).

29) Planaguma, A., Claria, J., Miquel, R., Lopez-Parra, M., Titos, E., Masferrer, J. L., Arroyo, V., Rodes, J. The selective cyclooxygenase-2 inhibitor SC-236 reduces liver fibrosis by mechanisms involving non-parenchymal cell apoptosis and PPARγ activation. *FASEB J.* **19**, 1120-1122 (2005).

30) Horrillo, R., Planaguma, A., Gonzalez-Periz, A., Ferre, N., Titos, E., Miquel, R., Lopez-Parra, M., Masferre,r J. L., Arroyo, V., Claria, J. Comparative protection against liver inflammation and fibrosis by a selective cyclooxygenase-2 inhibitor and a nonredox-type 5-lipoxygenase inhibitor. *J. Pharmacol. Exp. Ther.* **323**, 778-786 (2007).

31) Tu, C.-T., Guo, J.-S., Wang, M., Wang, J.-Y. Antifibrotic activity of rofecoxib in vivo is associated with reduced portal hypertension in rats with carbon tetrachloride-induced liver injury. *J. Gastroentorol. Hepatol.* **22**, 877-884 (2007).

32) Hui, A. Y., Leung, W. K., Chan, H. L. Y., Chan, F. K. L., Go, M. Y. Y., Chan, K. K., Tang, B. D., Chu, E. S. H., Sung, J. J. Y. Effect of celecoxib on experimental liver fibrosis in rat. *Liver Int.*, **26**, 125-136 (2006).

33) Schiffmann, S., Sandner, J., Schmidt, R., Birod, K., Wobst, I., Schmidt, H., Angioni, C., Geisslinger, G., Groesch, S. The selective COX-2 inhibitor celecoxib modulates sphingolipid synthesis. *J. Lipid Res.* **50**, 32-40 (2009).

Tables and legends

Table 1. Plasma ALT and AST and vitamin C level in the liver 24 h after CCl_4 intoxication

	CCl_4 + vehicle	CCl_4 + celecoxib	Sham (celecoxib+oil)	Control (oil only)
ALT (Karmen units)	3514.7 ± 431.1* #	1910.5 ± 243.3* #	29.5 ± 2.6	33.4 ± 1.4
AST (Karmen Units)	7675.7 ± 664.4*	3525.4 ± 412.6* #	67.5 ± 1.7	83.2 ± 5.9
Vitamin C (nmol/g Liver)	437.4 ± 68.6*	862.2 ± 49.4* #	1679.9 ± 46.6	1878.1 ± 162

CCl_4 (1 ml/kg; as a mixture of CCl_4:mineral oil=1:1) was orally administered to rats. After 24 h, plasma ALT and AST and concentration of vitamin C in the liver were determined as described in the text. After 12 h of fasting, the control rats received mineral oil alone (1 ml/kg body weight). The sham rats received celecoxib at 3 and 8 h after administration of mineral oil. Determinations for the control and sham were made 24 h after mineral oil administration. Values are means ± S.E. for 4 rats. Asterisk (*) indicates a significant difference from both the sham and control group and a signal (#) indicates a significant difference from the CCl_4+vehicle group (ANOVA Bonferroni/Dunn, $P<0.05$).

Table 2. Plasma level of ceramide (nmol/ml) 24 h after CCl_4 intoxication

	C 16:0	C 18:0	C 22:0	C 24:0	C 24:1	C 24:2	Total
Control (oil only)	0.50±0.04	0.05±0.01	0.37±0.03	3.62±0.27	2.63±0.20	0.75±0.05	7.92±0.60
CCl_4 + vehicle	1.33±0.19*	0.40±0.07*	1.13±0.10*	8.52±0.21*	6.18±0.24*	1.86±0.16*	19.4±0.82*
CCl_4 + celecoxib	0.93±0.09	0.24±0.03*	0.85±0.06*	6.68±0.36* #	4.90±0.26* #	1.55±0.12*	15.2±0.83* #
Sham (celecoxib+oil)	0.55±0.04	0.06±0.002	0.39±0.04	3.55±0.41	2.61±0.28	0.81±0.08	7.97±0.84

CCl_4 (1 ml/kg; as a mixture of CCl_4:mineral oil=1:1) was orally administered to rats. After 24 h, plasma ceramide concentrations were determined as described in the text. After 12 h of fasting, the control rats received mineral oil alone (1 ml/kg body weight). The sham rats received celecoxib at 3 and 8 h after administration of mineral oil. Determinations for the control and sham were made 24 h after mineral oil administration. Values are means ± S.E. for 4 rats. Asterisk (*) indicates a significant difference from both the sham and control group and a signal ($^{\#}$) indicates a significant difference from the CCl_4+vehicle group (ANOVA Bonferroni/Dunn, $P<0.05$).

Chapter 3

Increase in plasma ceramide levels via secretory sphingomyelinase activity in streptozotocin-induced diabetic rats

Abstract

Ceramide mediates apoptosis and is upregulated by oxidative stress. To reveal the causative agent of diabetes-induced complications, we examined the changes in ceramide metabolism during diabetes. Two and 8 weeks after intraperitoneal injection of streptozotocin (STZ: 40 mg/kg body weight) to rats, tissue ceramide levels were analyzed by liquid chromatography-electrospray tandem mass spectrometry (LC-MS/MS). Blood glucose was significantly increased 2 weeks after STZ administration. Alanine aminotransferase (ALT), aspartate aminotransferase (AST), and blood urea nitrogen (BUN) levels were also increased in the diabetic rats, suggesting that hepatic and renal damage was induced by STZ administration. Vitamin C, an indicator of oxidative stress, was significantly decreased in the plasma, liver, and kidney of rats 2 weeks after STZ administration. Although no differences in hepatic ceramide levels were observed between the control and diabetic rats, plasma and renal ceramide levels were significantly increased 8 weeks after STZ administration. In the liver and kidney, acid and neutral sphingomyelinase (SMase) activities were not increased, while secretory sphingomyelinase (sSMase) activity was increased in the plasma of diabetic rats after STZ administration. These data indicated that STZ administration induced the increase in plasma ceramide levels via the increase in sSMase activity. It was suggested that increased plasma ceramide levels were involved in the renal damage induced by STZ in diabetic rats accompanied with the enhancement of oxidative stress.

Abbreviations: aSMase, acid sphingomyelinase; ALT, alanine aminotransferase; AST, aspartate aminotransferase; BUN, blood urea nitrogen; NBD, nitrobenzofurazan; nSMase, neutral sphingomyelinase; ROS, reactive oxygen species; SM, sphingomyelin; SMase, sphingomyelinase; sSMase, secretory sphingomyelinase; STZ, streptozotocin

1. Introduction

Diabetes mellitus and its complications (such as nephropathy, atherosclerosis, retinopathy, neuropathy, and so on) are serious worldwide concerns in public health. Diabetes mellitus is a metabolic disease characterized by hyperglycaemia, and chronic hyperglycaemia and reactive oxygen species (ROS) are increased through non-enzymatic glycosylation and glucose autoxidation (1). Oxidative stress has been implicated in the development and progression of various diabetes-induced complications (2) and antioxidants decrease diabetes-induced complications by ameliorating the damage by free radicals (3).

Treatment of rats with the beta-cell toxin streptozotocin (STZ) results in a diabetic state characterized by insulin deficiency and is used as a model of type 1 diabetes (4). Generation of ROS is involved in cytotoxic actions in STZ-induced diabetic rats (5, 6), and STZ administration causes diabetes-induced complications in various tissues including the liver and kidney (7, 8). It is possible that toxic materials are increased by the enhanced oxidative stress during diabetic conditions, thereby damaging the liver and kidney.

Ceramide has been implicated in regulating cell cycle arrest, apoptosis, and cellular senescence (9), and serves as an intracellular second messenger in these processes (10). Oxidative stress such as UV light, antineoplastic drugs and radiation induces ceramide accumulation in cells (11-14). Ceramide is generated from sphingomyelin (SM) by sphingomyelinase (SMase), which is classified based on pH optimum, subcellular localization, and cation dependency (13, 15). Neutral SMase (nSMase) is localized in the plasma membrane and exhibits an optimal pH of around 7.5 and Mg^{2+} dependence. Acid SMase (aSMase), with an optimal pH of 4.8, operates in the endosomal-lysosomal compartments or plasma membrane. Lysosomal and secretory SMase (sSMase) is

derived from aSMase by differential protein trafficking of a common protein precursor (16), and sSMase is secreted by the vascular endothelium and macrophages and is the only enzyme responsible for sphingolytic activity in the plasma (17).

We previously reported that the ceramide level in the plasma, liver, and kidney was increased via nSMase activation when oxidative stress was induced by CCl_4 intoxication in rats (18, 19). In addition, other studies have demonstrated that SMase activation and the increase in ceramide levels were important participants in atherosclerosis (20, 21). Hyperglycaemia causes increased production of ROS in all tissues and plays a role in the development of complications in diabetes mellitus (22, 23). A recent study demonstrated that the ceramide level was elevated in the plasma of patients with type 2 diabetes (24). Therefore, in the STZ-induced diabetic rats, ceramide may also be a putative mediator of lipotoxicity in diabetes-induced complications. In order to find a target enzyme to prevent diabetic complications, we investigated whether ceramide metabolism was altered in damaged tissues by STZ administration, and whether ceramide accumulation is correlated with the pathogenesis of diabetes-induced complications.

2. Material and methods

2.1. Animals

This study was approved by the Animal Care Committee of Nara Women's University. Six-week-old male rats (SLC: Wistar strain) were obtained from Japan SLC Co. (Hamamatsu, Shizuoka, Japan). Diabetes was induced in overnight-fasted rats by intraperitoneal injection of STZ at a dose of 40 mg/kg body weight dissolved in citrate buffer (0.1 M, pH 4.5). Control rats received an equivalent volume of the buffer alone.

Rats were fed a commercial laboratory chow (MF, Oriental Yeast Co., Osaka, Japan) and water ad libitum for 2 and 8 weeks (wk).

2.2. Analytical methods

Two and 8 wk after STZ administration, rats were anaesthetized with diethyl ether and killed by exsanguination of the inferior vena cava using the anticoagulant sodium heparin. After perfusion of ice-cooled saline through the portal vein, the liver and kidney were removed. Plasma glucose levels, plasma aspartate aminotransferase (AST: EC 2.6.1.1) and alanine aminotransferase (ALT: EC 2.6.1.2) activities, and blood urea nitrogen (BUN) levels were measured using commercial kits (Wako Pure Chemical Industries, Osaka, Japan). Vitamin C level was determined by a specific and sensitive method (25) involving chemical derivatization and HPLC as mentioned in Chapter 1.

2.3. Measurement of ceramide species

Lipids from each tissue were extracted according to the method of Folch *et al*. (26). Quantitative measurements of ceramide species was made by LC-MS/MS (Finnigan MAT TSQ 7000) as described previously (14).

2.4. Assay of SMase activity

The enzyme assay of SMase (EC 3.1.4.12) was performed as described previously (27). The excised tissues were homogenized in 3 volumes of ice-cold phosphate-buffered saline (10 mM, pH 7.4). Protein concentrations were determined according to the method of Lowry *et al* (28). The homogenate (10-20 mg protein/ml) was dissolved in 300 μl of 0.2% Triton X-100 containing 10 mM Tris, pH 7.4 (supplemented with 25 μM genistein) for 10 min on ice. Nitrobenzofurazan (NBD) C_6-SM (Molecular Probes Inc., Eugene, OR, USA) was added to the lysates to achieve a final concentration of 20 μM

and the lysates were incubated at 4°C for 10 min. The lysates were added to a solution of 5 mM $MgCl_2$ in 10 mM Tris pH 7.4 for nSMase or 0.5 M acetate buffer pH 4.5 for the aSMase and the final volume was made 300 μl. Incubation was performed for 1 h at 37°C. For sSMase analysis, the 200-μl assay mixture consisted of 10 μl of a 1:20 dilution of the plasma in an assay buffer (0.1 mM Zn^{2+} sulphate, 1 nmol NBD C_6-SM, 0.1% Nonidet P-40, 0.1 M sodium acetate, pH 5.0), which was incubated for 1 h at 37°C. The reaction was stopped by adding 1 ml of methanol. Lipids were extracted according to the method of Bligh and Dyer. The samples (20 μl each) were directly analyzed by HPLC analysis, which was performed using a Nova Pak 4 μm C18 column (3.9 × 150 mm, Waters). Elution was performed at a flow rate of 1 ml/min with a mixture of water, acetonitrile, and phosphoric acid at a volume ratio of 35:65:0.2. The fluorescence of NBD in these compounds was determined using a fluorescence detector (Shimadzu, RF-10AXL, excitation at 466 nm and emission at 536 nm).

2.5. Statistical analysis

The data are expressed as means ± SEM. Differences between group means were considered significant at $P < 0.05$ using Fisher's protected least significant difference test.

3. Results

3.1. Changes in blood glucose levels, ALT and AST activities, and blood urea nitrogen levels

This study was approved by the Animal Care Committee of Nara Women's University. The blood glucose level in the diabetic group after STZ administration was significantly higher than that in the control group (Fig. 1a). Within the control and diabetic groups, no differences in blood glucose levels at 2 and 8 weeks (wk) were observed. To examine the effect of STZ administration on hepatic and renal injury, we analyzed alanine aminotransferase (ALT) and aspartate aminotransferase (AST) activities and blood urea nitrogen (BUN) levels. Plasma AST and ALT levels were significantly increased by STZ administration (Fig. 1b, c). These levels at 8 wk in the diabetic rats were further increased. At 2 wk, the BUN levels in the control group were almost equal to those in the diabetic group. However, these levels in the diabetic rats at 8 wk were significantly higher than those in the other groups (Fig. 1d).

3.2. Effect of STZ administration on vitamin C level in plasma, liver, and kidney

In the liver and kidney, the vitamin C level in the diabetic rats was significantly decreased 2 and 8 wk after STZ administration. In the diabetic rats, the hepatic and renal vitamin C levels at 8 wk were significantly lower than those at 2 wk (Fig. 2a, b). Although no significant differences were observed in plasma vitamin C levels between the control and diabetic groups at 2 wk, the diabetic rats exhibited a significant decrease in plasma vitamin C compared with the control group at 8 wk (Fig. 2c).

3.3. Effect of STZ administration on ceramide level in the liver, plasma, and kidney

Tissue ceramide concentration was determined using LC-MS/MS as described previously (14, 18). In the liver, the major ceramides were C24:0 and C24:1 (Fig. 3a). STZ administration did not increase hepatic ceramide levels except for that of C16:0 at 8 wk. However, in the diabetic rats, C24:1 and C24:2 levels were significantly increased at 8 wk compared with those at 2 wk.

C24:0 and C24:1 were also found to be major ceramides in the kidney (Fig. 3b). Levels of long-chain fatty acid ceramides, such as C22:0, C24:0, C24:1, and C24:2 and total ceramides in the kidney in the diabetic rats were higher than those in the control rats at 2 wk. The levels of these ceramides were further increased and a significant difference was also observed between the control and diabetic groups 8 wk after STZ administration.

The major ceramides in the plasma were C24:0 and C24:1 in the control and diabetic rats (Fig. 3c). Plasma C16:0 levels in the diabetic rats at 2 wk was increased compared to the control rats, and total plasma ceramide levels in the diabetic rats were higher than those in the control rats at 8 wk. In the diabetic groups, the total plasma ceramide levels at 8 wk were significantly higher than those at 2 wk.

3.4. Changes in the SMase activity in STZ-induced diabetic rats

SMase, which directly generates ceramide, is a key regulatory step in the ceramide-signalling cascade (9). In the liver, STZ administration did not affect nSMase activity at 2 or 8 wk (Fig. 4a). After 2 wk, hepatic aSMase activity in the diabetic group was significantly lower than that in the control group (Fig. 4b). Although renal nSMase activity in the diabetic rats was higher than that in the control rats at 2 wk (Fig. 4c), aSMase activity in the diabetic group at 2 and 8 wk was lower compared to that in the control group (Fig. 4d). Because the plasma ceramide level was increased in STZ-

induced diabetic rats, sSMase activity was measured. Plasma sSMase activity was found to be significantly increased 2 and 8 wk after STZ administration compared to that in the control group (Fig. 4e).

4. Discussion

Ceramide has been implicated in various diseases such as atherosclerosis (29, 30), which accompanies enhanced oxidative stress. STZ injection in animals produces various kinds of ROS such as superoxide, hydroxyl radical, and lipid hydroperoxides (5-8). In this study, we examined whether STZ administration caused tissue damage and affected ceramide metabolism at 2 wk (early) and 8 wk (advanced stage) during the progression of oxidative stress.

Chronic hyperglycaemia occurring in uncontrolled diabetes leads to significant long-term damage and failure of various organs. STZ-induced diabetic rats also exhibit many complications observed in human diabetic patients (31). Our results demonstrated that plasma ALT and AST levels were significantly augmented 2 wk after STZ injection and further increased after 8 wk, showing signs of liver injury as early as 2 wk after STZ administration. A major complication of diabetes is renal disease such as nephropathy (2). In this study, we also demonstrated that the plasma BUN level 8 wk after STZ administration was significantly increased in the diabetic group compared to the control group, showing that STZ injection induced diabetes-induced complications in the rat kidney. Similar increases in BUN and ceramide levels in the plasma and kidney have been reported under severe oxidative stress leading to renal failure during fulminant hepatic failure induced by CCl_4 intoxication (18).

Diabetic mellitus induces a requirement for antioxidants such as vitamin C (32) and enhancement of oxidative stress induces the development of diabetes. Our previous studies have showed that the concentrations of vitamin C, which is an outstanding hydrophilic antioxidant in tissues and is consumed primarily under conditions of enhanced oxidative stress, most sensitively reflects oxidative stress in the rat liver during chemical intoxication (33). In this study, the liver vitamin C level was significantly decreased 2 wk after STZ injection, showing that oxidative stress was enhanced in the liver. Therefore, the decrease in the level of antioxidants such as vitamin C may induce the liver injury in STZ-induced diabetic rats similar to chemically induced hepatitis (18, 34, 35) where hepatic vitamin C levels are decreased by a similar extent.

We have previously demonstrated that hepatic ceramide levels and nSMase activity were increased by CCl_4 administration, which enhances oxidative stress (18, 19). However, in this study, using STZ-induced diabetic rats, the hepatic ceramide level was almost identical to that in the control group, and hepatic nSMase and aSMase activities were not increased in diabetic rats compared with control rats. Although the hepatic ceramide level was increased in a rat model of type 2 diabetes (24, 36), our results indicated that the hepatic damage in type 1 diabetic rats was not due to ceramide accumulation. These results suggested that the enhancement of oxidative stress via hyperglycaemia led to liver dysfunction, and that the ceramide accumulation was not associated with the pathogenesis of liver injury in the STZ diabetic rats at least 8 wk after STZ administration.

Hyperglycaemia augments oxidative stress in the plasma due to the overproduction of free radicals and decreased efficiency of the antioxidant defense system. In this study, the plasma vitamin C level was decreased as early as 2 wk after STZ administration and its level remained this low level 8 wk after STZ administration. Two wk after STZ administration, only plasma C16:0 ceramide was significantly increased and this increase

may correspond to the elevation of plasma sSMase activity. However increase in other ceramides was not observed. This result suggests that catabolism system of ceramide for example in the kidney still effectively operated at the early phase of diabetes. At 8 wk the levels of all species of plasma ceramide were elevated, and the activity of plasma sSMase, the only sphingolytic enzyme in plasma, was significantly increased following STZ administration. Therefore, the increase in plasma ceramide level by STZ injection may be ascribed to the elevated sSMase activity. STZ-induced-β-cell destruction mediates the release of cytokines such as TNF-α (37), and that sSMase secretion from endothelial cells is stimulated by a variety of proinflammatory mediators such as TNF-α (38). Therefore, the increase in plasma sSMase activity might be stimulated by increased cytokine production.

Renal damage was confirmed based on BUN levels 8 wk after STZ administration when low concentration of renal vitamin C was maintained. Kashiba *et al*. (39) reported the impaired regeneration of renal vitamin C and urinary excretion of vitamin C were increased following STZ injection. Consistent with this study, which demonstrated that STZ administration induced renal deterioration along with the decrease of vitamin C, antioxidant supplements were found to inhibit the increased ROS production and effectively prevent renal dysfunction in STZ-induced diabetic rats (40). Because the cellular uptake of vitamin C is promoted by insulin and inhibited in conditions such as hyperglycaemia (41), it is reasonable that vitamin C treatment significantly decreased BUN levels in diabetic rats (42). Therefore, the enhancement of oxidative stress is an important factor leading to the development of renal damage at an advanced stage.

In the kidney, all long-chain fatty acid-bound ceramides except C16:0 and C18:0 were increased in STZ-induced diabetic rats. Therefore, accumulation of these ceramides may also contribute to the renal damage. In this study, renal nSMase and aSMase

activities did not increase in the diabetic rats at 8 wk compared with those in control rats, suggesting that increased ceramide levels at the advanced stage of diabetes was not due to the production but the transport of ceramides from the plasma. These results imply that ceramide accumulation is a cause of renal dysfunction in STZ-induced diabetic rats.

5. Conclusion

Ceramide accumulation was induced in the plasma and kidney of STZ-induced in diabetic rats, and accompanied by a decrease in vitamin C levels. Furthermore, elevated sSMase activity was suggested to be involved in the increase in plasma ceramide levels. Thus, the increase in plasma ceramide levels may play an important role in the pathogenesis of diabetes-induced complications. Therefore sSMase is a possible target to develop an inhibitor for the prevention of diabetic complications.

References

1) Oberley, L. W. Free radicals and diabetes. *Free Radic. Biol. Med.***5**, 113-124 (1988).
2) Baynes, J. Role of oxidative stress in development of complications in diabetes. *Diabetes* **40**, 405-412 (1991).
3) Peerapatdit, T., Likidlilid, A., Patchanans, N., Somkasetrin, A. Antioxidant status and lipid peroxidation end products in patients of type 1 diabetes mellitus. *J. Med. Assoc. Thai.* **89**, S141-146 (2006).
4) Le Marchand-Brustel, Y., Freychet, P. Effect of Fasting and Streptozotocin Diabetes on Insulin Binding and Action in the Isolated Mouse Soleus Muscle. *J. Clin. Invest.* **64**, 1505-1515 (1979).
5) Szkudelski, T. The mechanism of alloxan and streptozotocin action in B cells of the rat pancreas. *Physiol. Res.* **50**, 537-546 (2001).
6) Sun, F., Iwaguchi, K., Shudo, R., Nagaki, Y., Tanaka, K., Ikeda, K., Tokumaru S., Kojo, S. Change in tissue concentrations of lipid hydroperoxides, vitamin C and vitamin E in rats with streptozotocin-induced diabetes. *Clin. Sci.* **96**, 185-190 (1999).
7) Andican, G., Burcak, G. Oxidative damage to nuclear DNA in streptozotocin-diabetic rat liver. *Clin. Exp. Pharmacol. Physiol.* **32**, 663-666 (2005).
8) Kraynak, A. R., Storer, R. D., Jensen, R. D., Kloss, M. W., Soper, K. A., Clair, J. H., Deluca, J. G., Nichols, W. W., Eydelloth, R. S. Extent and Persistence of Streptozotocin-Induced DNA Damage and Cell Proliferation in Rat Kidney as Determined by in Vivo Alkaline Elution and BrdUrd Labeling Assays. *Toxicol. Appl. Pharmacol.* **135**, 279-286 (1995).
9) Hannun, Y. A., Obeid, L. M. The Ceramide-centric Universe of Lipid-mediated Cell Regulation: Stress Encounters of the Lipid Kind. *J. Biol. Chem.* **277**, 25847-25850 (2002).

10) Kolesnick, R. Ceramide: a novel second messenger. *Trends Cell. Biol.* **2**, 232-236 (1992).

11) Farrell, A. M., Uchida, Y., Nagiec, M. M., Harris, I. R., Dickson, R. C., Elias, P. M., Holleran, W. M. UVB irradiation up-regulates serine palmitoyltransferase in cultured human keratinocytes. *J. Lipid Res.* **39**, 2031-2038 (1998).

12) Santana, P., Pena, L. A., Haimovitz-Friedman, A., Martin, S., Green, D., McLoughlin, D. M., Cordon-Cardo, C., Schuchman, E. H., Fuks, Z., Kolesnick, R. Acid Sphingomyelinase–Deficient Human Lymphoblasts and Mice Are Defective in Radiation-Induced Apoptosis. *Cell* **86**, 189-199 (1996).

13) Merrill, A. H., Jones, D. D. An update of the enzymology and regulation of sphingomyelin metabolism. *Biochim. Biophys. Acta* **1044**, 1-12 (1990).

14) Yamada, Y., Kajiwara, K., Yano, M., Kishida, E., Masuzawa, Y., Kojo, S. Increase of ceramides and its inhibition by catalase during chemically induced apoptosis of HL-60 cells determined by electrospray ionization tandem mass spectrometry. *Biochim. Biophys. Acta* **1532**, 115-120 (2001).

15) Goni, F. M., Alonso, A. Sphingomyelinases: enzymology and membrane activity. *FEBS Lett.* **531**, 38-46 (2002).

16) Schissel, S. L., Keesler, G. A., Schuchman, E. H., Williams, K. J., Tabas, I. The Cellular Trafficking and Zinc Dependence of Secretory and Lysosomal Sphingomyelinase, Two Products of the Acid Sphingomyelinase Gene. *J. Biol. Chem.* **273**, 18250-18259 (1998).

17) Tabas, I. Secretory sphingomyelinase. *Chem. Phys. Lipids* **102**, 123-130 (1999).

18) Ichi, I., Kamikawa, C., Nakagawa, T., Kobayashi, K., Kataoka, R., Nagata, E., Kitamura, Y., Nakazaki, C., Matsura, T., Kojo, S., Neutral sphingomyelinase-induced ceramide accumulation by oxidative stress during carbon tetrachloride intoxication. *Toxicology* **261**, 33-40 (2009).

19) Ichi, I., Nakahara, K., Fujii, K., Iida, C., Miyashita, Y., Kojo, S., Increase of ceramide in the liver and plasma after carbon tetrachloride intoxication in the rat. *J. Nutr. Sci. Vitaminol.* **53**, 53-56 (2007).

20) Marathe, S., Kuriakose, G., Williams K. J., Tabas, I. Sphingomyelinase, an enzyme implicated in atherogenesis, is present in atherosclerotic lesions and binds to specific components of the subendothelial extracellular matrix. *Arterioscler. Thromb. Vasc. Biol.* **19**, 2648-2658 (1999).

21) Auge, N., Negre-Salvayre, A., Salvayre, R., Levade,T. Sphingomyelin metabolites in vascular cell signaling and atherogenesis. *Prog. Lipid Res.* **39**, 207-229 (2001).

22) Arun, N., Nalini, N. Efficacy of turmeric on blood sugar and polyol pathway in diabetic albino rats. *Plants Foods Hum. Nutr.* **57**, 41-52 (2002).

23) Allen, D. A., Harwood, S., Varagunam, M., Raftery M. J., Yaqoob, M. M., High glucose-induced oxidative stress causes apoptosis in proximal tubular epithelial cells and is mediated by multiple caspases. *Faseb J.*, **17**, 908-910, (2003).

24) Haus, J. M., Kashyap, S. R., Kasumov, T., Zhang, R., Kelly, K. R., DeFronzo, R. A., Kirwan, J. P., Plasma ceramides are elevated in obese subjects with type 2 diabetes and correlate with the severity of insulin resistance. *Diabetes* **58**, 337-343 (2009).

25) Kishida, E., Nishimoto, Y., Kojo, S. Specific determination of ascorbic acid with chemical derivatization and high-performance liquid chromatography. *Anal. Chem.* **64**, 1505-1507 (1992).

26) Folch, J., Ascoli, I., Lees, M., Meath J. A., LeBaron, N. Preparation of lipide extracts from brain tissue. *J. Biol. Chem.* **191**, 833-841 (1951).

27) Lightle, S. A., Oakley, J. I., Nikolova-Karakashian, M. N. Activation of sphingolipid turnover and chronic generation of ceramide and sphingosine in liver during aging. *Mech. Ageing Dev.* **120**, 111-125 (2000).

28) Lowry, O. H., Rosebrough, N. J., Farr, A. L., Randall, R. J. Protein measurement with the Folin phenol reagent. *J. Biol. Chem.* **19**, 265-275 (1951).

29) Park, T. S., Rosebury, W., Kindt, E. K., Kowala, M. C., Panek, R. L. Serine palmitoyltransferase inhibitor myriocin induces the regression of atherosclerotic plaques in hyperlipidemic ApoE-deficient mice. *Pharmacol. Res.* **58**, 45-51 (2008).

30) Ichi, I., Takashima, Y., Adachi, N., Nakahara, K., Kamikawa, C., Harada-Shiba, M., Kojo, S. Effects of dietary cholesterol on tissue ceramides and oxidation products of apolipoprotein B-100 in ApoE-deficient mice *Lipids* **42**, 893-900 (2007).

31) Rakieten, N., Rakieten M. L., Nadkarni, M. V. Studies on the diabetogenic action of streptozotocin. *Cancer Chemother. Rep.* **29**, 91-98 (1963).

32) Maxwell, S. R., Thomason, H., Sandler, D. Antioxidant status in patients with uncomplicated insulin-dependent and non-insulin-dependent diabetes mellitus. *Eur. J. Clin. Invest.*, **27**, 484-490 (1997).

33) Kojo, S. Vitamin C: basic metabolism and its function as an index of oxidative stress *Curr. Med. Chem.* **11**, 1041-1064 (2004).

34) Sun, F., Hamagawa, E., Tsutsui, C., Sakaguchi, N., Kakuta, Y., Tokumaru, S., Kojo, S. Evaluation of oxidative stress during apoptosis and necrosis caused by D-galactosamine in rat liver. *Biochem. Pharmacol*. **65**, 101-107 (2003).

35) Sun, F., Hayami, S., Ogiri, Y., Haruna, S., Tanaka, K., Yamada, Y., Tokumaru, S., Kojo, S. Evaluation of oxidative stress based on lipid hydroperoxide, vitamin C and vitamin E during apoptosis and necrosis caused by thioacetamide in rat liver. *Biochim. Biophys. Acta* **1500**, 181-185 (2000).

36) Turinsky, J., O'Sullivan D. M., Bayly, B. P. 1,2-Diacylglycerol and ceramide levels in insulin-resistant tissues of the rat in vivo. *J. Biol. Chem.* **265**, 16880-16885 (1990).

37) Herold, K. C., Vezys, V., Sun, Q., Viktora, D., Seung, E., Reinr, S., Brown, D. R. Regulation of cytokine production during development of autoimmune diabetes

induced with multiple low doses of streptozotocin *J. Immunol.*, **156**, 3521-3527 (1996).

38) Marathe, S., Schissel, S. L., Yellin, M. J., Beatini, N., Mintzer, R., Williams, K. J., Tabas, I. Human vascular endothelial cells are a rich and regulatable source of secretory sphingomyelinase. Implications for early atherogenesis and ceramide-mediated cell signaling. *J. Biol. Chem.* **273**, 4081-4088 (1998).

39) Kashiba, K., Oka, J., Ichikawa, R., Kasahara, E., Inayama, T., Kageyama, A., Kageyama, H., Osaka, T., Umegaki, K., Matsumoto, A., Ishikawa, T., Nishikimi, M., Inoue M., Inoue, S. Impaired ascorbic acid metabolism in streptozotocin-induced diabetic rats. *Free Radic. Biol. Med.* **33**, 1221-1230 (2002).

40) Manna, P., Sinha M., Sil, P. C. Prophylactic role of arjunolic acid in response to streptozotocin mediated diabetic renal injury: Activation of polyol pathway and oxidative stress responsive signaling cascades. *Chem. Biol. Interact.* **181**, 297-308, (2009).

41) Cunningham, J. J. The glucose/insulin system and vitamin C: implications in insulin-dependent diabetes mellitus. *J. Am. Coll. Nutr.* **17**, 105-108, (1998).

42) Al-Shamsi, M., Amin, A., Adeghate, E. Effect of vitamin C on liver and kidney functions in normal and diabetic rats. *Ann. N. Y. Acad. Sci.* **1084**, 371-390, (2006).

Figures and legends

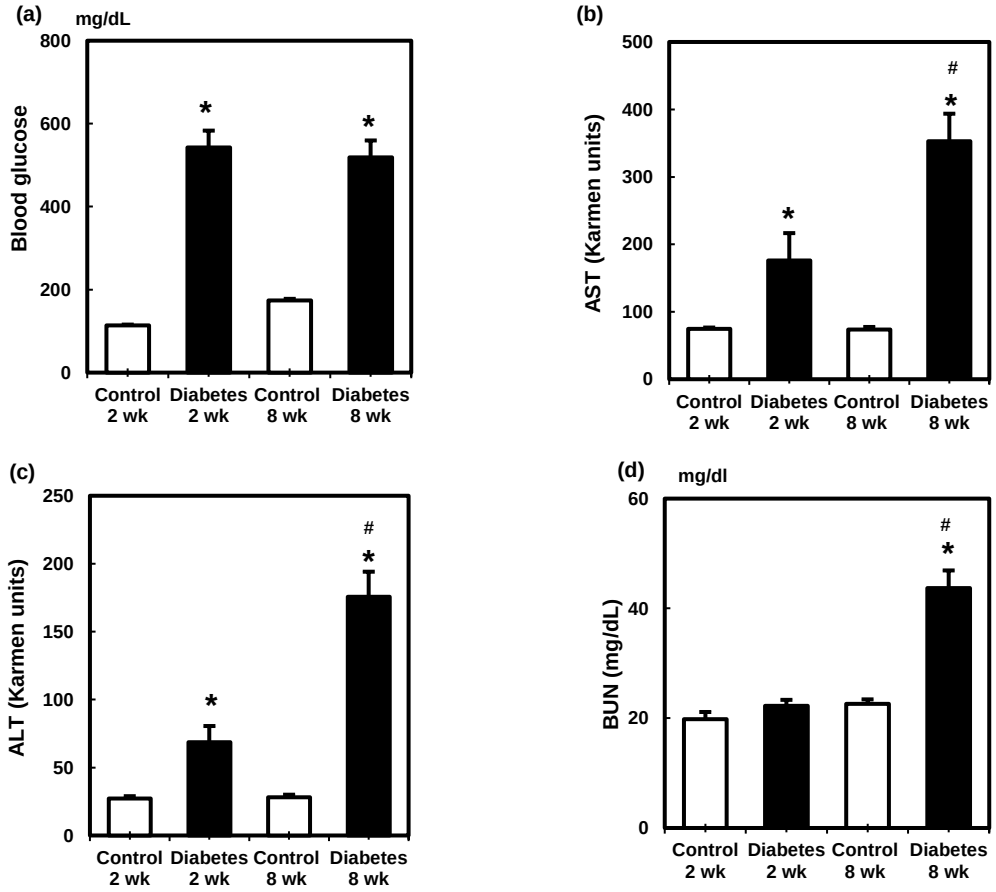

Fig. 1. Changes in blood glucose levels (a), plasma AST (b) and ALT (c) activities, and BUN levels (d) in STZ-induced diabetic rats. Values are mean ± SEM (n=5 or 6 in each group). *Significant difference between the control and diabetic groups ($p < 0.05$). #Significant difference between the 2- and 8-week groups ($p < 0.05$).

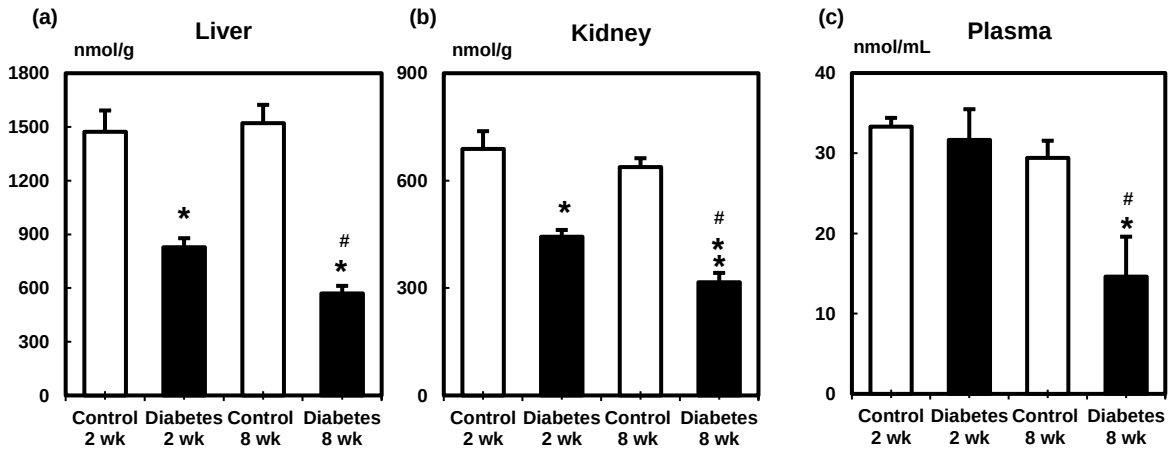

Fig. 2. Effect of STZ administration on the level of vitamin C in the liver (a), kidney (b), and plasma (c) of the control and diabetic rats. Values are mean ± SEM (n=5 or 6 in each group). *Significant difference between the control and diabetic groups ($p < 0.05$). #Significant difference between 2- and 8-week groups ($p < 0.05$).

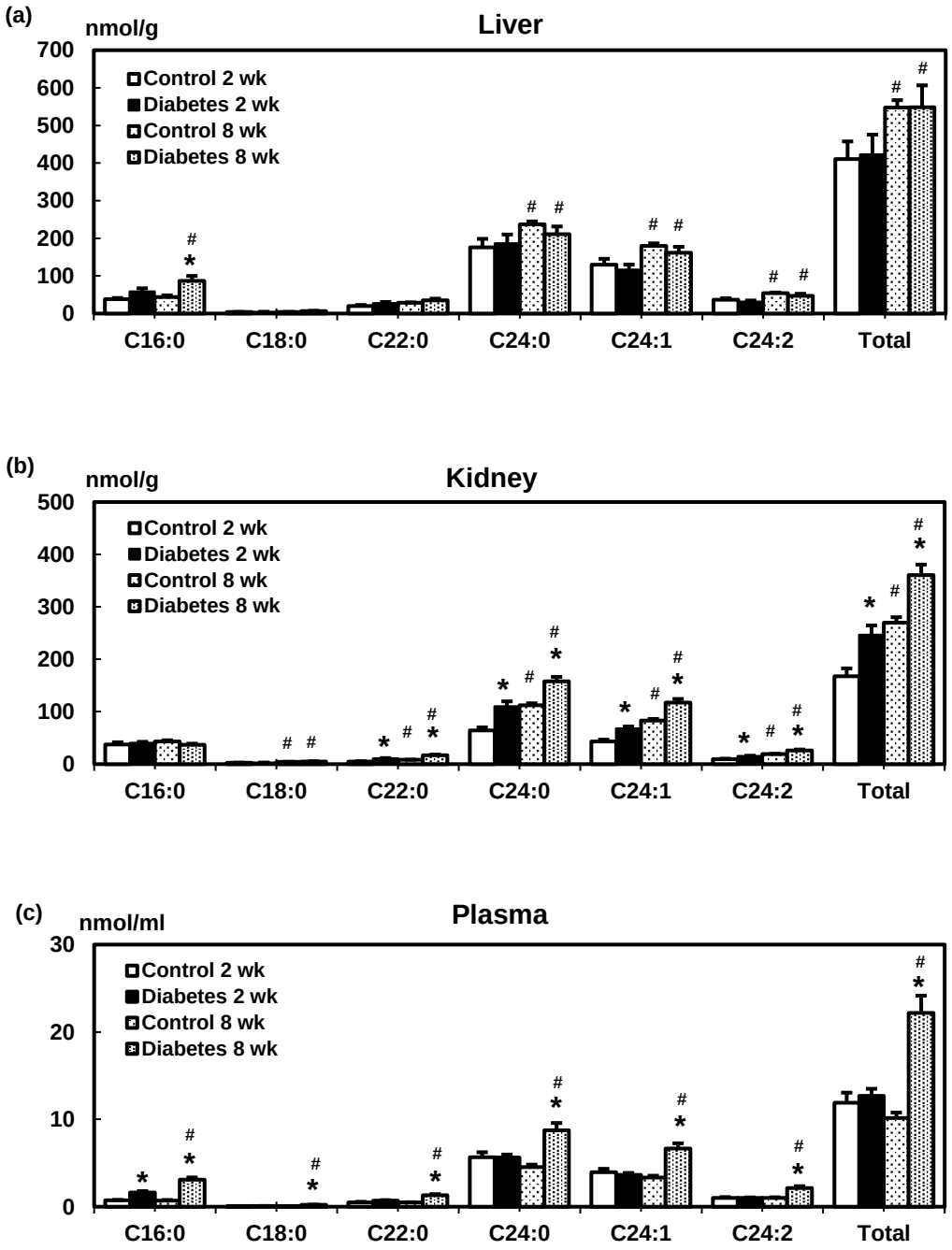

Fig. 3. Effect of STZ administration on the level of ceramide in the liver (a), kidney (b), and plasma (c) of the control and diabetic rats. Values are mean ± SEM (n=5 or 6 in each group). *Significant difference between the control and diabetic groups ($p < 0.05$). #Significant difference between 2- and 8-week groups ($p < 0.05$).

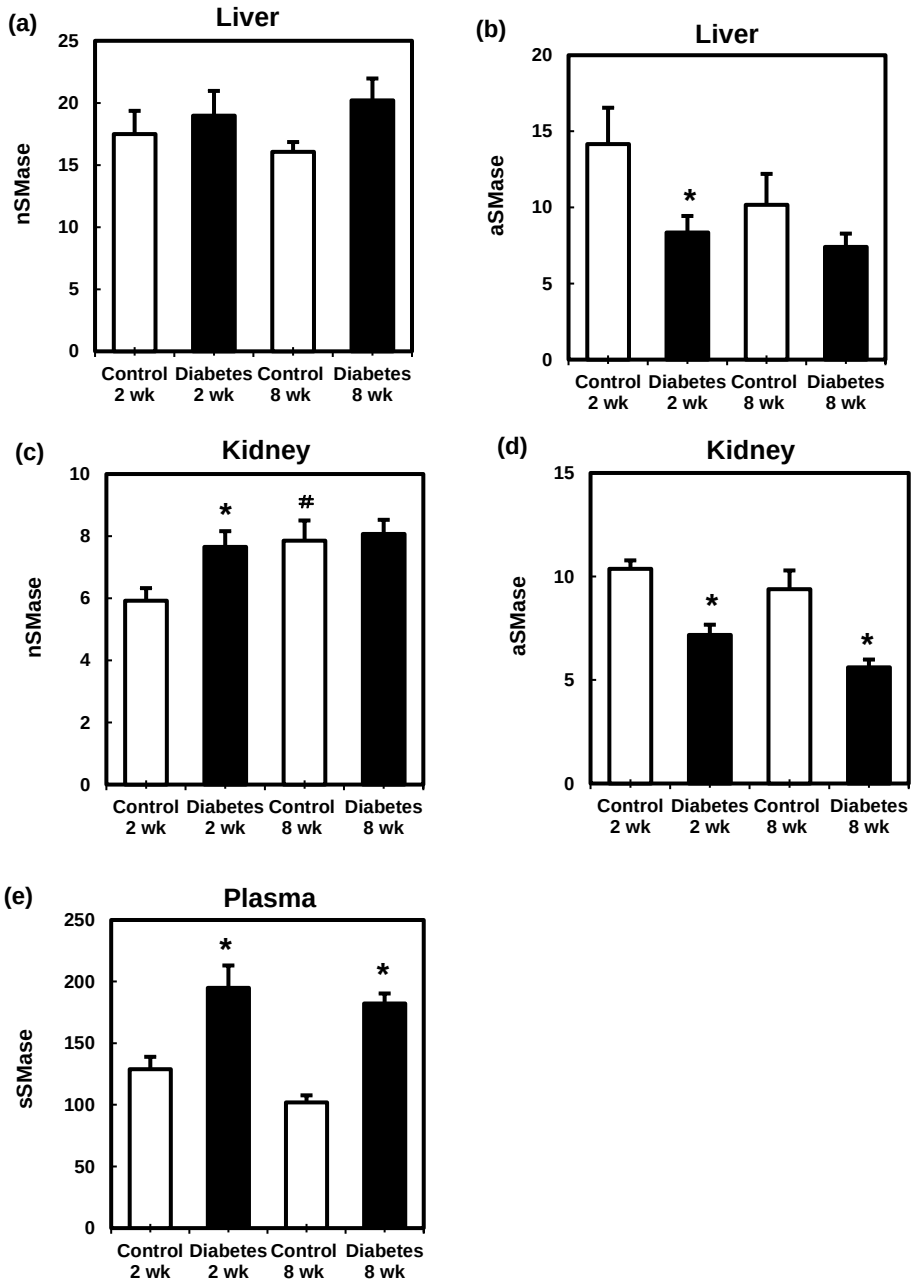

Fig. 4. Effect of STZ administration on nSMase activity in the liver (a) and kidney (c), aSMase activity of liver (b) and kidney (d), and sSMase activity (e) in the control and diabetic rats. Values are mean ± SEM (n=5 or 6 in each group). *Significant difference between the control and diabetic groups ($p < 0.05$). #Significant difference between 2- and 8-week groups ($p < 0.05$).

Chapter 4

Increase in secretory sphingomyelinase activity and specific ceramides in the aorta of apolipoprotein E knockout mice during aging

Abstract

Atherosclerosis is caused by many factors, one of which is oxidative stress. We recently demonstrated that systemic oxidative stress increased secretory sphingomyelinase activity and generated ceramides in the plasma of diabetic rats. In addition, we also showed that the total ceramide level in human plasma correlated with the level of oxidized low-density lipoprotein. To investigate the relationship between ceramide species and atherogenesis during aging, we compared age-related changes in ceramide metabolism in apolipoprotein E knock out mice (apoE$^{-/-}$) and wild type mice (WT). Although the total plasma ceramide level was higher in apoE$^{-/-}$ than that in WT at all ages, it decreased with increasing age. Secretory sphingomyelinase activity increased at 65 weeks (w) of age in both strains of mice. When apoE$^{-/-}$ developed atherosclerosis at 15 w of age, C18:0, C22:0, and C24:0 ceramide levels in the apoE$^{-/-}$ aorta significantly increased. Furthermore, at 65 w of age C16:0 and C24:1 ceramide levels were significantly higher than those in WT. These results suggested that elevation in levels of specific ceramide species due to sSMase activity contributed to atherogenesis during aging.

Abbreviations: apoE$^{-/-}$, apolipoprotein E knockout mice; aSMase, acid sphingomyelinase; CerS, ceramide synthase; LC-MS/MS, liquid chromatography-electrospray tandem mass spectrometry; NBD, nitrobenzofurazan; nSMase, neutral sphingomyelinase; oxLDL, oxidized apolipoprotein B-100; SM, sphingomyelin; SMase, sphingomyelinase; sSMase, secretory sphingomyelinase; TLC, thin-layer chromatography; WT, wild-type mice

1. Introduction

Cardiovascular disease is associated with aging. Hyperlipidemia and long-term exposure to various stimuli such as oxidative stress lead to atherosclerosis.

Despite several indications that aging causes atherosclerosis, a specific factor associated with atherosclerosis that increases or decreases with aging is yet to be entirely identified. One possible factor is elevation of bioactive lipid such as ceramide. Ceramide regulates cell cycle arrest, apoptosis, and cellular senescence (1), and serves as an intracellular second messenger in these processes (2). Oxidative stress inducers such as UV light, antineoplastic drugs, and radiation stimulate ceramide accumulation in the cell (3-6). Ceramide belongs to the sphingolipid family and comprises a saturated or unsaturated fatty acid of C16-C26 chain length bound to the amino group of sphingosine.

Ceramide is generated by de novo synthetic pathway as well as from the hydrolysis of sphingomyelin (SM) by sphingomyelinase (SMase). Sphingomyelinases are classified into five types on the basis of their optimum pH, subcellular localization, and cation dependence (5, 7). Among these enzymes acid SMase (aSMase) (optimal pH = 4.8) operates in the endosomal/lysosomal compartment or plasma membrane (8). Of note, the aSMase gene (*smpd1*) gives rise to two different enzymes lysosomal SMase *i.e.*, aSMase, and secretory SMase (sSMase) via alternative trafficking of the same protein precursor (9, 10). The vascular endothelium and macrophages secrete sSMase, which is the only enzyme responsible for sphingolytic activity in plasma (11).

Elevated ceramide levels were recently shown to correlate with atherogenetic processes such as low-density lipoprotein (LDL) aggregation (12), and form cell migration (13). In relation to atherogenesis, we previously reported that the ceramide level in human plasma was positively correlated with both total cholesterol and oxidized apolipoprotein B-100 (oxLDL) levels (14). Deevska *et al*. (15) reported that LDL-SM content and sSMase activity in LDL receptor knockout mice, which were fed an atherogenic diet, were

increased. Excessive cholesterol intake increased plasma ceramides in apolipoprotein E knockout mice (apoE$^{-/-}$), a typical animal model for atherosclerosis (16). In addition, we previously reported that the increase in plasma ceramide level was caused by increased activity of sSMase in the streptozotocin-induced diabetic rats (17), thus suggesting that the elevation of plasma ceramide was an important factor in atherogenesis. sSMase activity also increased in response to stimulation of macrophages obtained from patients with chronic heart failure (18) and type 2 diabetes (19). These studies indicated that oxidative stress resulted in ceramide accumulation by increasing sSMase activity.

To investigate the effect of aging on ceramide metabolism, we compared changes in tissue ceramides and related enzymes in apoE$^{-/-}$ with wild-type mice (WT), particularly focusing on SMase activity, which increased because of oxidative stress (17, 20, 21).

2. Materials and methods

2.1. Materials

All the solvents were purchased from Wako Pure Chemical Industries, Ltd. (Osaka, Japan). All other reagents were obtained from Nacalai Tesque Inc. (Kyoto, Japan). Authentic ceramides were purchased from Avanti Polar Lipids Inc. (Alabaster, AL, USA). Nitrobenzofurazan (NBD) C_6-SM was purchased from Molecular Probes Inc. (Eugene, OR, USA).

2.2. Animals

This study was approved by the Animal Care Committee of Nara Women's University. Female WT (SLC: C57BL/6J; 4 or 13 weeks of age) were obtained from Japan SLC Co. (Hamamatsu, Shizuoka, Japan). Female apoE$^{-/-}$ were obtained from the Jackson

Laboratory. The animals were housed in a room maintained at 24±2°C, with a 12h/12h light/dark cycle. Animals were fed commercial laboratory chow (CE-2, Oriental Yeast Co., Osaka, Japan) and water *ad libitum*. Mice were sacrificed at the age of 7, 15, and 65 weeks (w) of age.

2.3. Sampling Methods

Mice were anesthetized with Nembutal, and blood samples were collected by left ventricular puncture using a syringe containing sodium heparin as an anticoagulant. After perfusion with saline, the liver and aorta were dissected out. Plasma was separated from whole blood sample by centrifugation.

2.4. SMase Activity Assay

SMase activities were measured using NBD C_6-SM as a substrate, and the assay was principally performed based on previous studies (17, 22). For sSMase analysis, a 800 μL assay mixture consisted of 15 μL of plasma and 785 μL of an assay buffer (0.1 mM $ZnSO_4$, 1 nmol NBD C_6-SM, 0.1% Nonidet P-40, 0.1 M sodium acetate buffer at pH 5.0) was incubated for 2 h at 37 °C. The reaction was stopped by adding 1 mL of methanol. For aortic aSMase, which depended on zinc ion, the aorta was dissected and cleaned of visible fat debris. The tissue was homogenized on ice in 400 μL of phosphate buffered saline (10 mM, pH 7.4). Protein concentrations were determined according to the method of Lowry *et al* (23). Aortic aSMase activity was determined by suspending the homogenate (1-2 mg protein/mL) in 800 μL assay mixture comprising of 0.1 mM $ZnSO_4$, 1 nmol NBD C_6-SM, 0.1% NP-40/62, and 0.1 M sodium acetate (pH 5.0). The reaction was continued for 2 h at 37°C and stopped by the addition of 2 mL methanol.

NBD C_6-SM and generated NBD C_6-Ceramide were subsequently extracted according to the method of Bligh and Dyer (24). The extract was dissolved in 0.5mL methanol and

analyzed using HPLC as described below. The samples (20 μL) were directly analyzed by HPLC with a Nova Pak 4 μm C18 column (3.9 × 150 mm, Waters Corporation, Milford, MA, USA). Elution was performed at a flow rate of 1 mL/min with a mixture of water, acetonitrile, and phosphoric acid at a volume ratio of 35:65:0.2. NBD fluorescence was determined using a fluorescence detector (Shimadzu, RF-10AXL, excitation at 466 nm and emission at 536 nm).

Data were expressed as mean ± SEM, and analyzed by multiple comparison tests using Statcel software (OMS Publishing Inc., Tokyo, Japan). Using the Tukey-Kramer Procedure, the differences between group means were significant at $p < 0.05$.

2.5. Ceramide Measurement

Lipids were extracted according to the method of Folch *et al* (25). Lipids were dissolved in chloroform and subjected to chromatography on Silica gel 60 thin-layer chromatography (TLC) plates (Merck, Darmstradt, Germany). Separation was performed using silica gel 60 TLC plates (Merck, Germany) as previous studies (6, 26). In brief, the first elution was made with a mixture of n-butanol/acetic acid/water (30:10:10, v/v/v) to the one third of the plate and the second elution was made to the top of the plate with a mixture of diethyl ether/n-hexane/acetic acid (90:10:1, v/v/v). The ceramide spot was visualized under the UV by staining with primulin spay. The ceramide spot was scratched from the TLC plates and collected into a glass tube. Extraction was made with 2 mL of a mixture of $H_2O/CH_3OH/CHCl_3$ (20:30:50, v/v/v) under shaking for 30 min. After centrifugation, the lower layer was collected. To the upper phase was added 1.5 mL of $CHCl_3$, and extraction was made an additional two times. The collected $CHCl_3$ solution was evaporated and resuspended in a mixture of 10 mL (liver) or 2 mL (aorta and plasma) of $CHCl_3/CH_3OH$ (1:9, v/v). Standards and tissue ceramide extracts were stored at -20°C. The quantities of major ceramide species were measured by LC-MS/MS using a triple-

quadrupole mass spectrometer [the ACQUITY TQD mass spectrometer (Waters Corporation, Milford, MA, USA)] equipped with the ACQUITY ultra performance liquid chromatography (UPLC) system (Waters Corporation, Milford, MA, USA). The ceramide species were separated using a column, [ACQUITY UPLC BEH, 1.7 μm, 2.1 × 50 mm, C18, (Waters Corporation, Milford, MA, USA)] at 50°C. UPLC gradient elution was applied beginning with 15% of mobile phase A (water containing 0.2% formic acid and 5 mM ammonium acetate) and 85% of mobile phase B (methanol containing 0.2% formic acid and 5 mM ammonium acetate) at a flow rate of 0.4 mL/min. The initial solvent condition was maintained for 3 min, and the percentage of the B solution was gradually increased with a linear gradient to 99% for 6 min. The column was equilibrated for 4 min with 85% mobile phase B prior to next injection. The total run time per injection was 13 min. The mass spectrometry settings were as follows: ESI positive ion mode, capillary voltage, 3.0 kV; cone voltage, 20 V; source temperature, 120°C; and desolvation temperature, 350°C. The flow rates of nitrogen gas in the cone and desolvation gas were 50 and 600 L/h, respectively. Argon gas was used for collision-induced dissociation and maintenance of collision cell pressure at 10^{-4} mbar. Results were analyzed using multiple reaction monitoring (MRM). Mass spectra (m/z) for an internal standard (IS) and six major ceramides were set up at 426.4 → 264.2 for C8:0 ceramide (IS), and 538.4 → 264.2, 566.5 → 264.2, 622.5 → 264.3, 650.6 → 264.3, 648.6 → 264.3, 646.6 → 264.3 for C16:0, C18:0, C22:0, C24:0, C24:1, and C24:2 ceramides, respectively. Data acquisition was carried out by MassLynx software (version 4.1, Waters Corporation). Ceramide species were quantified using standard curves and ratios of the integrated peak areas of each ceramide species and C8:0 ceramide, which was used as an internal standard for quantification of the other ceramide species. Total ceramide content was calculated by addition of the amount of C16:0, C18:0, C22:0, C24:0, C24:1, and C24:2 ceramides. Data were expressed as an mean ± SEM.

3. Results

3.1. Change in SMase Activity

Plasma sSMase activity was significantly elevated at 65 w of age in both apoE$^{-/-}$ and WT compared with level observed at 7 w of age (Table. 1). At 7 w of age, plasma sSMase activity was lower in apoE$^{-/-}$ than that in WT.

Aortic aSMase activity in WT was significantly elevated at 15 w of age compared with the level observed at 7 w of age, the level increased further at 65 w of age (Table. 1). In contrast, aortic aSMase activity in apoE$^{-/-}$ was unchanged at 15 w of age compared with that at 7 w of age and declined significantly at 65 w of age. Liver aSMase and neutral SMase activities were unchanged during aging in both apoE$^{-/-}$ and WT (data not shown).

3.2. Changes in Tissue Ceramide Levels

The total aortic ceramide level in WT at 65 w of age increased significantly compared with that observed at 7 w of age (2.6-fold increase) (Table 2A). In the apoE$^{-/-}$ aorta, the total ceramide level was increased at 15 w and 65 w of age compared with the level observed at 7 w of age (2.0 and 1.9-fold, respectively). The total aortic ceramide concentration of apoE$^{-/-}$ was similar to that of WT at 7 w of age (Table 2A); however, it was significantly higher than that of WT (2.7-fold) at 15 w of age. Table 2A demonstrates the six major ceramide levels. In the WT aorta, C24:0, C24:1, and C24:2 ceramide levels at 65 w of age were significantly higher than those at 7 w of age (2.6, 2.9, and 6.0-fold, respectively). In contrast, C18:0, C22:0, and C24:0 ceramide levels in apoE$^{-/-}$ aorta increased at 15 w of age compared with those observed at 7 w of age (2.7, 2.4, and 2.2-fold, respectively). The C16:0, C24:1, and C24:2 ceramide levels in apoE$^{-/-}$ aorta at 65 w of age increased compared with those at 7 w of age (2.5, 2.3, and 2.6-fold, respectively) (Table 2A).

Although the levels of almost all ceramide species changed in a similar manner to the total level, some ceramides showed a different behavior (Table 2A). The levels of C16:0, C18:0, C22:0, and C24:0 ceramides in the apoE$^{-/-}$ aorta were significantly higher than those of WT (2.4, 4.1, 3.5, and 3.5-fold, respectively) at 15 w of age.

The total plasma ceramide level in apoE$^{-/-}$ was significantly higher (4.4-5.9-fold) than that observed in WT at all ages (Table 2B). Almost all plasma ceramide species in apoE$^{-/-}$ decreased with age with the exception of C24:2 ceramide (Table 2B).

The total ceramide level in WT liver increased at 15 w at age (Table 2C) and the levels of C16:0, C18:0, C22:0, and C24:1 ceramides were highest at 15 w of age (Table 2C). In apoE$^{-/-}$ liver, C22:0 ceramide level at 7 w of age was significantly higher than that observed in WT, whereas C22:0 ceramide level and total ceramide level at 65 w of age were significantly lower in apoE$^{-/-}$ than those in WT.

4. Discussion

The total plasma ceramide level in apoE$^{-/-}$ was comparable to that reported for human atherosclerotic subjects (14), and was significantly higher than the level observed in WT at all ages, indicating that the aorta of apoE$^{-/-}$ was exposed to a higher plasma ceramide level throughout aging. The difference in the plasma ceramide levels between WT and apoE$^{-/-}$ may be attributed to the LDL level in plasma because LDL is the major ceramide carrier (27, 28). The plasma ceramide level correlated with the LDL cholesterol and oxLDL levels in human samples (14). The plasma ceramide level in apoE$^{-/-}$ decreased during aging. As a similar phenomemon was reported for oxLDL by Itabe *et al.* (29): the level of oxLDL increased at 20 w of age and decreased toward the basal level at 40 w of age in apoE$^{-/-}$. These authors suggested that oxLDL appeared before the development of

atherosclerotic lesions. Moreover, Schissel *et al*. (30) indicated that ceramides, generated by sSMase from the lesional LDL, but not from the plasma LDL, participated in LDL aggregation. Combining these reports with the results from this study, in which aortic ceramide levels increased at 15 w of age in apoE$^{-/-}$, it is suggested that an elevation in ceramide level at the beginning of atherogenesis is involved in the pathogenesis of atherosclerosis.

Although the aortic ceramide level increased significantly in both WT and apoE$^{-/-}$, the distribution pattern of ceramide species in WT and apoE$^{-/-}$ was different. At 15 w of age, when atherogenesis was assumed to initiate in apoE$^{-/-}$ (31, 32), the levels of C16:0, C18:0, C22:0, and C24:0 ceramides in the aorta increased significantly, whereas only C16:0 and C24:1 ceramide levels increased at 65 w of age. The aortic levels of C18:0, C22:0, and C24:0 ceramides caused a similar change in aortic SMase activity. On the basis of these results, we suggest that the increase in C18-24 ceramide levels and the elevation of aortic aSMase activity may play a role in the initiation of atherogenesis. In addition, this is the first study showing elevation of aortic ceramide level during aging in apoE$^{-/-}$ as well as in WT.

In contrast to C24 ceramide, C16:0 ceramide, a major ceramide in the aorta of apoE$^{-/-}$ that increased at 15 and 65 w of age, seemed to have a different function. Ceramide chain length affects the physicochemical properties of lipid membranes (33); thus, C16:0 ceramide easily mixes with cholesterol in contrast to C24 ceramide (34). Mesicek *et al*. (35) reported that the overexpression of ceramide synthase (CerS) 5 lead to generation of C16:0 ceramide and an increase in apoptosis, whereas overexpression of CerS2 yielded C24 ceramide and provoked pro-survival signals. Furthermore, in the liver of CerS2 null mice, elevated ROS levels are associated with an increase in C16:0 ceramide and a decrease in mitochondria complex IV activity (36). In this regard, cellular homeostasis appears to be maintained by a balance between C16:0 and C24:0 ceramides. Although the

present study showed that C16:0 ceramide behaved in a manner similar to the very long, unsaturated C24:1 ceramide, the relationship between atherogenesis and apoptosis caused by ceramides, particularly C16:0 and C24 ceramides, requires further examination.

Liver ceramide levels were unchanged with aging in either apoE$^{-/-}$ or WT. Similar results were obtained in diabetic rats (17). These observations suggested that aging did not affect hepatic ceramide metabolism.

In conclusion, this study suggests that elevation of ceramide species such as C16:0 in the aorta as a result of sSMase activity in the plasma contributes to atherogenesis during aging.

References

1) Hannun, Y. A., Obeid, L. M., The Ceramide-centric universe of lipid-mediated cell regulation: stress encounters of the lipid kind. *J. Biol. Chem*. **277**, 25847–25850 (2002).
2) Kolesnick, R., Ceramide: a novel second messenger. *Trends Cell Biol*. **2**, 232–236 (1992).
3) Farrell, A. M., Uchida, Y., Nagiec, M. M., Harris, I. R., Dickson, R. C., Elias, P. M., Holleran, W. M., UVB irradiation up-regulates serine palmitoyltransferase in cultured human keratinocytes. *J. Lipid Res*. **39**, 2031–2038 (1998).
4) Santana, P., Pena, L. A., Haimovitz-Friedman, A., Martin, S., Green, D., McLoughlin, D. M., Cordon-Cardo, C., Schuchman, E. H., Fuks, Z., Kolesnick, R., Acid sphingomyelinase-deficient human lymphoblasts and mice are defective in radiation-induced apoptosis. *Cell* **86**, 189–199 (1996).
5) Merrill, A. H., Jones, D. D., An update of the enzymology and regulation of sphingomyelin metabolism. *Biochim. Biophys. Acta*, **1044**, 1–12 (1990).
6) Yamada, Y., Kajiwara, K., Yano, M., Kishida, E., Masuzawa, Y., Kojo, S., Increase of ceramides and its inhibition by catalase during chemically induced apoptosis of HL-60 cells determined by electrospray ionization tandem mass spectrometry. *Biochim. Biophys. Acta*. **1532**, 115–120 (2001).
7) Goni, F. M., Alonso, A., Sphingomyelinases: enzymology and membrane activity. *FEBS Lett.* **531**, 38–46 (2002).
8) Schuchman, E. H., Acid sphingomyelinase, cell membranes and human disease: lessons from Niemann-Pick disease. *FEBS Lett.* **584**, 1895–1900 (2010).
9) Schissel, S. L., Keesler, G. A., Schuchman, E. H., Williams, K. J., Tabas, I., The cellular trafficking and zinc dependence of secretory and lysosomal sphingomyelinase, two products of the acid sphingomyelinase gene. *J. Biol. Chem.* **273**, 18250–18259 (1998).

10) Jenkins, R. W., Canals, D., Idkowiak-Baldys, J., Simbari, F., Roddy, P., Perry, D. M., Kitatani, K., Luberto, C., Hannun, Y. A., Regulated secretion of acid sphingomyelinase: implications for selectivity of ceramide formation. *J. Biol. Chem.* **285**, 35706-35718 (2010).

11) Tabas, I., Secretory sphingomyelinase. *Chem. Phys. Lipids* **102**, 123–130 (1999).

12) Walters, M. J., Werenn, S. P., Effect of sphingomyelinase-mediated generation of ceramide on aggregation of low-density lipoprotein. *Langmuir* **24**, 9642-9647 (2008)

13) Morita, S. Y., Kawabe, M., Sakurai, A., Okumura, K., Vartut-Doi, A., Nakano, M., Handa, T., Ceramide in lipid particles enhances heparan sulfate proteoglycan and low density lipoprotein receptor-related protein-mediated uptake by macrophages. *J. Biol. Chem.* **279**, 24355-24361 (2004).

14) Ichi, I., Nakahara, K., Miyashita, Y., Hidaka, A., Kutsukake, S., Inoue, K., Maruyama, T., Miwa, Y., Harada-Shiba, M., Tsushima, M., Kojo, S., Association of ceramides in human plasma with risk factors of atherosclerosis. *Lipids* **41**, 859–863 (2006).

15) Deevska, G. M., Sunkara, M., Morris, A. J., Nikolova-Karakashian, M. N., Characterization of secretory sphingomyelinase activity, lipoprotein sphingolipid content and LDL aggregation in $ldlr^{-/-}$ mice fed on a high-fat diet. *Bio. Rep.* **32**, 479-490 (2012).

16) Ichi, I., Takashima, Y., Adachi, N., Nakahara, K., Kamikawa, C., Harada-Shiba, M., Kojo, S., Effects of dietary cholesterol on tissue ceramides and oxidation products of apolipoprotein B-100 in ApoE-deficient mice. *Lipids* **42**, 893–900 (2007).

17) Kobayashi, K., Ichi, I., Nakagawa, T., Kamikawa, C., Kitamura, Y., Koga, E., Washino, Y., Hoshinaga, Y., Kojo, S., Increase in plasma ceramide levels via secretory sphingomyelinase activity in streptozotocin-induced diabetic rats. *Med. Chem. Commun.* **2**, 536-541 (2011).

18) Doehner, W., Bunck, A. C., Rauchhaus, M., von Haehling, S., Brunkhorst, F. M., Cicoira, M., Tschope, C., Ponikowski, P., Claus, R. A., Anker, S. D., Secretory sphingomyelinase is upregulated in chronic heart failure: a second messenger system of immune activation relates to body composition, muscular functional capacity, and peripheral blood flow. *Eur. Heart J.* **28**, 821–828 (2007)

19) Gorska, M., Baranczuk, E., Dobrzyn, A., Secretory Zn^{2+}-dependent sphingomyelinase activity in the serum of patients with type 2 diabetes is elevated. *Horm. Metab. Res.* **35**, 506–507 (2003).

20) Filosto, S., Fry, W., Knowlton, A. A., Goldkorn, T., Neutral sphingomyelinase 2 (nSMase2) is a phosphoprotein regulated by calcineurin (PP2B). *J. Biol. Chem.* **285**, 10213-10222 (2010).

21) Ichi, I., Kamikawa, C., Nakagawa, T., Kobayashi, K., Kataoka, R., Nagata, E., Kitamura, Y., Nakazaki, C., Matsura, T., Kojo, S., Neutral sphingomyelinase-induced ceramide accumulation by oxidative stress during carbon tetrachloride intoxication. *Toxicology* **261**, 33-40 (2009).

22) Lightle, S. A., Oakley, J. I., Nikolova-Karakashian, M. N., Activation of sphingolipid turnover and chronic generation of ceramide and sphingosine in liver during aging. *Mech. Ageing. Dev.* **120**, 111-125 (2000).

23) Lowry, O. H., Rosebrough, N. J., Farr, A. L., Randall, J., Protein measurement with the Folin phenol reagent. *J. Biol. Chem.* **19**, 265-275 (1951).

24) Bligh, E. G., Dyer, W. J., A rapid method of total lipid extraction and purification. *Can. J. Biochiem. Physiol.* **37**, 911-917 (1959).

25) Folch, J., Ascoli, I., Lees, M., Meath, J. A., LeBaron, N., Preparation of lipide extracts from brain tissue. *J. Biol. Chem.* **191**, 833-841 (1966).

26) Yano, M., Kishida, E., Murayuki, Y., Masuzaka, Y., Quantitative analysis of ceramide molecular species bu high performance liquid chromatography. *J. Lipid Res.* **39**, 2091-2098 (1998).

27) Wiesner, P., Leidl, K., Boettcher, A., Schmitz, G., Liebisch, G., Lipid profiling of FPLC-separated lipoprotein fractions by electrospray ionization tandem mass spectrometry. *J. Lipid. Res*. **50**, 574-585 (2009).

28) Hammad, S. M., Pierce, J. S., Soodavar, F., Smith, K. J., Al Gadban, M. M., Rembiesa, B., Klein, R. L., Hannun, Y. A., Bielawski, J., Bielawska, A., Blood sphingolipidomics in healthy humans: impact of sample collection methodology. *J. Lipid. Res*. **51**, 3074-3087 (2010).

29) Kato, R., Mori, C., Kitasato, K., Arata, S., Obama, T., Mori, M., Takahashi, K. Aiuchi, T., Takano, T., Itabe, H., Transient increase in plasma oxidized LDL during the progression of atherosclerosis in apolipoprotein E knockout mice. *Arterioscler. Thromb. Vasc. Biol.* **29**, 33-39 (2009).

30) Schissel, S. L., Tweedie-Hardman, J., Rapp, J. H., Graham, G., Williams, K. J., Tabas, I., Rabbit aorta and human atherosclerotic lesions hydrolyze the sphingomyelin of retained low-density lipoprotein. Proposed role for arterial-wall sphingomyelinase in subendothelial retention and aggregation of atherogenic lipoproteins. *J. Clin. Invest.* **98,** 1455-1464 (1996).

31) Plump, A.S., Smith, J. D., Hayek, T., Aalto-Setala, K., Walsh, A., Verstuyft, J. G., Rubin, E. M., Breslow, J. L., Severe hypercholesterolemia and atherosclerosis in apolipoprotein E-deficient mice created by homologous recombination in ES cells. *Cell* **71**, 343-353 (1992).

32) Zhang, S. H., Reddick, R. L., Piedrahita, J. A., Maeda, N., Spontaneous hypercholesterolemia and arterial lesions in mice lacking apolipoprotein E. *Science* **258**, 468-471 (1992).

33) Grosch, S., Schiffmenn, S., Geisslinger, G., Chain length-specific properties of ceramides. *Prog. Lipid Res.* **51**, 50-62 (2012).

34) ten Grotenhuis, E., Demel, R. A., Ponec, M., Boer, D. R., van Miltenburg, J. C., Bouwstra, J. A., Phase behavior of stratum corneum lipids in mixed Langmuir-Blodgett monolayers. *Biophys. J.* **71**, 1389-1399 (1996).

35) Mesicek, J., Lee, H., Feldman, T., Jiang, X., Skobeleva, A., Berdyshev, E. V., Haimovitz-Fridman, A., Fuks, Z., Kolesnick, R., Ceramide synthases 2, 5, and 6 confer distinct roles in radiation-induced apoptosis in HeLa cells *Cell. Signal.* **22**, 1300-1307 (2010).

36) Zigdon, H., Kogot-Levin, A., Park, J. W., Goldschmidt, R., Kelly, S., Merrill, A. H., Scherz, A. Jr, Pewzner-Jung, Y., Saada, A., Futerman, A. H., Ablation of Ceramide Synthase 2 Causes Chronic Oxidative Stress due to Disruption of the Mitochondrial Respiratory Chain. *J. Biol. Chem.* **288**, 4947-4956 (2013).

Tables and legends

Table 1. Changes in sSMase activity in plasma (pmol/mL/hour) and aortic aSMase activity (pmol/mg protein/min) of wild-type and apoE$^{-/-}$ mice

	7 w WT	15 w WT	65 w WT	7 w apoE$^{-/-}$	15 w apoE$^{-/-}$	65 w apoE$^{-/-}$
sSMase	1599.6 ± 171.6^{ab}	1666.7 ± 83.6^{ab}	2688.7 ± 175.1^{c}	657.3 ± 86.9^{d}	1187.2± 121.7^{ad}	1990.2 ± 207.1^{b}
aortic aSMase	79.2 ± 9.4^{a}	130.8 ± 12.5^{bc}	271.5 ± 14.3^{d}	113.8 ± 13.5^{ab}	167.1 ± 8.3^{c}	66.4 ± 5.0^{a}

Values are presented as mean ± SEM for 4 or 5 animals in each group. Different superscript letters indicate significant differences at $p < 0.05$ (Tukey-Kramer post hoc test).

Table 2. Levels of ceramides in the aorta (A), plasma (B), and liver (C) of wild-type and apoE$^{-/-}$ mice

(A) Aorta ceramide levels (nmol/mg protein)

Aorta	7 w WT	15 w WT	65 w WT	7 w apoE$^{-/-}$	15 w apoE$^{-/-}$	65 w apoE$^{-/-}$
C16:0	1.08 ± 0.18^{a}	1.53 ± 0.15^{a}	2.48 ± 0.32^{ac}	2.03 ± 0.46^{ac}	3.70 ± 0.52^{bc}	4.98 ± 0.53^{b}
C18:0	0.38 ± 0.04^{a}	0.38 ± 0.03^{a}	0.74 ± 0.07^{a}	0.58 ± 0.14^{a}	1.53 ± 0.14^{b}	0.47 ± 0.04^{a}
C22:0	0.45 ± 0.06^{ab}	0.44 ± 0.05^{b}	0.95 ± 0.13^{a}	0.66 ± 0.14^{ab}	1.56 ± 0.18^{bc}	0.94 ± 0.08 ^{a}
C24:0	1.36 ± 0.21^{ac}	1.33 ± 0.10^{a}	3.52 ± 0.46^{bd}	2.10 ± 0.39^{ad}	4.69 ± 0.55^{b}	3.03 ± 0.29^{cd}
C24:1	0.58 ± 0.12^{a}	1.03 ± 0.12^{ab}	1.70 ± 0.15^{b}	1.22 ± 0.24^{ab}	1.79 ± 0.25^{b}	2.82 ± 0.31^{c}
C24:2	0.17 ± 0.03^{a}	0.39 ± 0.06^{a}	1.02 ± 0.13^{b}	0.45 ± 0.08^{a}	0.50 ± 0.10^{a}	1.15 ± 0.13^{b}
Total	4.02 ± 0.58^{a}	5.09 ± 0.48^{a}	10.40 ± 1.17^{bc}	7.03 ± 1.42^{ab}	13.77 ± 1.73^{cd}	13.39 ± 1.23^{cd}

Values are presented as mean ± SEM for 4 or 5 animals in each group. Total values are sum of six ceramide species. Different superscript letters indicate significant differences at $p < 0.05$ (Tukey-Kramer post hoc test).

(B) Plasma ceramide levels (nmol/mL)

Plasma	7 w WT	15 w WT	65 w WT	7 w apoE$^{-/-}$	15 w apoE$^{-/-}$	65 w apoE$^{-/-}$
C16:0	0.53 ± 0.04^{a}	0.50 ± 0.09^{a}	0.47 ± 0.05^{a}	5.63 ± 0.42^{b}	4.33 ± 0.26^{c}	3.34 ± 0.39^{c}
C18:0	0.14 ± 0.03^{a}	0.20 ± 0.03^{a}	0.16 ± 0.02^{a}	0.82 ± 0.10^{b}	0.85 ± 0.05^{b}	0.47 ± 0.07^{c}
C22:0	1.06 ± 0.12^{a}	0.98 ± 0.15^{a}	0.79 ± 0.06^{a}	8.50 ± 1.12^{b}	6.61 ± 0.44^{b}	3.77 ± 0.26^{c}
C24:0	4.86 ± 0.48^{a}	3.89 ± 0.68^{a}	2.96 ± 0.38^{a}	25.76 ± 3.44^{b}	16.81 ± 0.82^{c}	12.08 ± 0.64^{c}
C24:1	2.82 ± 0.46^{a}	3.20 ± 0.55^{a}	2.33 ± 0.24^{a}	14.84 ± 1.90^{b}	12.93 ± 0.58^{bc}	9.43 ± 0.59^{c}
C24:2	0.20 ± 0.05^{a}	0.22 ± 0.04^{a}	0.21 ± 0.02^{a}	1.05 ± 0.05^{a}	1.01 ± 0.07^{ab}	1.37 ± 0.44^{b}
Total	9.62 ± 1.14^{a}	8.99 ± 1.48^{a}	6.92 ± 0.72^{a}	56.60 ± 6.54^{b}	42.53 ± 1.81^{c}	30.46 ± 1.74^{c}

Values are presented as mean ± SEM for 4 or 5 animals in each group. Total values are sum of six ceramide species. Different superscript letters indicate significant differences at $p < 0.05$ (Tukey-Kramer post hoc test).

(C) Liver ceramide levels (nmol/g tissue)

Liver	7 w WT	15 w WT	65 w WT	7 w apoE$^{-/-}$	15 w apoE$^{-/-}$	65 w apoE$^{-/-}$
C16:0	47.03 ± 4.12^{a}	72.29 ± 5.66^{b}	60.20 ± 5.22^{ab}	52.47 ± 4.87^{ab}	56.07 ± 2.02^{ab}	55.09 ± 3.71^{ab}
C18:0	8.03 ± 0.85^{a}	16.48 ± 2.15^{b}	13.10 ± 0.29^{ab}	10.19 ± 1.54^{a}	12.02 ± 1.35^{ab}	8.07 ± 0.98^{a}
C22:0	44.14 ± 1.96^{a}	65.93 ± 3.69^{b}	67.06 ± 3.28^{b}	66.16 ± 7.25^{b}	65.48 ± 4.23^{b}	38.75 ± 2.36^{a}
C24:0	128.87 ± 5.43^{ab}	169.37 ± 10.78^{a}	156.39 ± 16.47^{ab}	178.40 ± 19.69^{a}	153.40 ± 6.30^{ab}	105.94 ± 4.78^{b}
C24:1	201.38 ± 11.52^{a}	283.16 ± 13.98^{b}	239.44 ± 12.91^{ab}	200.30 ± 8.90^{a}	247.01 ± 11.85 ^{ab}	208.74 ± 10.94^{a}
C24:2	16.67 ± 0.97	22.33 ± 1.70	20.40 ± 3.24	21.30 ± 1.83	24.23 ± 1.11	24.11 ± 3.87
Total	446.12 ± 22.95^{ac}	629.55 ± 29.14^{b}	556.58 ± 26.09^{ab}	528.82 ± 35.68^{abc}	558.22 ± 15.30^{ab}	440.69 ± 19.06^{c}

Values are presented as mean ± SEM for 4 or 5 animals in each group. Total values are sum of six ceramide species. Different superscript letters indicate significant differences at $p < 0.05$ (Tukey-Kramer post hoc test).

Chapter 5

Strong inhibition of secretory sphingomyelinase by catechins, particularly by (-)-epicatechin 3-*O*-gallate and (-)-3′-*O*-methylepigallocatechin 3-*O*-gallate

Abstract

Sphingomyelinases (SMases) are key enzymes involved in many diseases, which are caused by oxidative stress such as atherosclerosis, diabetes mellitus, nonalcoholic fatty liver disease, and Alzheimer's disease. SMases hydrolyze sphingomyelin to generate ceramide, a well-known pro-apoptotic lipid. SMases are classified into five types based on pH optimum, subcellular localization, and cation dependence. Previously, we demonstrated that elevation of secretory sphingomyelinase (sSMase) activity increased the plasma ceramide concentration under oxidative stress induced by diabetes and atherosclerosis in murine models. These results suggest that sSMase inhibitors can prevent the progress of these diseases. The present study demonstrated that sSMase activity was activated by oxidation and inhibited by reduction. Furthermore, we examined whether catechins inhibited the sSMase activity in a physiological plasma concentration. Among catechins, (-)-epicatechin 3-*O*-gallate (ECg) exhibited strong inhibitory effect on sSMase (IC_{50}=25.7 μM). This effect was attenuated by methylation at the 3″- or 4″-position. On the other hand, (-)-epigallocatechin 3-*O*-gallate (EGCg) and (-)-catechin 3-*O*-gallate (Cg) exhibited weaker inhibitory activity than ECg, and (-)-epicatechin and (-)-epigallocatechin did not affect sSMase activity. Additionally, one synthetic catechin, (-)-3′-*O*-methylepigallocatechin 3-*O*-gallate (EGCg-3′-O-Me), showed the strongest inhibitory effect (IC_{50}=1.7 μM) on sSMase. This phenomenon was not observed for (-)-4′-*O*-methylepigallocatechin 3-*O*-gallate. These results suggest that the reduction potential, the presence of the galloyl residue at the C-3 position, and the steric requirement to interact with sSMase protein are important for effective inhibition of sSMase.

Abbreviations: aSMase, acid sphingomyelinase; Cg, (-)-catechin 3-*O*-gallate; EC, (-)-epicatechin; ECg, (-)-epicatechin 3-*O*-gallate; ECg-3′-*O*-Me, (-)-3′-O-methylepicatechin 3-*O*-gallate; ECg-4′-O-Me, (-)-4′-*O*-methylepicatechin 3-*O*-gallate; ECg-3″-O-Me, (-)-epicatechin 3-*O*-(3″-*O*-methyl)gallate; ECg-4″-O-Me, (-)-epicatechin 3-*O*-(4″-*O*-methyl)gallate; EGC, (-)-epigallocatechin; EGC-3′-O-Me, (-)-epigallocatechin 3′-*O*-methylether; EGCg, (-)-epigallocatechin 3-*O*-gallate; EGCg-3′-O-Me, (-)-3′-*O*-methylepigallocatechin 3-*O*-gallate; EGCg-4′-O-Me, (-)-4′-*O*-methylepigallocatechin 3-*O*-gallate; GA, Gallic acid; GSH, reduced glutathione; MG, methyl gallate; NBD, nitrobenzofurazan; nSMase, neutral sphingomyelinase; SM, sphingomyelin; SMase, sphingomyelinase; sSMase, secretory sphingomyelinase; PGG, penta-*O*-galloyl-β-D-glucose

1. Introduction

Sphingomyelinases (SMases) are involved in the pathogenesis of many diseases such as atherosclerosis, diabetes mellitus, coronary heart disease, nonalcoholic fatty liver disease, Alzheimer's disease, and tumor metastasis (1-6). SMases hydrolyze sphingomyelin to generate ceramide, which is a well-known pro-apoptotic lipid (7) and serves as an intracellular second messenger (8). Oxidative stress caused, for example, by UV light, antineoplastic drugs, and radiation induces SMase activation and ceramide accumulation in the cell (9-11).

SMases are classified into five types based on pH optimum, subcellular localization, and cation dependence (12). Among them, acid SMase (aSMase) with an optimal pH of 4.8 functions in the endosomal-lysosomal compartments or plasma membrane (13). The gene coding aSMase (*smpd1*) produces two different enzymes, —lysosomal SMase and secretory SMase (sSMase)— through alternative trafficking of the same protein precursor (14, 15). sSMase is secreted by the vascular endothelium and macrophages, and is the only enzyme responsible for sphingolytic activity in the plasma (16).

Previously, we demonstrated that increased sSMase activity resulted in an increase of the ceramide in the plasma of diabetic and atherosclerotic murine models, which had been exposed to systemic oxidative stress (17, 18). These results suggest that inhibition of sSMase activity is effective in the prevention of these diseases.

Although many studies were conducted on the aSMase functional inhibitor, FIASMA (19), no report is available concerning sSMase. Because neutral SMase is inhibited by gluthathione (GSH) (20), some chemicals with strong reducing power might affect sSMase activity.

In the present study, we investigated whether sSMase was affected by redox, as well as the inhibitory activity of catechins, well-known antioxidants, on sSMase to find effective sSMase inhibitors in food materials.

2. Materials and methods

2.1. Materials.

All the solvents, catalase, and (-)-epicatechin 3-*O*-gallate (ECg) were purchased from Wako Pure Chemicals Co. (Osaka, Japan). (-)-Catechin 3-*O*-gallate (Cg) and penta-*O*-galloyl-β-D-glucose (PGG) hydrate were purchased from Sigma-Aldrich (St. Louis, MO, USA). Seven methylated catechins were obtained from Nagara Science Co., Ltd (Gifu, Japan); (-)-epigallocatechin 3′-*O*-methylether (EGC-3′-O-Me), (-)-3′-*O*-methylepigallocatechin 3-*O*-gallate (EGCg-3′-O-Me), (-)-4′-*O*-methylepigallocatechin 3-*O*-gallate (EGCg-4′-O-Me), (-)-3′-*O*-methylepicatechin 3-*O*-gallate (ECg-3′-O-Me), (-)-4′-*O*-methylepicatechin 3-*O*-gallate (ECg-4′-O-Me), (-)-epicatechin 3-*O*-(3″-*O*-methyl)gallate (ECg-3″-O-Me) and (-)-epicatechin 3-*O*-(4″-*O*-methyl)gallate (ECg-4″-O-Me). (-)-Epigallocatechin 3-*O*-gallate (EGCg) was a gift from Mitsui-Nourin Inc. (Tokyo, Japan). Gallic acid (GA) and methyl gallate (MG) were purchased from Fuji Chemical Industry Co., Ltd (Wakayama, Japan). Procyanidin B1 was purchased from Extrasynthese S. A. (Lyon, France). Nitrobenzofurazan (NBD) C_6-SM was purchased from Molecular Probes Inc. (Eugene, OR, USA). All other reagents, (-)-epicatechin (EC), and (-)-epigallocatechin (EGC) were obtained from Nacalai Tesque Inc. (Kyoto, Japan). The structures of these catechins are shown in Fig.1.

2.2. sSMase enzyme from rats.

This study was approved by the Animal Care Committee of Nara Women's University. We used the plasma of ten-week-old male rats (SLC: Sprague-Dawley strain), which were obtained from Japan SLC Co. (Hamamatsu, Shizuoka, Japan). The animals were housed in a room at 24 ± 2 °C, with a 12 h/12 h light–dark cycle. Animals were fed commercial laboratory chow (CE-2, Oriental Yeast Co., Osaka, Japan) and water *ad libitum*. The rats were anesthetized with pentobarbital, and sacrificed by collecting the blood from the inferior vena cava using a syringe containing sodium heparin as an anticoagulant. The plasma was separated from the blood sample by centrifugation and used as an enzyme solution.

2.3. Change in sSMase activity by the redox state.

sSMase activities were measured using NBD C_6-SM as a substrate, as previously described (17, 18). To examine the effect of oxidation on sSMase activity, 100 µL of rat plasma was incubated with 500 µL of H_2O_2 solution at 0, 10, 100, and 1000 mM final concentrations for 15 min at 37 °C in 20 mM Tris-HCl buffer (pH 7.5) (the oxidized sample). To examine the effect of reduction, 100 µL of plasma was incubated with 500 µL of reduced glutathione (GSH) at 0, 4, 10, and 20 mM final concentrations for 15 min at 37 °C in 20 mM Tris-HCl buffer (pH 7.5) (the reduced sample). To examine the effect of redox cycling, sSMase in 100 µL of plasma was treated with H_2O_2 at 100 mM final concentration for 15 min at 37 °C, then H_2O_2 was removed by 920 units of catalase (Wako Pure Chemicals Co., 9200 units per mg), and the resulting enzyme solution was incubated with GSH at 7, 10, 14, and 20 mM final concentrations for 15 min at 37 °C (the redox cycling sample). To prepare the reoxidized sample, H_2O_2 was added to the sample reduced by 10 mM GSH at 1000 mM final concentration (the reoxidized sample).

2.4.Inhibition of sSMase by catechins and other compounds.

Five catechins, seven methylated catechins, and galloyl compounds (50 μM final concentration) were incubated with sSMase in 15 μL of plasma for 15 min at 37 °C. The total volume of the incubation mixture was 800 μL containing 0.1 mM $ZnSO_4$, 0.1% Nonidet P-40, and 62 mM sodium acetate (pH 5.0). After incubation, 4 nmol of NBD C_6-SM in 10 μL of methanol was added as a substrate. The enzymatic reaction was performed for 2 h at 37 °C, and was stopped by adding 2 mL of chloroform and methanol. After vortexing and centrifugation, the chloroform layer was collected, evaporated, and dissolved in 500 μL of methanol. Twenty μL of the solution was directly applied to HPLC system (Waters, 1525 Binary HPLC Pump) using a Nova Pak 4 μm C18 column (3.9×150 mm, Waters Corp. Milford, MA USA). NBD C_6-ceramide generated from NBD C_6-SM was eluted at a flow rate of 1 mL/min with a mixture of water, acetonitrile, and phosphoric acid at a volume ratio of 35:65:0.2. The fluorescence of NBD of these compounds was recorded with a fluorescence detector (Waters, type 2479, excitation at 466 nm and emission at 536 nm).

2.5. Kinetic data analysis.

To determine the inhibition pattern, sSMase was reacted in the presence of 0, 2.5, and 5 μM concentrations of EGCg-3′-O-Me and the contents of NBD C_6-SM were changed in a range from 1 to 8 nmol. Duplicated experiments were performed to determine Km and Vmax. The kinetic data of Km and Vmax were analyzed by using the R (Free Software under the terms of the Free Software Foundation’s GNU General Public License). The velocities were fitted to the Michaelis-Menten model by using package “drc” and its function “drm”. Figure was drawn as double reciprocal plot by Excel.

2.6. Statistical analyses.

Data were expressed as mean ± SEM and analyzed through a multiple comparison test using the Statcel software (OMS Publishing Inc., Tokyo, Japan). Differences between group means were considered significant at $p < 0.01$ using the Scheffe's method generated by this program.

3. Results

3.1. Change in sSMase activity by the redox state

To examine whether sSMase is affected by the redox state, we determined the change in sSMase activity under oxidative and reductive conditions. sSMase was activated by H_2O_2 in a dose dependent manner (Fig. 2A). H_2O_2 at 100 mM (final concentration) significantly activated sSMase compared with the control without H_2O_2. H_2O_2 at 1000 mM significantly activated sSMase more than H_2O_2 at 100 mM (Fig. 2A).

On the contrary, addition of GSH decreased the sSMase activity in a dose-dependent manner. GSH at 10 mM significantly inhibited the sSMase activity, as compared with the control without GSH, and GSH at 20 mM further inhibited sSMase (Fig. 2B). Additionally, dithiothreitol showed a stronger inhibition effect than GSH (data not shown).

Next, we examined whether the effect of the redox state on sSMase was reversible. The sSMase activity was activated by 100 mM H_2O_2 followed by H_2O_2 decomposition by catalase. This activation was suppressed by treatment with 7 mM and higher GSH concentrations (Fig. 2C). Moreover, sSMase, which was activated by 100 mM H_2O_2 and then inhibited by 10 mM of GSH, was activated again by 1000 mM of H_2O_2 (Fig. 2D). However 100 mM of H_2O_2 did not activate the reduced sSMase by GSH, probably because H_2O_2 was promptly decomposed by GSH.

Since sSMase was easily activated in aerobic condition, we presented the sSMase activities as relative values versus the corresponding control values.

3.2. Inhibition of sSMase by five catechins

Catechins are well-known antioxidants with a strong reducing power. We examined the inhibitory effect by five catechins contained in green tea on sSMase (Fig. 3). ECg significantly inhibited sSMase. Other gallate-type catechins such as EGCg and Cg also significantly inhibited sSMase; however, these catechins had a weaker inhibitory effect than ECg. On the contrary, EC and EGC did not affect sSMase activity. Among these catechins, ECg showed the strongest inhibitory effect on sSMase. The IC_{50} value of ECg was 25.7 μM.

3.3. sSMase inhibition by ECg and its reversal by H_2O_2

The sSMase activated by 100 mM H_2O_2 that is followed by decomposition of H_2O_2 with catalase was incubated with 50 μM ECg for 15 min at 37 °C. The activity of the resulting sSMase was reduced significantly to 17% of the oxidized enzyme with H_2O_2 (Fig. 4). Then the reduced enzyme was significantly reactivated by 1000 mM of H_2O_2 (Fig. 4).

3.4. sSMase inhibition by galloyl compounds and catechin dimer

The inhibition of sSMase by various catechins indicated that the galloyl group was essential. We investigated the effect of some galloyl compounds on the sSMase activity (Fig. 5). Gallic acid (GA) and methyl gallate (MG) did not show any inhibitory effect. PGG with five galloyl residues exhibited a significant inhibitory effect, which was weaker than that by ECg. In addition, procyanidin B1, which is a dimer of catechin (epicatechin-(4β-8)-catechin), had no effect on sSMase.

3.5. sSMase inhibition by seven methylated catechins

To determine the necessary hydroxyl group(s) for the inhibitory activity of catechins, the inhibitions of sSMase by four methylated ECgs were compared. The inhibitory activity of ECg was significantly attenuated by methylation at the 3′-, 4′-, 3″-, or 4″-position of the galloyl residue (Fig. 6A, and B). The inhibitory activity of ECg-3′-O-Me was significantly stronger than that of ECg-4′-O-Me ($p<0.01$).

Furthermore, the inhibitory activity of two methylated EGCgs (Fig. 6C) was examined. EGCg-3′-O-Me showed the strongest inhibitory effect on sSMase (IC_{50}=1.7 μM) among the catechins examined in the present study. It was much stronger than that of ECg. The inhibitory activity of EGCg-4′-O-Me was significantly weaker than that of EGCg. EGC and EGC-3′-O-Me did not inhibit sSMase (Fig. 6D).

To determine the inhibitory pattern of EGCg-3′-O-Me, sSMase was reacted with 0, 2.5, and 5 μM concentrations of EGCg-3′-O-Me and fitted to the Michaelis-Menten model. The Vmax and Km values were different in each reaction condition (Table. 1). In addition, the three plots in the double reciprocal plot did not intersect at one point (Fig. 7). These results indicated that the inhibition of sSMase by EGCg-3′-O-Me did not follow the competitive inhibition mechanism.

4. Discussion

Although aSMase was activated by copper-promoted oxidation (21), this is the first study demonstrating that sSMase in plasma is also activated by oxidation. Furthermore, sSMase is inhibited by reductants such as GSH and dithiothreitol, and the redox regulation of the sSMase activity is found to be reversible. Therefore it is expected that the sSMase activity reflects the oxidative stress in plasma and it is a useful marker of diseases such as diabetes (17) and atherosclerosis (18), because oxidative stress is involved in their pathogenicity.

Since the activity of sSMase is attenuated by reduction, an antioxidant may affect the sSMase activity. This study demonstrated that catechins, a typical food-derived antioxidant and reductant, effectively inhibited sSMase. Four catechins —EC, EGC, ECg, and EGCg— are the main components of green tea. Among them, ECg showed a strong inhibitory effect on sSMase. EGCg also exerted an inhibitory effect, although it was weaker than ECg. However, reducing ability of EGCg was stronger than that of ECg (22), suggesting that the steric interaction of the sSMase protein with ECg is more favorable than that with EGCg.

The results concerning gallate type catechins (Fig. 3) indicate that the presence of the galloyl group at the C-3 position is important for the inhibitory effect on sSMase. The same phenomenon is observed in procyanidin B1 with no galloyl residue (Fig. 5). In addition, the results of ECg-3″-O-Me and ECg-4″-O-Me (Fig. 6A) indicated that the galloyl structure was important. Meanwhile, the inhibitory activity of PGG with five galloyl residues was not stronger than that of ECg (Fig. 5). It is suggested that both the alcohol part and the flavanol structure of ECg are necessary to exhibit the inhibitory activity on sSMase. This idea is consistent with the results for methyl gallate, which had no inhibitory effect (Fig.5).

It is worthwhile to note that the catechol structure of B-ring is important for the inhibition of sSMase. On the other hand, Cg, which is the epimer of ECg and has a catechol structure similar to that of ECg showed weaker inhibitory activity on sSMase than that of ECg. Since the reduction potential of Cg may approximate that of ECg, the difference between these epimers at the C-2 position may be ascribed to the steric discrimination by the sSMase protein.

There are some green teas, that contain methylated catechins, such as Benifuuki. Methylated catechins have an anti-allergic effect (23). Among seven types of methylated catechins, EGCg-3′-O-Me showed the strongest inhibitory effect on sSMase (IC_{50}=1.7

μM). Matsuura *et al*. (21) reported that the pattern of electric potential of EGCg-3′-O-Me resembled that of ECg, indicating that the redox character of the pyrogallol moiety of EGCg-3′-O-Me was changed to that of catechol by methylation of the 3′-position, which also caused stabilization of EGCg. On the other hand, the redox pattern of EGCg-4′-O-Me resembled that of MG, showing that methylation of the 4′-position of the B-ring of EGCg abolished the redox character of its B-ring (21). From these results, it is suggested that the *ortho*-diphenol structure at the B-ring was necessary to inhibit sSMase.

Gallate-type catechins have been reported to easily form a conjugated bond to the cysteine of many proteins such as albumin, and GAPDH (24, 25). Such an addition reaction could occur between the cysteine residue at the C-terminal domain of sSMase and catechins. However, considering the result that the inhibition by ECg was reversed by oxidation with H_2O_2 similar to the case of GSH, reduction of the cysteine group(s) may be a preferred mechanism for the inhibition of sSMase by catechins.

It is worthwhile to note that catechins have metal ion chelating activity. As sSMase needs zinc ion, inhibitory effect of catechins might be due to its chelating activity. However, the zinc-chelating activities of EC, ECg, EGCg, and procyanidin B1 were almost similar as detected by the decrease of the fluorescence emission of zinc-Zinquin complexes (26). Therefore, it is concluded that the zinc-chelating activity does not primarily contribute to the sSMase inhibition.

The results of the Michaelis-Menten model and the double reciprocal plot indicate that EGCg-3′-O-Me mainly affects sSMase activity through reduction reaction and does not compete with SM for the binding site of the enzyme. (Fig. 7, Table 1).

Oxidative stress is implicated in the pathogenesis of diabetes and atherosclerosis. Moreover, sSMase activity, which is activated by oxidation, is increased in these diseases, resulting in increased plasma ceramide (17,18). Ceramide is suggested to be a risk factor for these diseases (27, 28, 29). Therefore, it is possible that the inhibition of sSMase

effectively prevents these diseases. The beneficial effects of catechins in preventing these diseases are well documented (30), and the present study suggests that one of these effects of catechins is ascribed to their ability to inhibit sSMase.

In conclusion, EGCg-3′-O-Me and ECg have a strong inhibitory effect on sSMase in a physiological plasma concentration, i.e., micromolar order. This inhibition may be due to their specific structures such as methoxycatechol and galloyl residue, and it depends on the reducing power as well as the steric interaction with the sSMase protein.

References

1) Marathe, S., Kuriakose, G., Williams, K. J., Tabas, I. Sphingomyelinase, an enzyme implicated in atherogenesis, is present in atherosclerotic lesions and binds to specific components of the subendothelial extracellular matrix. *Atherioscler. Thromb. Vasc. Biol.* **19**, 2648 -2658 (1999).

2) Górska, M., Barańczuk, E., Dobrzyń, A. Secretory Zn^{2+}-dependent sphingomyelinase activity in the serum of patients with type 2 diabetes is elevated. *Horm. Metab. Res.* **3**, 506 -507 (2003).

3) Pan, W., Yu, J., Shi, R., Yan, L., Yang, T., Li, Y., Zhang, Z., Yu, G., Bai, Y., Schuchman, E. H., He, X., Zhang, G. Elevation of ceramide and activation of secretory acid sphingomyelinase in patients with acute coronary syndromes. *Coron. Artery. Dis.* **25**, 230 -235 (2014).

4) Fucho, R., Martínez, L., Baulies, A., Torres, S., Tarrats, N., Fernandez, A., Ribas, V., Astudillo, A. M., Balsinde, J., Garcia-Rovés, P., Elena, M., Bergheim, I., Lotersztajn, S., Trautwein, C., Appelqvist, H., Paton, A. W., Paton, J. C., Czaja, M. J., Kaplowitz, N., Fernandez-Checa, J. C., García-Ruiz, C. ASMase regulates autophagy and lysosomal membrane permeabilization and its inhibition prevents early stage non-alcoholic steatohepatitis. *J. Hepatol.* **61**, 1126 -1134 (2014).

5) Wang, G., Dinkins, M., He, Q., Zhu, G., Poirier, C., Campbell, A., Mayer-Proschel, M., Bieberich, E. Astrocytes secrete exosomes enriched with proapoptotic ceramide and prostate apoptosis response 4 (PAR-4): potential mechanism of apoptosis induction in Alzheimer disease (AD). *J. Biol. Chem.* **287**, 21384 -21395 (2012).

6) Carpinteiro, A., Becker, K. A., Japtok, L., Hessler, G., Keitsch, S., Požgajovà, M., Schmid, K. W., Adams, C., Müller, S., Kleuser, B., Edwards, M. J., Grassmé, H., Helfrich, I., Gulbins, E. Regulation of hematogenous tumor metastasis by acid sphingomyelinase. *EMBO. Mol. Med.* **7**, 714 -734 (2015).

7) Hannun, Y. A., Obeid, L. M. The ceramide-centric universe of lipid-mediated cell regulation: stress encounters of the lipid kind. *J. Biol. Chem.* **277**, 25847–25850 (2002).

8) Kolesnick, R. Ceramide: a novel second messenger. *Trends Cell Biol.* **2**, 232 –236 (1992).

9) Farrell, A. M., Uchida, Y., Nagiec, M. M., Harris, I. R., Dickson, R. C., Elias, P. M., Holleran, W. M. UVB irradiation up-regulates serine palmitoyltransferase in cultured human keratinocytes. *J. Lipid Res.* **39**, 2031 –2038 (1998).

10) Yamada, Y., Kajiwara, K., Yano, M., Kishida, E., Masuzawa, Y., Kojo, S. Increase of ceramides and its inhibition by catalase during chemically induced apoptosis of HL-60 cells determined by electrospray ionization tandem mass spectrometry. *Biochim. Biophys. Acta.* **1532**, 115 –120 (2001).

11) Santana, P., Pena, L. A., Haimovitz-Friedman, A., Martin, S., Green, D., McLoughlin, D. M., Cordon-Cardo, C., Schuchman, E. H., Fuks, Z., Kolesnick, R. Acid sphingomyelinase-deficient human lymphoblasts and mice are defective in radiation-induced apoptosis. *Cell* **86**, 189 ‑199 (1996).

12) Goni, F. M., Alonso, A. Sphingomyelinases: enzymology and membrane activity. *FEBS Lett.* **531**, 38 –46 (2002).

13) Schuchman, E. H., Acid sphingomyelinase, cell membranes and human disease: lessons from Niemann-Pick disease. *FEBS Lett.* **584**, 1895 –1900 (2010).

14) Schissel, S. L., Keesler, G. A., Schuchman, E. H., Williams, K. J., Tabas, I. The cellular trafficking and zinc dependence of secretory and lysosomal sphingomyelinase, two products of the acid sphingomyelinase gene. *J. Biol. Chem.* **273**, 18250 –18259 (1998).

15) Jenkins, R. W., Canals, D., Idkowiak-Baldys, J., Simbari, F., Roddy, P., Perry, D. M., Kitatani, K., Luberto, C., Hannun, Y. A. Regulated secretion of acid

sphingomyelinase: implications for selectivity of ceramide formation. *J. Biol. Chem.* **285**, 35706 -35718 (2010).

16) Tabas, I., Secretory sphingomyelinase. *Chem. Phys. Lipids* **102**, 123 –130 (1999).

17) Kobayashi, K., Ichi, I., Nakagawa, T., Kamikawa, C., Kitamura, Y., Koga, E., Washino, Y., Hoshinaga, Y., Kojo, S. Increase in plasma ceramide levels via secretory sphingomyelinase activity in streptozotocin-induced diabetic rats. *Med. Chem. Commun.* **2**, 536 -541 (2011).

18) Kobayashi, K., Nagata, E., Sasaki, K., Harada-Shiba, M., Kojo, S., Kikuzaki, H. Increase in secretory sphingomyelinase activity and specific ceramides in the aorta of apolipoprotein E knockout mice during aging. *Biol. Pharm. Bull.* **36**,1192 -1196 (2013).

19) Kornhuber, J., Tripal, P., Reichel, M., Mühle, C., Rhein, C., Muehlbacher, M., Groemer, T. W., Gulbins, E. Functional inhibitors of acid sphingomyelinase (FIASMAs): a novel pharmacological group of drugs with broad clinical applications. *Cell Physiol. Biochem.* **26**, 9 -20 (2010).

20) Liu, B., Hannun, Y. A. Inhibition of the neutral magnesium-dependent sphingomyelinase by glutathione. *J. Biol. Chem*. **272**, 16281 -16287 (1997).

21) Qiu, H., Edmunds, T., Baker-Malcolm, J., Karey, K. P., Estes, S., Schwarz, C., Hughes, H., Van Patten, S. M. Activation of human acid sphingomyelinase through modification or deletion of C-terminal cysteine. *J. Biol. Chem.* **278**, 32744 -32752 (2003).

22) Matsuura, K., Usui, Y., Kan, T., Ishii, T., Nakayama, T. Structural specificity of electric potentials in the coulometric-array analysis of catechins and theaflavins. *J. Clin. Biochem. Nutr.* **55**, 103 -109 (2014).

23) Maeda-Yamamoto, M., Inagaki, N., Kitaura, J., Chikumoto, T., Kawahara, H., Kawakami, Y., Sano, M., Miyase, T., Tachibana, H., Nagai, H., Kawakami, T. O-

methylated catechins from tea leaves inhibit multiple protein kinases in mast cells. *J. Immunol.* **172**, 4486 -4492 (2004).

24) Ishii, T., Mori, T., Tanaka, T., Mizuno, D., Yamaji, R., Kumazawa, S., Nakayama, T., Akagawa, M. Covalent modification of proteins by green tea polyphenol (-)-epigallocatechin-3-gallate through autoxidation. *Free Radic. Biol. Med.* **45**, 1384 -1394 (2008).

25) Li, M., Hagerman, A. E. Role of the flavan-3-ol and galloyl moieties in the interaction of (-)-epigallocatechin gallate with serum albumin. *J. Agric. Food Chem.* **62**, 3768 -3775 (2014).

26) Quesada, I. M., Bustos, M., Blay, M., Pujadas, G., Ardèvol, A., Salvadó, M. J., Bladé, C., Arola, L., Fernández-Larrea, J. Dietary catechins and procyanidins modulate zinc homeostasis in human HepG2 cells. *J. Nutr. Biochem.* **2**, 153 -163 (2001).

27) Ichi, I., Nakahara, K., Kiso, K., Kojo, S. The effect of dietary cholesterol and high fat on ceramide concentration in rat tissues. *Nutrition* **23**, 570 -574 (2007).

28) Ichi, I., Takashima, Y., Adachi, N., Nakahara, K., Kamikawa, C., Harada-Shiba, M., Kojo, S. Effects of dietary cholesterol on tissue ceramides and oxidation products of apolipoprotein B-100 in apoE deficient mice. *Lipids* **42**, 893 -900 (2007).

29) Ichi, I., Nakahara, K., Miyashita, Y., Hidaka, A., Kutsukake, S., Inoue, K., Maruyama, T., Miwa, Y., Harada-Shiba, M., Tsushima, M., Kojo, S., Kisei Cohort Study Group. Association of ceramides in human plasma with risk factors of atherosclerosis. *Lipids* **41**, 859 -863 (2006).

30) Crespy, V., Williamson, G. A review of the health effects of green tea catechins in in vivo animal models. *J. Nutr.* **134**, 3431S -3440S (2004).

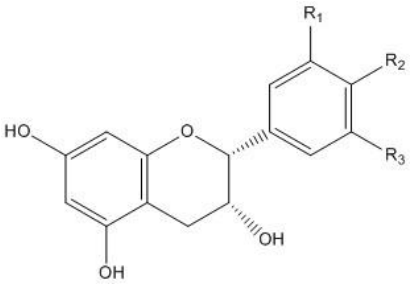

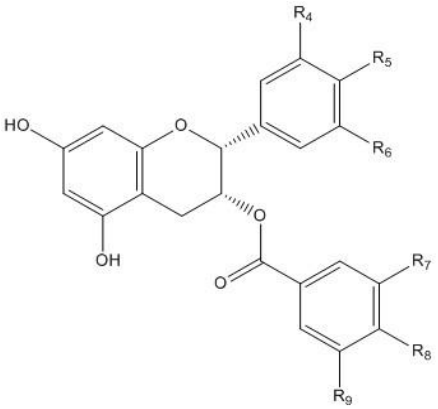

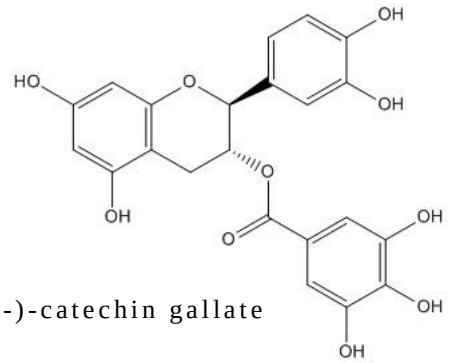

(-)-catechin gallate

compound name	abbreviation	R_1	R_2	R_3
(-)-epicatechin	EC	OH	OH	H
(-)-epigallocatechin	EGC	OH	OH	OH
(-)-epigallocatechin 3′-*O*-methylether	EGC-3′-O-Me	OCH_3	OH	OH

compound name	abbreviation	R_4	R_5	R_6	R_7	R_8	R_9
(-)-epicatechin 3-*O*-gallate	ECg	OH	OH	H	OH	OH	OH
(-)-3′-*O*-methylepicatechin 3-*O*-gallate	ECg-3′-O-Me	OCH_3	OH	H	OH	OH	OH
(-)-4′-*O*-methylepicatechin 3-*O*-gallate	ECg-4′-O-Me	OH	OCH_3	H	OH	OH	OH
(-)-epicatechin 3-*O*-(3″-*O*-methyl)gallate	ECg-3″-O-Me	OH	OH	H	OCH_3	OH	OH
(-)-epicatechin 3-*O*-(4″-*O*-methyl)gallate	ECg-4″-O-Me	OH	OH	H	OH	OCH_3	OH
(-)-epigallocatechin 3-*O*-gallate	EGCg	OH	OH	OH	OH	OH	OH
(-)-3′-*O*-methylepigallocatechin 3-*O*-gallate	EGCg-3′-O-Me	OCH_3	OH	OH	OH	OH	OH
(-)-4′-*O*-methylepigallocatechin 3-*O*-gallate	EGCg-4′-O-Me	OH	OCH_3	OH	OH	OH	OH

Figure 1. Structures of catechins.

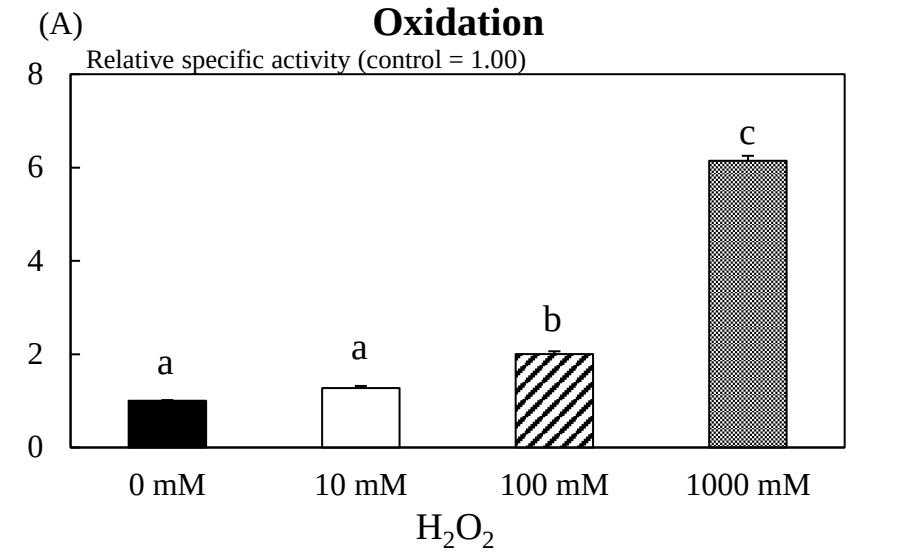
(A)
Oxidation
Relative specific activity (control = 1.00)
8
6
4
2
0
a
a
b
c
0 mM
10 mM
100 mM
1000 mM
H2O2

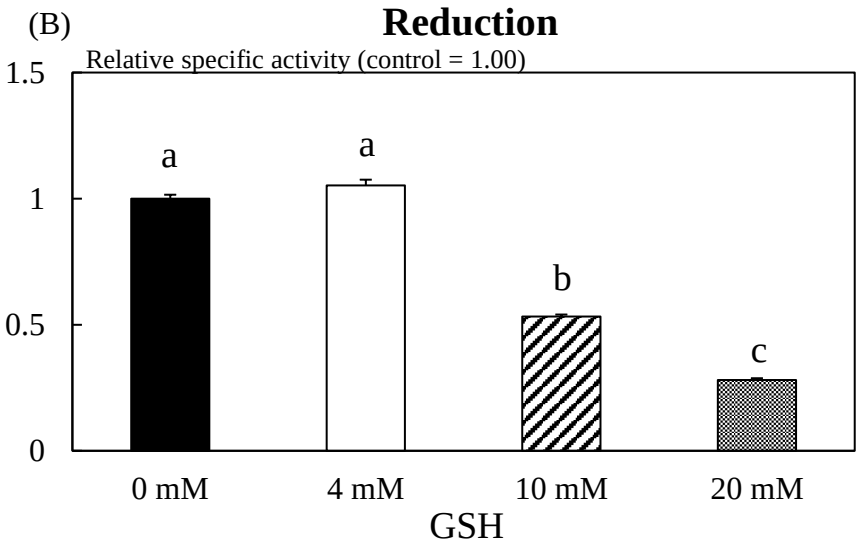
(B)
Reduction
Relative specific activity (control = 1.00)
1.5
1
0.5
0
a
a
b
c
0 mM
4 mM
10 mM
20 mM
GSH

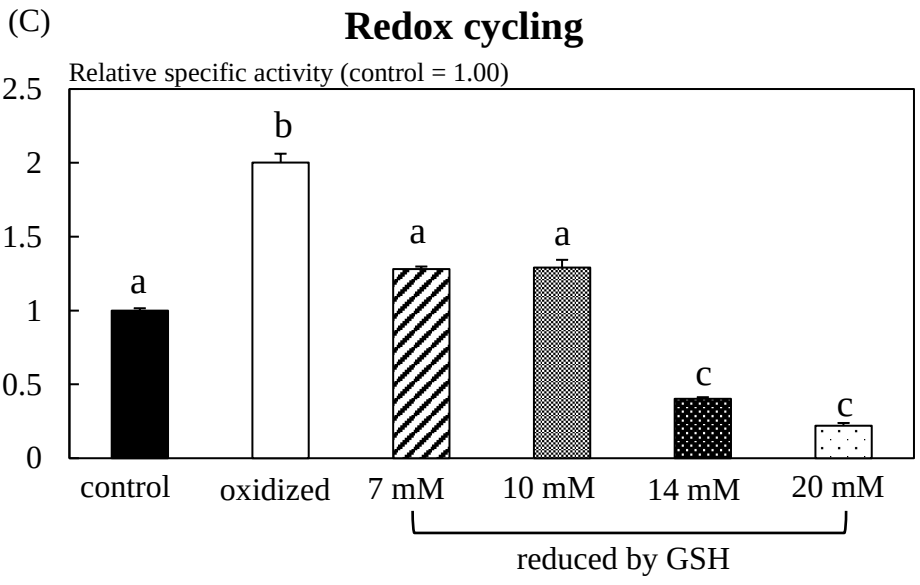
(C)
Redox cycling
Relative specific activity (control = 1.00)
2.5
2
1.5
1
0.5
0
a
b
a
a
c
c
control
oxidized
7 mM
10 mM
14 mM
20 mM
reduced by GSH

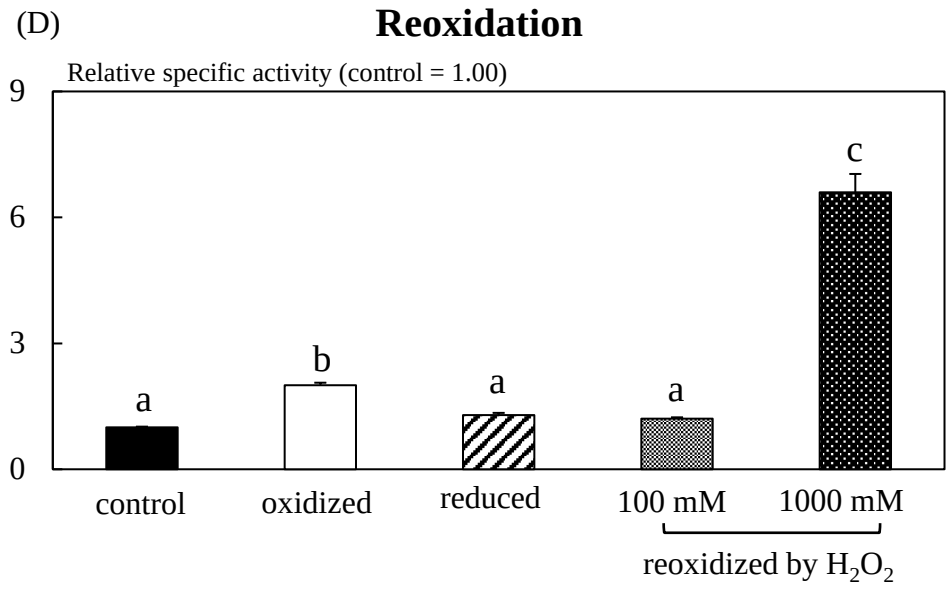

Figure 2. Changes in sSMase activity under oxidation by H_2O_2 (A) and reduction by GSH (B). sSMase was oxidized by 0, 10, 100, and 1000 mM of H_2O_2. To prepare reduced sSMase, sSMase was incubated with 0, 4, 10, and 20 mM of GSH. Values are mean ± SEM for 4 -12 runs. Different superscript letters indicate significant differences at $p < 0.01$ (Scheffe's method).

Effect of redox cycling on sSMase activity (C). sSMase was reduced by 7, 10, 14, and 20 mM of GSH after the oxidation by 100 mM of H_2O_2. Different superscript letters indicate significant differences at $p < 0.01$ (Scheffe's method).

Changes in sSMase activity by reoxidation (D). sSMase was oxidized by 100 mM of H_2O_2. After removing the residual H_2O_2 by catalase, GSH was added to a final concentration of 10 mM. Then the enzyme solution was reoxidized in the presence of 100 and 1000 mM of H_2O_2. Values are mean ± SEM for 4 -12 runs in each group. Different superscript letters indicate significant differences at $p < 0.01$ (Scheffe's method).

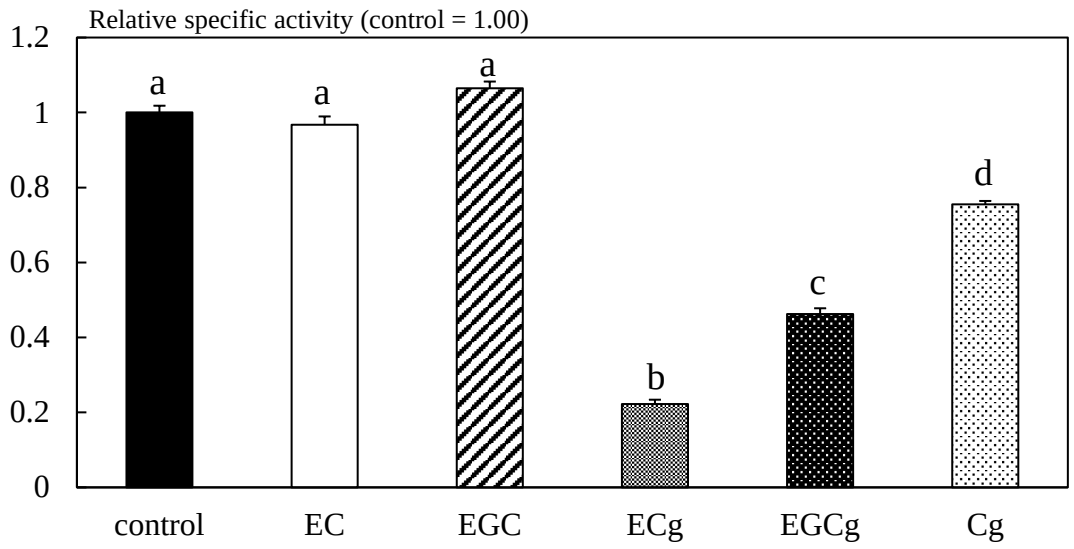

Figure 3. Changes in sSMase activity under incubation by catechins. sSMase was incubated by five types of catechins ; EC, EGC, ECg, EGCg, and Cg (50 μM as final concentration). Values are mean ± SEM for 4-8 runs in each catechin group and 8 runs in the control. Different superscript letters indicate significant differences at $p < 0.01$ (Scheffe's method).

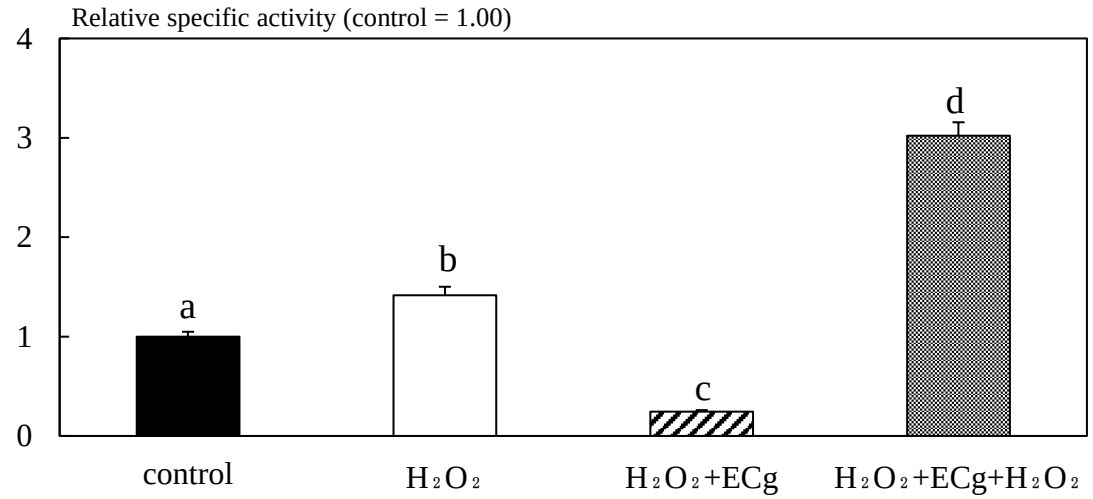

Figure 4. Inhibition reversal of sSMase activity by catechins by reoxidation. sSMase was oxidized by 100 mM of H_2O_2. After removing the residual H_2O_2 by catalase, 50 μM of ECg was added. Then, the enzyme solution was reoxidized with 1000 mM of H_2O_2. Values are mean ± SEM for 4 runs in each group. Different superscript letters indicate significant differences at $p < 0.01$ (Scheffe's method).

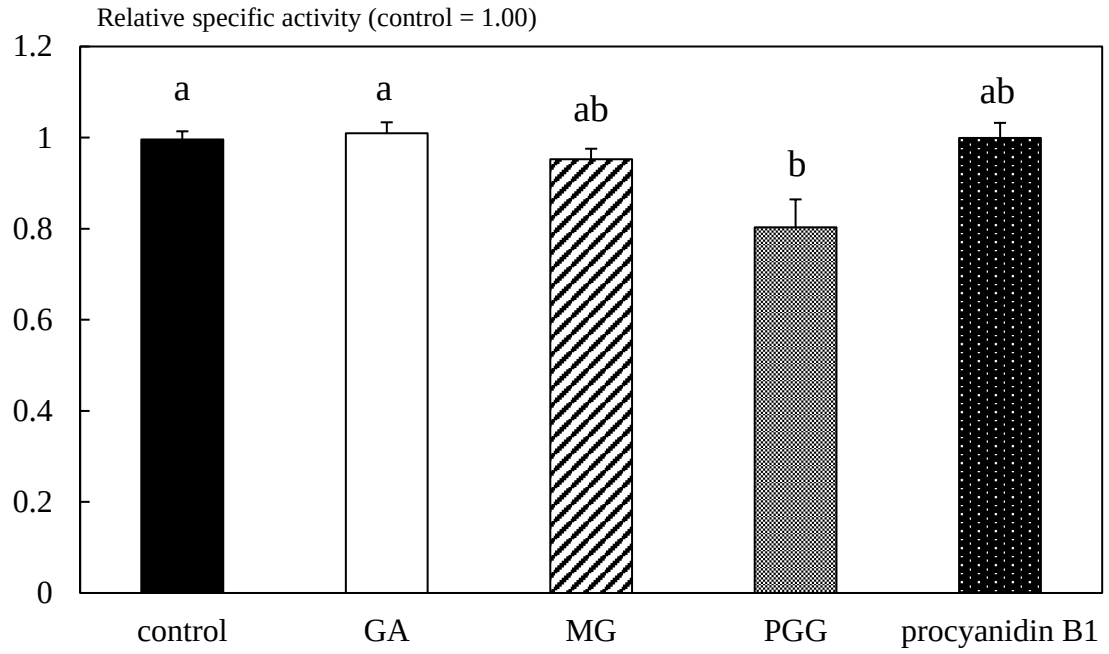

Figure 5. Inhibition of sSMase activity by galloyl chemicals and catechin dimer. sSMase was incubated with GA, MG, PGG, and procyanidin B1 (final concentration at 50μM). Values are mean ± SEM for 4 -9 runs in each group. Different superscript letters indicate significant differences at $p < 0.01$ (Scheffe's method).

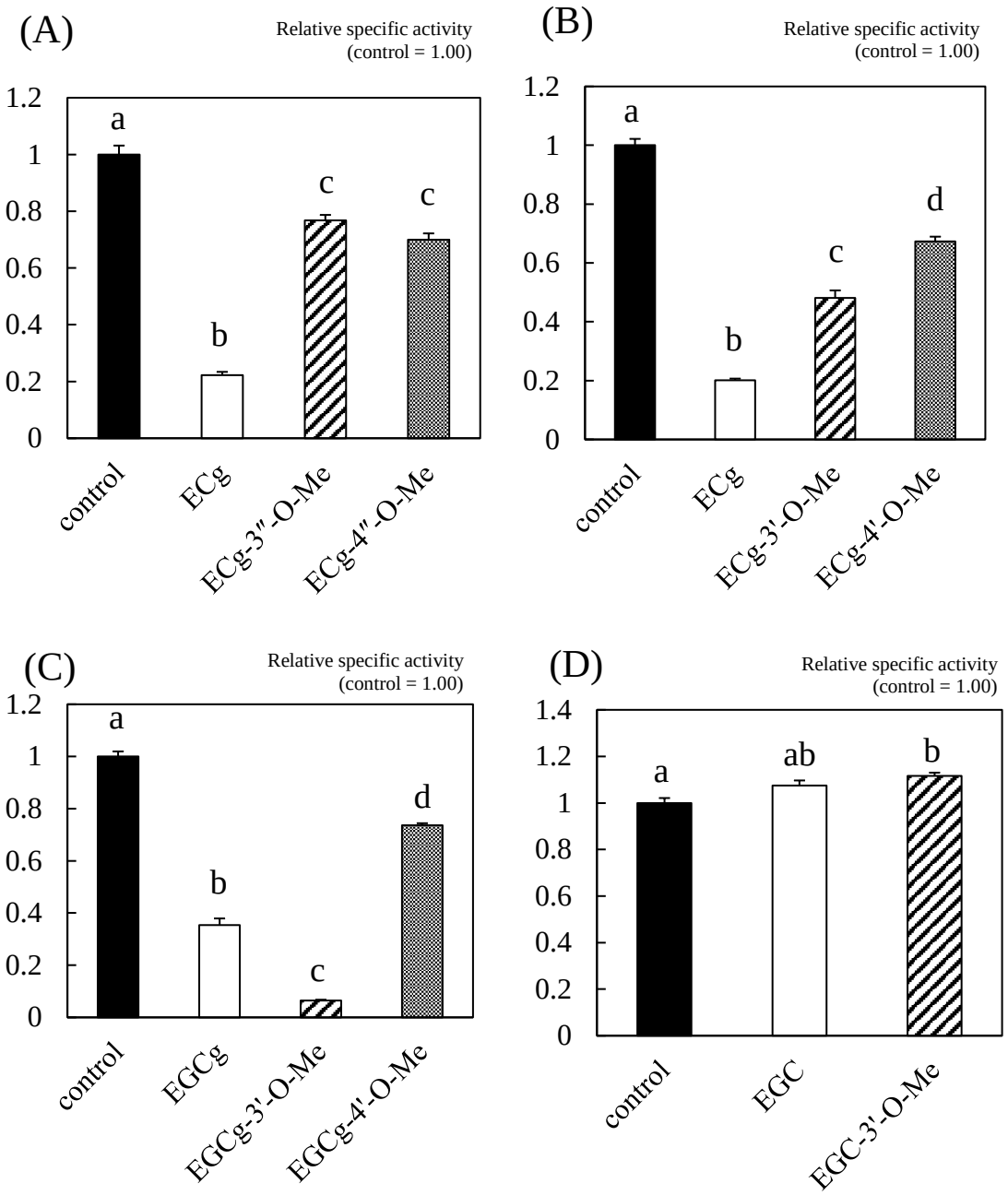

Figure 6. Inhibition of sSMase activity by methylated ECg molecules (A, B). Values are mean ± SEM for 4 runs in each group. Different superscript letters indicate significant differences at $p < 0.01$ (Scheffe's method).

Inhibition of sSMase activity by methylated EGCg (C). Values are mean ± SEM for 4 runs in each group. Different superscript letters indicate significant differences at $p < 0.01$ (Scheffe's method).

Inhibition of sSMase activity by methylated EGC (D). Values are mean ± SEM for 4 runs in each group. Different superscript letters indicate significant differences at $p < 0.01$ (Scheffe's method).

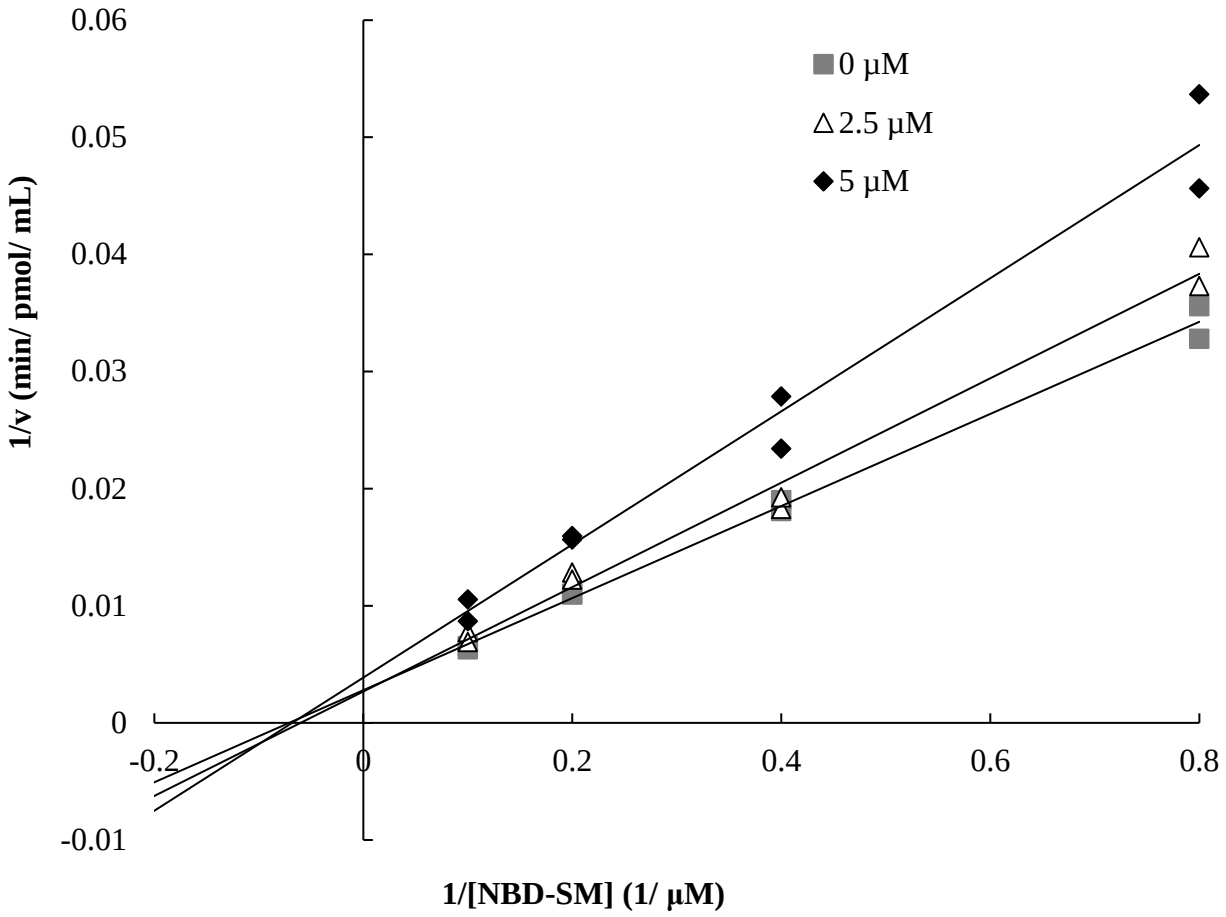

Figure 7. Double reciprocal plot of sSMase activity versus NBD C_6-SM concentrations in the presence of EGCg-3′-O-Me.

	EGCg-3′-O-Me concentration		
	0 μM	2.5 μM	5 μM
Vmax (pmol/ mL/ min)	455.10	343.02	261.64
Km (μM)	19.31	15.27	15.03

Data were fitted to the Michaelis-Menten model by using the R.

Table 1. The change of Km values and Vmax values when sSMase was inhibited by EGCg-3′-O-Me.

Conclusion

Oxidative stress was related to the accumulation of ceramide in many diseases, but the mechanism causing the ceramide increase was not clearly elucidated. Based on studies of this thesis, I found that oxidative stress increased ceramide by stimulating SMase *in vivo*.

In Chapter 1, I found that the increased plasma ceramide was due to the activation of liver nSMase in CCl_4-intoxicated rats. I also found that the increased plasma ceramide was derived from the liver, indicating that ceramide was transported to other tissues such as brain via blood flow in acute oxidative stress. On the other hand, I found that the increased plasma ceramide was due to the increase in plasma sSMase activity in diabetes mellitus in Chapter 3. Moreover, it was revealed that the increased aorta ceramide was derived from the elevated activity of sSMase in atherosclerosis during aging in Chapter 4. Finally I found that sSMase is activated by oxidation and inhibited by reduction in Chapter 5.

SMases are classified into five types based on pH optimum, subcellular localization, and cation dependence. Since nSMase activity also depends on its redox state, the active site of all SMases seems to have a common structure. Therefore the activation of SMase may depend on the location of oxidative stress among tissues and also in the cell. In addition the timecourse of oxidative stress, for example acute or chronic, may affect the selectivity, which SMase is activated. Further studies are necessary to reveal the detailed mechanism of the SMase activation including the difference in the sensitivity of tissues against oxidative stress.

I also found that oxidative stress induced many physiological responses such as activation of SMase and Kupffer cells containing COX-2 and phospholipase A_2. In Chapter 2, it is revealed that increased ceramide and activity of COX-2 have an important role in the second phase of CCl_4 intoxication.

In addition, I found that a strong reductant such as ECg and EGCg-3′-O-Me is a probable candidate for preventing atherosclerosis and complications of diabetes by inhibiting the increase of sSMase activity and ceramide.

Oxidative stress has been known to cause many diseases such as atherosclerosis, diabetes mellitus, chronic heart diseases, NAFLD, Alzheimer's disease, and so on. However, the underlying mechanism that oxidative stress causes tissue dysfunction is not clearly elucidated. Ceramide is popular as the major constituent of lamellar structure and plays an important role in maintaining cutaneous barrier function because of its water-holding capacity. In this study, I found that ceramide and SMase had an important role in the post-oxidative stress state and that the ceramide metabolism was one of probable mechanisms that leaded to tissue injury as a new aspect. This investigation provides new insights into the progression of metabolic syndrome and the effective food materials, which prevent these diseases.

Publications List

Publications included in this thesis

1. Neutral sphingomyelinase-induced ceramide accumulation by oxidative stress during carbon tetrachloride intoxication. I. Ichi, C. Kamikawa, T. Nakagawa, K. Kobayashi, R. Kataoka, E. Nagata, Y. Kitamura, C. Nakazaki, T. Matsura, and S. Kojo, *Toxicology*, **261**, 33-40 (2009).
2. Effect of celecoxib, a selective cyclooxygenase-2 inhibitor on carbon tetrachloride intoxication in rats. Y. Washino, E. Koga, Y. Kitamura, C. Kamikawa, K. Kobayashi, T. Nakagawa, C. Nakazaki, I. Ichi, and S. Kojo, *Biol. Pharm. Bull.*, **33**, 707-709 (2010).
3. Increase in plasma ceramide levels via secretory sphingomyelinase activity in streptozotocin-induced diabetic rats. K. Kobayashi, I. Ichi, T. Nakagawa, C. Kamikawa, Y. Kitamura, E. Koga, Y. Washino, Y. Hoshinaga and S. Kojo, *Med. Chem. Commun.*, **2**, 536-541(2011).
4. Increase in secretory sphingomyelinase activity and specific ceramides in the aorta of apolipoprotein E knockout mice during aging. K. Kobayashi, E. Nagata, K. Sasaki, M. Harada-Shiba, S. Kojo, and H. Kikuzaki, *Biol. Pharm.Bull*., **36**, 1192-1196 (2013).
5. Strong inhibition of secretory sphingomyelinase by catechins, particularly by (-)-epicatechin 3-*O*-gallate and (-)-3′-*O*-methylepigallocatechin 3-*O*-gallate. K. Kobayashi, Y. Ishizaki, S. Kojo, and H. Kikuzaki, *J. Nutr. Sci. Vitaminol.*, **62**, 125-131 (2016).

Other publications

1. The role of Kupffer cells in carbon tetrachloride intoxication in mice. K. Kiso, S. Ueno, M. Fukuda, I. Ichi, K. Kobayashi, T. Sakai, K. Fukui, and S. Kojo, *Biol. Pharm. Bull.*, **35**, 980-983 (2012).

2. Racemization of the aspartic acid residue of amyloid-β peptide by a radical reaction. K. Tambo, T. Yamaguchi, K. Kobayashi, E. Terauchi, I. Ichi, and S. Kojo, *Biosci. Biotechnol. Biochem.*, **77**, 416-418 (2013).

Acknowledgement

The author wishes to express her deep gratitude to Emeritus Professor Shosuke Kojo, Faculty of Humen Life and Environment, Nara Women's University, for his warm guidance, advice and continuous encouragement throughout this study. The author also express her gratitude to Lecturer Ikuyo Ichi, Faculty of Human Life and Environmental Sciences, Ochanomizu University, for her encouragement and helpful advice in completing this study.

The author is grateful to Professor Hiroe Kikuzaki, Faculty of Humen Life and Environment, Nara Women's University, for the guidance and invaluable support. The sincere appreciation is also expressed to Professor Yasunori Ogura, Professor Satoru Matsuda and Associate Professor Rieko Nakata for the critical reading of this manuscript and helpful advice.

She would like to thank her collaborators, Ms. Chiaki Kamikawa, Ms. Tomoka Nakagawa, Ms. Yukiko Hoshinaga, Ms. Kazuki Sasaki, Ms. Eri Nagata, Ms. Yukiko Washino, Ms. Eriko Koga, Ms. Ryoko Kataoka, Ms. Yuko Kitamura, Ms. Chihiro Nakazaki and Ms. Yuki Ishizaki for their close, warm-hearted collaboration and valuable contributions to the experimental works that are essential in this study.

In addition, she wishes to thank Professor Tatsuya Matsura, Tottori University, for his useful advice. She also thank Dr. Mariko Harada-Shiba, National Cardiovascular Center Research Institute, for kindly providing apoE$^{-/-}$ mice.

Finally, the author is thankful to my family for their continuous encouragement, love and unlimited support throughout this study.